

AN ABSTRACT OF THE DISSERTATION OF

Emily Amanda Caffrey for the degree of Doctor of Philosophy in Radiation Health Physics presented on January 8, 2016.

Title: Development and Application of Voxelized Dosimetric Models for Biota: Characterization of the Uncertainty in the International Commission on Radiological Protection's Wildlife Dosimetry System.

Abstract approved:

Kathryn A. Higley

A system for radiological dosimetry for nonhuman biota developed by International Commission on Radiological Protection (ICRP) relies on calculations that utilize the Monte Carlo simulations of simple, ellipsoidal geometries with internal radioactivity distributed homogeneously throughout. In this manner it is quick and easy to estimate whole-body dose rates to biota. This system relies on the validity of three major assumptions. First, that any organism can be reasonably represented by a simplified dosimetric phantom; second, that for dosimetric purposes four-component human tissue (composed of hydrogen, carbon, nitrogen, and oxygen) adequately mimics real tissue,

and third, that assuming a homogeneous distribution of radionuclides within an organism's body is not a large source of uncertainty. This work characterizes the uncertainty each of these assumptions adds to wildlife dosimetry calculations by comparing ellipsoidal and voxel calculated dose rates for a rabbit to determine whether or not ellipsoidal models are fit for regulatory purposes. The voxel model is then used to compare homogeneous versus particulate lung dose rates resulting from exposures to small, highly radioactive fragments of material incorporated into metallic matrices (i.e. hot particles).

Voxel models are detailed anatomical phantoms that were first used for calculating radiation dose to humans, which are now being extended to nonhuman biota dose calculations. These more complex phantoms can be used to test the validity of simple ellipsoidal models by comparing dose rate estimates from each. Here we show that the ellipsoidal method provides conservative estimates of organ dose rates to small mammals. Organ dose rates were calculated for environmental source terms from Maralinga, the Nevada Test Site, Hanford and Fukushima using both the ellipsoidal and voxel techniques, and in all cases the ellipsoidal method yielded more conservative dose rates by factors of 1.2–1.4 for photons and 5.3 for beta particles. Dose rates for alpha-emitting radionuclides are identical for each method as full energy absorption in source tissue is assumed. The voxel procedure includes contributions to dose from organ-to-organ irradiation (shown here to comprise 2–50% of total dose from photons and 0–93% of total dose from beta particles) that is not specifically quantified in the ellipsoidal approach. The maximum potential uncertainty added to the wildlife dosimetry calculation

from geometry is a factor of 5.3, and the assumption is conservative (i.e. ellipsoidal model over predicts dose rates as compared to the voxel model).

In most voxel models created to date, human tissue composition and density values have been used in lieu of biologically accurate values for nonhuman biota. This has raised questions regarding variable tissue composition and density effects on the fraction of radioactive emission energy absorbed within tissues (e.g. the absorbed fraction – AF). The results of this study on rabbits indicates that the variation in composition between two mammalian tissue types (e.g. human vs rabbit bones) made little difference in self-AF (SAF) values (within 5% over most energy ranges). However, variable tissue density (e.g. bone vs liver) can significantly impact SAF values. AFs for electron energies of 0.1, 0.2, 0.4, 0.5, 0.7, 1.0, 1.5, 2.0, and 4.0 MeV and photon energies of 0.01, 0.015, 0.02, 0.03, 0.05, 0.1, 0.2, 0.5, 1.0, 1.5, 2.0, and 4.0 MeV are provided for eleven rabbit tissues. The maximum potential uncertainty added to the wildlife dosimetry calculation from tissue composition and density is a factor of 1.5, and the assumption is not conservative (i.e. ellipsoidal model under predicts dose rates as compared to the voxel model).

Hot particles are commonly found at nuclear weapons test and accident sites, and can be inhaled by wildlife. Inhaled particles often partition heterogeneously in the lungs, with aggregation occurring in the periphery of the lung, and are tenaciously retained. However, dose rates are typically calculated as if the material were homogeneously distributed throughout the entire organ. Here we quantify the variation in dose rates for alpha, beta, and gamma emitting radionuclides with particles sizes from 1-150 μm and considering three averaging volumes- the entire lung, a 10 cm^3 and a 1 cm^3 volume of tissue. Dose rates from beta-emitting particles (e.g. ^{90}Sr) were approximately one order of

magnitude higher than those from gamma-emitting radionuclides (e.g. ^{137}Cs). Self-shielding within the particle was negligible for gammas and minor for betas. For alpha-emitting particles (e.g. ^{239}Pu) it was found that particles in the respirable size range of less than 5 μm are not greatly self-shielded, but rather deposit a significant amount of energy into the surrounding tissue. As such particles may remain lodged deep in the lung, they represent a considerable contribution to long term lung dose rates. This study demonstrates one possible approach to dose assessments for biota in environments contaminated by radioactive particles, which may prove useful for those engaged in environmental radioprotection.

Overall, the voxel models provide robust dosimetry for the nonhuman mammals considered in this study, and though the level of detail is likely extraneous to demonstrating regulatory compliance today, voxel models may nevertheless be advantageous in resolving ongoing questions regarding the effects of ionizing radiation on wildlife.

©Copyright by Emily Amanda Caffrey
January 8, 2016
All Rights Reserved

Development and Application of Voxelized Dosimetric Models for Biota:
Characterization of the Uncertainty in the International Commission on Radiological
Protection's Wildlife Dosimetry System

by
Emily Amanda Caffrey

A DISSERTATION

submitted to

Oregon State University

in partial fulfillment of
the requirements for the
degree of

Doctor of Philosophy

Presented January 8, 2016
Commencement June 2016

Doctor of Philosophy dissertation of Emily Amanda Caffrey presented on January 8, 2016

APPROVED:

Major Professor, representing Radiation Health Physics

Head of the School of Nuclear Science and Engineering

Dean of the Graduate School

I understand that my dissertation will become part of the permanent collection of Oregon State University libraries. My signature below authorizes release of my dissertation to any reader upon request.

Emily Amanda Caffrey, Author

ACKNOWLEDGEMENTS

I am exceedingly grateful to the Australian Nuclear Science and Technology Organization (ANSTO), and particularly Mathew Johansen, for the opportunity to gain valuable lab and fieldwork experience during my Endeavor Fellowship. Many staff at ANSTO were critical to this work, including David P. Child, Emma Davis, Jenifer J. Harrison, and Michael A.C. Hotchkis, who provided the Maralinga site data. Thanks also to the Australian Radiation Protection and Nuclear Safety Agency for facilitating access to the Maralinga site. This work was supported financially by the Nuclear Methods in Earth Systems Project, Institute for Environmental Research, ANSTO.

At Oregon State University, I extend a heartfelt thank you to Scott Menn, Janet Knudson, Heidi Braly, Casey Mills, Shaun Bromagem, and Chris Thompson, without whom I would not have made it to the end. I thank my fellow research group members for your insights, time, and all the laughs we shared – this project would not have been possible without you all! I am indebted to my doctoral committee, Alena Paulenova, Camille Palmer, Sarah Emerson, Andreas Schmittner, and Mathew Johansen, whose hours of guidance and assistance have made this study considerably more vigorous.

My adviser, Kathy Higley, has provided me not only with financial support over the last three years, but also with excellent guidance and numerous opportunities for professional development and networking. I endeavor to follow in her footsteps in mentoring younger colleagues and future students.

Finally, I would like to express my appreciation for my husband, Jarvis, who spent countless hours helping me learn MCNP, proofreading my papers, and pouring over my data. This project would not have been possible without his unfailing support.

CONTRIBUTION OF AUTHORS

Dr. Mathew Johansen provided substantial feedback on all three manuscripts. He also performed a great deal of quality control on the Excel spreadsheets used to calculate biota dose rates, and provided access to the Maralinga site data. Jarvis Caffrey provided substantial assistance in the MCNP calculations, particularly in reference to the third manuscript. He also reviewed each manuscript and provided editorial comments. Dr. Kathryn Higley supported the research financially.

TABLE OF CONTENTS

	<u>Page</u>
1. INTRODUCTION	1
2. VOXEL MODELING OF RABBITS FOR USE IN RADIOLOGICAL DOSE RATE CALCULATIONS	3
Abstract	4
2.1. Introduction	5
2.2. Materials and Methods	6
2.3. Results and Discussion	14
2.3.1. Absorbed Fractions	15
2.3.2. Sensitivity Analysis	17
2.3.3. Life-stage Comparisons	21
2.4. Conclusions	24
2.5. Supplementary Information.....	25
2.6. References	25
3. ORGAN DOSE RATE CALCULATIONS FOR SMALL MAMMALS AT MARALINGA, THE NEVADA TEST SITE, HANFORD, AND FUKUSHIMA: A COMPARISON OF ELLIPSOIDAL AND VOXELIZED DOSIMETRIC METHODOLOGIES	26
Abstract	27
3.1. Introduction.....	28
3.2. Materials and Methods.....	29
3.2.1. Organ dose rate comparison methodology	30
3.2.2. Rabbit voxel model DCFs	31
3.2.3. Ellipsoidal model DCFs.....	32
3.3.4. Sites and Data	32
3.3.4.1. Maralinga	33
3.3.4.2. Nevada Test Site	35
3.3.4.3. Hanford	36
3.3.4.4. Fukushima.....	36
3.3. Results and Discussion	37
3.3.1. K-Ratios	37
3.3.2. Organ Dose Rates	39

TABLE OF CONTENTS (Continued)

	<u>Page</u>
3.3.3. ¹³⁷ Cs at NTS, Hanford, Maralinga	43
3.3.4. ^{134, 137} Cs depuration at Fukushima	43
3.3.5. ⁹⁰ Sr at NTS, Hanford, and Maralinga	45
3.3.6. ^{239, 240} Pu at NTS and Maralinga	47
3.3.7. ²⁴¹ Am at NTS	47
3.3.8. Utility of organ-specific dose rates	47
3.4. Conclusions	49
3.5. Supplementary Information.....	50
3.6. References	50
4. COMPARISON OF HOMOGENEOUS AND PARTICULATE LUNG DOSE RATES FOR SMALL MAMMALS	51
Abstract.....	52
4.1. Introduction.....	53
4.2. Materials and Methods.....	55
4.3. Results and Discussion	60
4.3.1. Photon Emitters	60
4.3.2. Electron Emitters	61
4.3.3. Alpha Emitters.....	61
4.4. Conclusions.....	65
4.5. References.....	66
5. CONCLUSIONS	67
6. REFERENCES	69
7. APPENDICIES.....	76
7.1. APPENDIX A – Rabbit tissue density and composition data.....	77
7.2. APPENDIX B – Photon absorbed fractions for adult <i>Lepus californicus</i>	83
7.3. APPENDIX C - Electron absorbed fractions for adult <i>Lepus californicus</i>	95
7.4. APPENDIX D - Photon absorbed fractions for juvenile <i>Lepus californicus</i> .	107
7.5. APPENDIX E - Electron absorbed fractions for juvenile <i>Lepus californicus</i> 119	119
7.6. APPENDIX F – Photon self-absorbed fractions for adult versus juvenile <i>Lepus californicus</i>	131

TABLE OF CONTENTS (Continued)

	<u>Page</u>
7.7. APPENDIX G – Electron self-absorbed fractions for adult versus juvenile <i>Lepus californicus</i>	133
7.8. APPENDIX H – Electron and photon self-absorbed fractions for the sensitivity analysis on tissue composition in adult <i>Lepus californicus</i>	136
7.9. APPENDIX I – Electron and photon self-absorbed fractions for the sensitivity analysis on tissue density in adult <i>Lepus californicus</i>	139
7.10. APPENDIX J – Dose conversion factors for adult <i>Lepus californicus</i> derived from voxel model.....	147
7.11. APPENDIX K – Dose conversion factors for adult <i>Lepus californicus</i> derived from ERICA Version 1.2	148
7.12. APPENDIX L – NTS, Hanford, Fukushima radionuclide concentration data	149
7.13. APPENDIX M – NTS, Hanford, Fukushima, Maralinga organ dose rates....	150

LIST OF FIGURES

<u>Figure</u>	<u>Page</u>
Figure 2-1: Adult <i>Lepus californicus</i> anatomy shown on a sagittal CT scan slice.....	8
Figure 2-2: 3D rendering of adult rabbit model from 3D Doctor	9
Figure 2-3: Adult rabbit AFs in various organs/tissues given a photon source in liver....	16
Figure 2-4: Ratio of photon SAFs for the sensitivity analysis on composition. Ratio is rabbit tissue SAF to human tissue SAF. A ratio of unity indicates measured value = standard value	20
Figure 2-5: Electron SAF for the sensitivity analysis on density	21
Figure 2-6: Electron SAFs for the adult and juvenile rabbit reproductive organs.....	22
Figure 3-1: K-ratios for all radionuclides and segments considered. A K-ratio of 1 indicates that dose rates predicted by the voxel model are identical to those predicted by the ellipsoidal model. K < 1 indicates the ellipsoidal model is conservative.	38
Figure 3-2: Voxel dose rate versus mass-ratio dose rate for: $^{134,137}\text{Cs}$, ^{137}Cs (blue); ^{90}Sr (orange); ^{241}Am , $^{239,240}\text{Pu}$, $^{238,239}\text{Pu}$ (green). Letters correspond to organs as follows: bone=B, heart=H, kidneys=K, liver=V, lungs=L, feces=F, testes=T, GI tract=G, stomach contents=C, skin=S, and muscle=M.	40
Figure 3-3: $^{134,137}\text{Cs}$ dose rates in various organ segments for small rodents at Fukushima calculated using voxel and mass-ratio methods.....	45
Figure 4-1: Rabbit voxel model with alpha particle tracks in lung tissue shown to approximately scale.	56
Figure 4-2: Lung dose rates for various particle sizes assuming placement of the particle deep within the lung. Closed symbols are for ^{137}Cs , open symbols for ^{90}Sr . The models compare the same activity in the lung, either distributed homogeneously or contained within a single particle.	60
Figure 4-3: ^{239}Pu energy deposition in the source particle and a 1 cm ³ dose volume as a percent of initial energy.	62
Figure 4-4: Dose rates for 1 cm ³ (closed symbols) and 100 μm^3 (open symbols) dose volumes assuming 1%, 10%, and 50% of the particle is plutonium. Here the amount of plutonium in each particle is no longer a constant, but increases with particle size.....	64

LIST OF TABLES

<u>Table</u>	<u>Page</u>
Table 2-1: Organ segment details	10
Table 2-2: Human tissue equivalents	18
Table 3-1: Summary of data used in this study.....	33
Table 3-2: $^{134},^{137}\text{Cs}$ depuration at Fukushima demonstrated by muscle tissue dose rates at three time intervals at three time intervals in a contaminated forest outside Fukushima.	44
Table 3-3: ^{90}Sr bone dose rates for NTS, Hanford, and Maralinga.	46
Table 3-4: Internal whole body dose rates (in $\mu\text{Gy/day}$) for rabbits at Maralinga, NTS, and Hanford calculated using ERICA Version 1.2.....	48

LIST OF APPENDICES

	<u>Page</u>
APPENDIX A – Rabbit tissue density and composition data	77
APPENDIX B – Photon absorbed fractions for adult <i>Lepus californicus</i>	83
APPENDIX C - Electron absorbed fractions for adult <i>Lepus californicus</i>	95
APPENDIX D - Photon absorbed fractions for juvenile <i>Lepus californicus</i>	107
APPENDIX E - Electron absorbed fractions for juvenile <i>Lepus californicus</i>	119
APPENDIX F – Photon self-absorbed fractions for adult versus juvenile <i>Lepus californicus</i>	131
APPENDIX G – Electron self-absorbed fractions for adult versus juvenile <i>Lepus californicus</i>	133
APPENDIX H – Electron and photon self-absorbed fractions for the sensitivity analysis on tissue composition in adult <i>Lepus californicus</i>	136
APPENDIX I – Electron and photon self-absorbed fractions for the sensitivity analysis on tissue density in adult <i>Lepus californicus</i>	139
APPENDIX J – Dose conversion factors for adult <i>Lepus californicus</i> derived from voxel model.....	147
APPENDIX K – Dose conversion factors for adult <i>Lepus californicus</i> derived from ERICA Version 1.2.....	148
APPENDIX L – NTS, Hanford, Fukushima radionuclide concentration data	149
APPENDIX M – NTS, Hanford, Fukushima, Maralinga organ dose rates	150

1. INTRODUCTION

Generally, radiation dose to nonhuman biota from environmental source terms are calculated using dose conversion factors (DCFs), which are absorbed dose rates per unit activity concentration ($\mu\text{Gy d}^{-1}$ per Bq kg^{-1}). The current method for calculating DCFs recommended by the International Commission on Radiological Protection (ICRP), and implemented in the ERICA Integrated Approach [1], utilizes Monte Carlo simulations of an ellipsoidal organism geometry with homogeneously distributed radioactivity throughout [2], [3]. These models are composed of four-component human tissue of unit density. This presents three major assumptions that this work seeks to quantify:

- (1) That any organism can be represented by a simplified dosimetric phantom;
- (2) That for dosimetric purposes, four-component human tissue of unit density (hydrogen, carbon, nitrogen, and oxygen) adequately mimics real tissue;
and
- (3) That assuming a homogeneous distribution of radionuclides within an organism's body is not a large source of uncertainty.

In order to characterize the uncertainty associated with each assumption, two models of a rabbit were created. A rabbit was selected due to its ubiquity in a wide variety of environments, as well as the plethora of data present on radionuclide distribution in rabbits present at nuclear weapons test and accident sites such as Hanford and Maralinga. ERICA Version 1.2 was used to create an ellipsoidal model that corresponded precisely to the size and mass of the rabbit used to construct the voxel model, thus eliminating one

potential source of discrepancy. The first paper published in this work (Chapter 2) describes the creation of the voxel model, and provides a sensitivity analysis on tissue composition and density between rabbits and humans. The second paper (Chapter 3) provides dose rate calculations for small mammals from environmental data across four sites - the Nevada Test Site, Maralinga, Hanford, and Fukushima, for environmentally relevant concentrations of ^{134}Cs , ^{137}Cs , ^{238}Pu , ^{239}Pu , ^{240}Pu , ^{90}Sr , and ^{241}Am . It compares dose calculation methodologies (mass-ratio/ellipsoidal and voxel) for the rabbit, and quantifies organ-to-organ (termed crossfire) contributions to dose which is included in voxel, but not ellipsoidal models. The third paper (Chapter 4) uses the voxel model to determine dose rates of localized alpha, beta, and gamma emitting hot particles on small mammal lung tissue including the effects of self-shielding, and compares homogeneous and particulate dose rates to determine the extent to which traditional models may misrepresent dose from particles. These results are then placed in a regulatory context to determine if ellipsoidal models are sufficient to demonstrate that the environment is sufficiently protected from radiation.

2. VOXEL MODELING OF RABBITS FOR USE IN RADIOLOGICAL DOSE RATE CALCULATIONS

Caffrey, E.A., Johansen, M.P., Higley, K.A.

Article and electronic supplementary information can be found online at:
<http://www.sciencedirect.com/science/article/pii/S0265931X15001265>

and

https://www.dropbox.com/sh/2z8z88gx0fb1otg/AAAppfhRa8_Np2e4eQXKM5maa?dl=0

Caffrey E.A., Johansen M.P., Higley K.A., 2015. Voxel Modeling of Rabbits for Use in Radiological Dose Rate Calculations. *Journal of Environmental Radioactivity*.
doi:10.1016/j.jenvrad.2015.04.008.

Abstract

Radiation dose to biota is generally calculated using Monte Carlo simulations of whole body ellipsoids with homogeneously distributed radioactivity throughout. More complex anatomical phantoms, termed voxel phantoms, have been developed to test the validity of these simplistic geometric models. In most voxel models created to date, human tissue composition and density values have been used in lieu of biologically accurate values for nonhuman biota. This has raised questions regarding variable tissue composition and density effects on the fraction of radioactive emission energy absorbed within tissues (e.g. the absorbed fraction - AF), along with implications for age-dependent dose rates as organisms mature. The results of this study on rabbits indicates that the variation in composition between two mammalian tissue types (e.g. human vs rabbit bones) made little difference in self-AF (SAF) values (within 5% over most energy ranges). However, variable tissue density (e.g. bone vs liver) can significantly impact SAF values. An examination of differences across life-stages revealed increasing SAF with testis and ovary size of over an order of magnitude for photons and several factors for electrons, indicating the potential for increasing dose rates to these sensitive organs as animals mature. AFs for electron energies of 0.1, 0.2, 0.4, 0.5, 0.7, 1.0, 1.5, 2.0, and 4.0 MeV and photon energies of 0.01, 0.015, 0.02, 0.03, 0.05, 0.1, 0.2, 0.5, 1.0, 1.5, 2.0, and 4.0 MeV are provided for eleven rabbit tissues. The data presented in this study can be used to calculate accurate organ dose rates for rabbits and other small rodents; to aide in extending dose results among different mammal species; and to validate the use of ellipsoidal models for regulatory purposes.

2.1. Introduction

Voxel models allow for organ dose rate calculations and the consideration of organ-to-organ contributions to dose. Generally, radiation dose to nonhuman biota from environmental source terms are calculated using dose conversion factors (DCFs), which are absorbed dose rates per unit activity concentration ($\mu\text{Gy d}^{-1}$ per Bq kg^{-1}). The current method for calculating DCFs recommended by the International Commission on Radiological Protection (ICRP), and implemented in the ERICA Integrated Approach [1], utilizes Monte Carlo simulations of an ellipsoidal organism geometry with homogeneously distributed radioactivity throughout [2], [3]. Current research efforts are focused on creating voxel phantoms, which include distinct organs and tissues, to determine the degree of uncertainty introduced when using the simplifying assumptions of ellipsoidal shapes and homogeneous radionuclide distributions (see Ruedig et al. 2014 for details) and to evaluate if voxel DCFs are consistent with those from the simple models developed by the ICRP [2]. Voxel models completed to date and utilized in an environmental context include a crab, flatfish, trout, rat, mouse, and frog [5]–[9]. Additional voxel models available to interested researchers include, but are not limited to, Digimouse, and two different canine models [10]–[12]. Additionally, there are two “compromise” options between the basic single ellipsoid models and voxel models that are worth mentioning. The first is the stylized model. In stylized models, pertinent organs are included as ellipsoids (see Martinez et al. 2014 for an example of a stylized model). This has the advantage of allowing researchers to calculate dose to sensitive organs, while still maintaining much of the simplicity of using ellipsoidal models. The second is a technique developed by Gómez-Ros et al. (2008) wherein organ dose rates can be

obtained by multiplying whole body dose rates by a ratio of the whole body mass to the mass of the organ of interest.

Voxel models are particularly useful in scenarios in which the radionuclides disproportionately partition into the specific organs/tissues of mammals after internalization [14]–[16]. For example, proportionally high accumulation of plutonium in bone ($83\% \pm 10\%$) compared to that in liver ($6\% \pm 6\%$) of mammalian wildlife at the former British nuclear weapons test site at Maralinga, Australia [17]. These data for wildlife contrast with that from mainly laboratory experiments summarized by the ICRP (45-50% bone, 30-45% liver) [15], and organ-specific dose models may provide insight into the dose implications of the higher accumulation in bone.

In this study, adult and juvenile rabbit models were created to answer longstanding questions regarding voxel modeling. First, the models were used to examine the effects of variable tissue composition and density on absorbed fraction (AF) values to determine the validity of using human data in nonhuman mammalian models. Second, the models were used to examine variations across life-stages. Adult versus juvenile self-AFs (SAF; source and target are the same organ/tissue) were compared across all major organ systems. An in-depth analysis was performed on internal electron emitters in testes and ovaries of varying sizes to elucidate the effects of organ size on SAF value.

2.2. Materials and Methods

Two black-tailed jackrabbits (*Lepus californicus*) were obtained post-mortem, an adult male weighing approximately 2 kg (4.5 lb), and a juvenile female weighing about 0.8 kg

(1.8 lb). Computed tomography (CT) scans were conducted at the Oregon State University School of Veterinary Medicine on a Toshiba Aquilion 64 slice machine. Axial plane images were used for image reconstruction for both specimens. Voxel dimensions of the adult were 0.679 mm x 0.679 mm x 2 mm, resulting in a 3D pixel matrix of 276 rows x 276 columns x 202 planes. Voxel dimensions of the juvenile were 0.395 mm x 0.395 mm x 2 mm, resulting in a 3D pixel matrix of 268 rows x 268 columns x 141 planes. Figure 2-1 depicts adult rabbit anatomy, shown on a sagittal slice of the CT scan.

Voxel phantom geometry is created via organ segmentation performed on the axial CT scan slices. Identifiable organs were manually contoured using 3D Doctor Software¹, and a 3D model was created (see Figure 2-2).

¹ Able Software Corp. 5 Appletree Lane, Lexington MA 02420. <http://www.ablesw.com/3d-doctor/>.

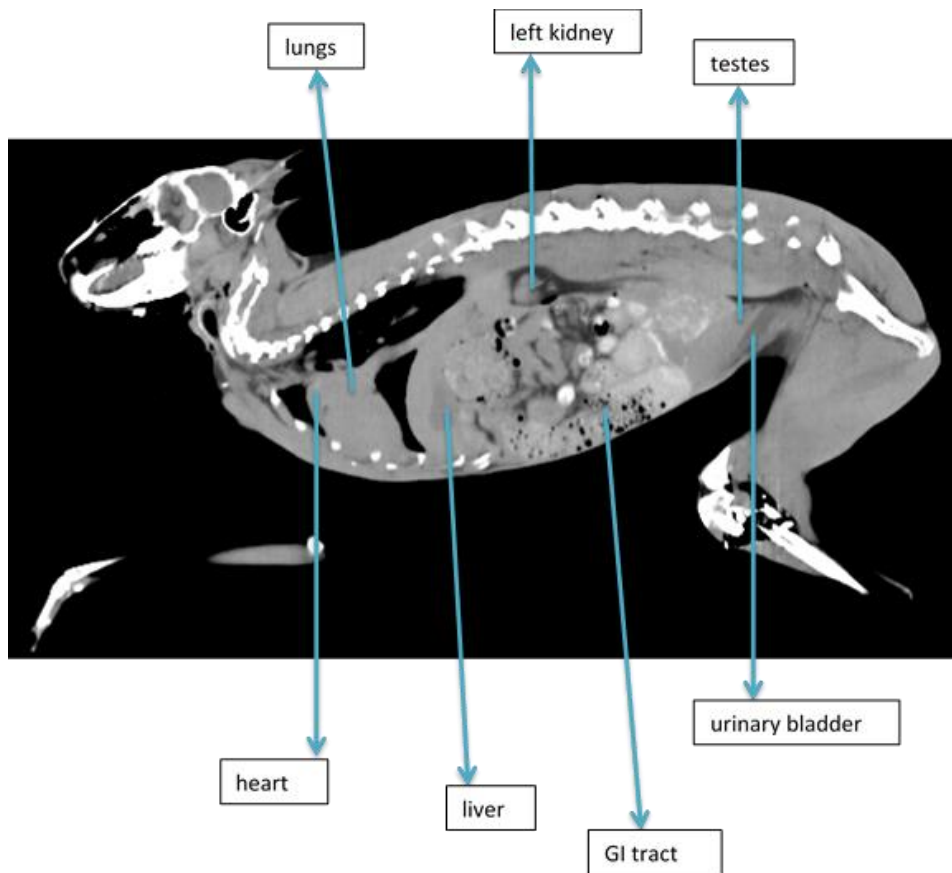


Figure 2-1: Adult *Lepus californicus* anatomy shown on a sagittal CT scan slice

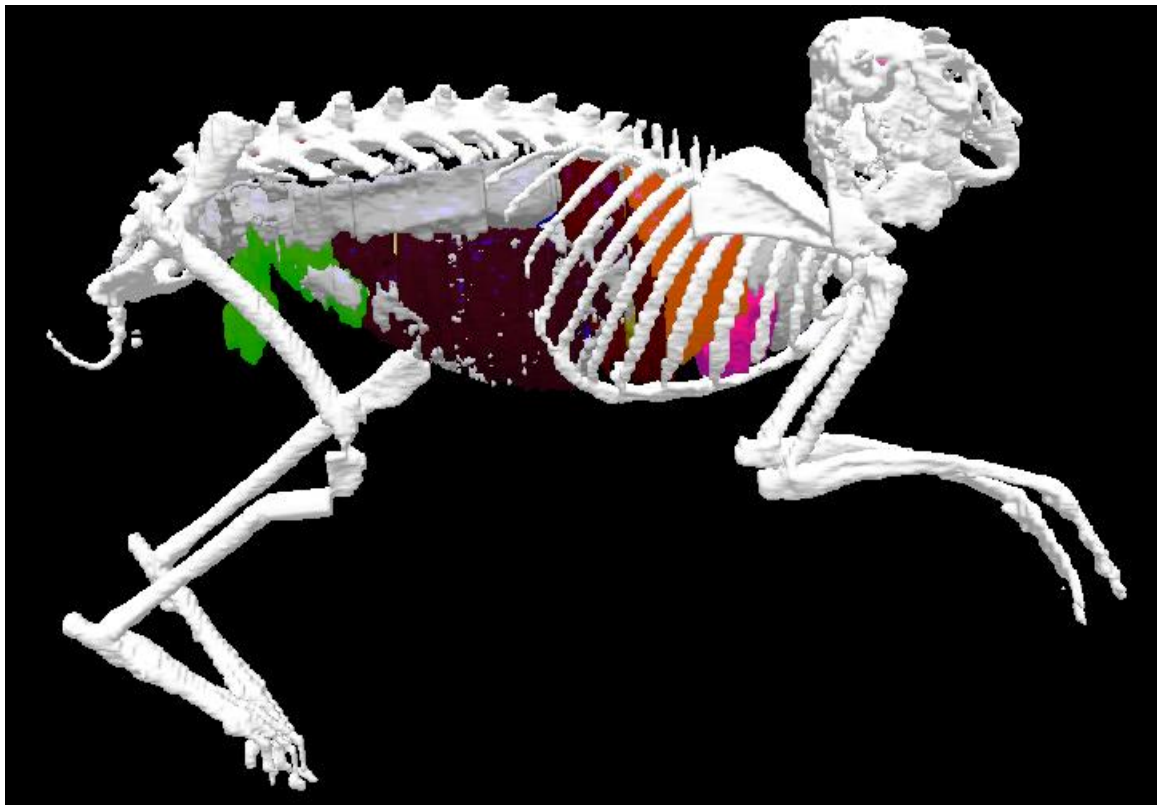


Figure 2-2: 3D rendering of adult rabbit model from 3D Doctor

Identifiable organs included the following for both the adult and the juvenile: bone, bone marrow, liver, gallbladder, testes/ovaries, lungs, kidneys, heart, gastrointestinal (GI) tract, stomach contents, feces, brain, fat, blood, muscle tissue (not shown in Figure 2-2), and skin (also not shown in Figure 2-2; see

Table 2-1 for organ segment details). The urinary bladder of the adult specimen was full and therefore visible on the CT scan, and was also segmented. Segment data is exported from 3D Doctor via a boundary file. The boundary file specifies the start and stop points of each contoured organ or tissue on each slice of the CT scan. This information is

imported into Lattice Tool² (also known as Voxelizer) [18], and converted into a repeated structures lattice format for use in Monte Carlo N-Particle (MCNP) simulations [19]. Once converted to MCNP format, tissue density and composition information can be added. Previous voxel models have utilized human tissue compositions due to the lack of available organism tissue compositions [5], [9], [20]. In order to obtain realistic organism tissue composition and density, and to avoid adding additional uncertainty to the dose calculations, both rabbits were dissected post CT scans, and an elemental analysis performed on selected organs.

Table 2-1: Organ segment details

Tissue or Organ and Inclusive Sections		Adult or Juvenile	Organ	Density³	Composition⁴
			Mass (g)	(g/cm³)	
Testes	testes	adult	28.3	1.1 (m)	m
Fat	removable fat content	adult	25.0	0.92 ⁵	m
Liver	liver and gallbladder	adult	114.0	1.1 (m)	m
Kidneys	kidneys	adult	11.1	1.1 (m)	m
Muscle	muscle and connective tissue	adult	47.4	1.1 (m)	m

² Human Monitoring Laboratory, Radiation Surveillance Division, Radiation Protection Bureau, 775 Brookfield Road A.L. 6302D1, Ottawa, Ontario K1A 1C1, Canada.

³ m=measured via displacement; otherwise cited. All ICRP values were obtained from NIST 2010.

⁴ m=measured via EOA; h=human value used.

⁵ ICRP adipose tissue.

Urinary bladder	bladder sac and contents	adult	2.3	1.0	m (unity)
Feces	recoverable feces in pellet form	adult	14.4	1.0	m (unity)
Stomach contents	removable contents	adult	19.9	1.0	m (unity)
GI tract	stomach, cecum, colon, large and small intestines	adult	116.3	1.0	m (unity)
Lungs	lungs and trachea/esophagus	adult	55.3	1.05 ⁶	m
Heart	heart, pulmonary vasculature, and vena cava	adult	21.6	1.2 (m)	m
Bone	left femur	adult	11.5	1.5 (m)	m
Brain	brain; not removed in dissection	adult	9.7 ⁷	1.03 ⁸	h ⁶
Skin	Skin, fur, ears, feet	adult	214.4	1.0 ⁹	h ¹⁰
Ovaries	ovaries (not recovered in dissection)	juvenile	0.2 ⁷	1.0	h ¹¹ (unity)
Fat	Removable fat content	juvenile	5.4	0.92 ³	h ³
Liver	Liver and gallbladder	juvenile	50.9	1.1 (m)	m

⁶ ICRP lung.⁷ From 3D Doctor model.⁸ ICRP brain.⁹ ICRP skin.¹⁰ Data is from NIST 2010¹¹ Woodard & White 1986.

Kidneys	kidneys	juvenile	8.4	1.1 (m)	m
Muscle	Muscle and connective tissue	juvenile	21.9	1.1 (m)	m
Feces	Recoverable feces (e.g. pellet form)	juvenile	13.6	1.0 (unity)	m
Stomach contents	Removable contents	juvenile	16.0	1.0 (unity)	m
GI tract	stomach, cecum, colon, large and small intestines	juvenile	62.0	1.0 (unity)	m
Lungs	Lungs and trachea/esophagus	juvenile	10.6	1.05 ⁴	m
Heart	Heart and pulmonary vasculature	juvenile	5.6	1.2 (m)	m
Bone	Left femur	juvenile	5.2	1.3 (m)	m
Brain	Brain (not removed in dissection)	juvenile	5.6 ⁶	1.03 ⁶	h ⁶
Skin	Skin, fur, ears, feet	juvenile	88.6	1.0 ⁷	h ⁸

The displacement technique used in this work was developed specifically for this study, drawing information from a study by Webb (1990) that measured the density of benthic fish organs. A Pyrex graduated cylinder was filled with plain water. Organs were carefully lowered and completely submerged into water using tweezers, and gently massaged as needed to remove air bubbles. Water displacement was recorded. This was repeated for all organs excluding the GI tract, stomach contents, and feces of both

specimens, the juvenile spleen, and the adult urinary bladder. For muscle density calculations, a large section of the inner thigh of each rabbit was used for displacement measurements. Density calculated for muscle samples was assumed to apply to the whole body muscle area [21]. The left femur of each specimen was used to obtain a reasonable value for rabbit bone density.

Organ composition was determined using the elemental analyzer facility in the Oregon State University College of Earth, Ocean, and Atmospheric Sciences. Elemental organic analysis (EOA) is the determination of the elemental composition of organic compounds [22]. With the exception of the brain and skin of both specimens, and the ovaries of the juvenile, small samples of each organ for both the adult and juvenile were removed and placed into a sample tray for analysis. Three individual samples from the inside of each organ were taken to help avoid cross-contamination from other organs or body fluids. This was completed by slicing open each organ, and then using clean tweezers and scissors to take each sample, cutting a piece of the organ and placing it in a separate bin in the sample tray, thus ensuring that each sample is a representation of the organ. As there were no significant outliers, composition averages of all three tissues were used. The machine used in this study is a Carlo-Erba NA 1500 analyzer, designed for the simultaneous determination of total hydrogen, carbon, nitrogen, and oxygen in a wide variety of both organic and inorganic samples [23]. Oxygen is calculated via subtraction, and human trace metal amounts are used where possible as obtaining actual rabbit trace metal data is tedious and expensive. With the exception of bone, rabbit tissue is essentially a less fatty version of human tissue, and as trace metals account for less than

one percent of the total composition, it is expected that this assumption will not substantially increase the error.

Table 2-1 gives details of each organ segment.

After sample densities and compositions were determined, particle transport simulations were performed using MCNPX [19]. The default electron energy cutoff of 1 keV was used, and no variance reduction techniques were employed. The term “source segment” refers to the organ from which the simulated particles were emitted, and “target segment” refers to the organ or tissue in which these particles deposited energy. Several simulations were run, each with a different source segment, until energy deposition data had been collected for all segments via the energy deposition tally, as done in previous works [5], [7]. Particle transport was run for electron energies of 0.1, 0.2, 0.4, 0.5, 0.7, 1.0, 1.5, 2.0, and 4.0 MeV and photon energies of 0.01, 0.015, 0.02, 0.03, 0.05, 0.1, 0.2, 0.5, 1.0, 1.5, 2.0, and 4.0 MeV. The radionuclides were considered to be distributed homogeneously in each source segment. Absorbed fractions (AFs) are the average fraction of a particle’s energy deposited in a target tissue. AFs are tabulated for each source-target segment combination (see supplementary information online).

2.3. Results and Discussion

All segmented organs were used as targets in both the adult and juvenile models. With the exception of the fat, blood volume, brain, and urinary bladder (adult rabbit only), all organs were also used as sources in both the adult and juvenile models. Caution should be exercised when using AF values given for the fat and blood volumes, as these are likely

to vary among individuals in a given population of rabbits. Additionally, it should be noted that the skin is simply ICRP human skin placed over the entire model, and does not account for the rabbit's fur. The external value listed as a target is a measure of the amount of energy that escapes the rabbit entirely. All tabulated AF data have coefficients of variance (COV) of less than 10%. For AFs with COV between 5 and 10%, the AF is underlined in the data tables as a cautionary note.

2.3.1. Absorbed Fractions

AF results for a photon source in the liver of the adult rabbit are shown in Figure 2-3. Extensive tabular data that detail AFs as a function of source, target, energy, and radiation type for both the adult and juvenile rabbit are provided as electronic supplementary information in the online article.

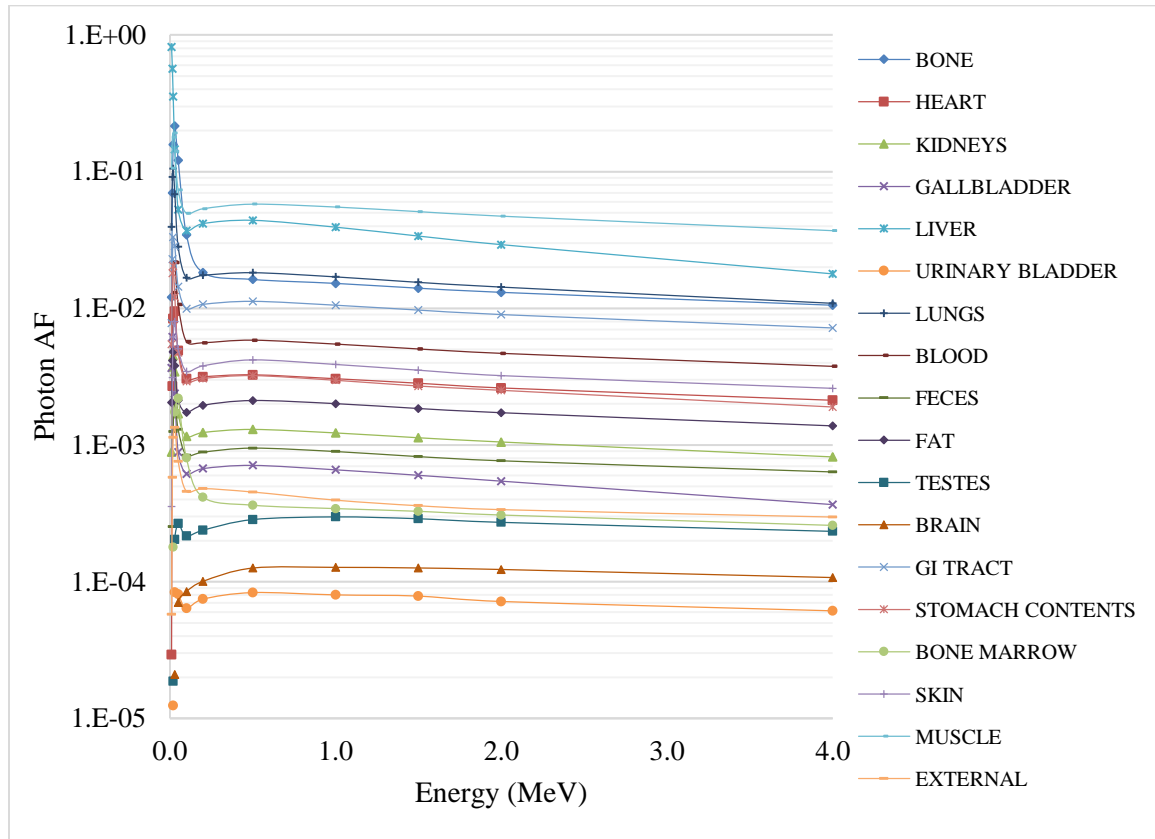


Figure 2-3: Adult rabbit AFs in various organs/tissues given a photon source in liver

All photon AF data for both the adult and juvenile follow the general trends seen in Figure 2-3. For photons, a small fraction of source particle energy is deposited in the source organ, with the remainder deposited in other organs or escaping the rabbit altogether. As photon energy is increased, more particles escape the source organ without interacting. Source organ location relative to the target, mass, and density are highly relevant parameters in determining energy deposition, but maximum deposition is predominantly influenced by the distance between source and target, as charged particle buildup reaches a maximum value for a given energy at a particular depth [7]. For the example of a photon-emitting radionuclide in liver, AFs were, in decreasing order:

muscle, liver, bone, lungs, GI tract, and then the remainder over the range of most energies.

In human dosimetry, electron AFs are generally assumed to be unity, where all electron energy is absorbed in the source organ [7]. As we consider smaller and smaller organisms, this assumption becomes less robust. At the lowest electron energies, total absorption in the source tissue is reasonable, but for high energy electrons, it becomes increasingly relevant to consider electron energy deposited in adjacent organs [3], [13]. Assuming similar tissue densities, the maximum energy deposition is heavily dependent on target size. Generally, the amount of energy that will escape is a function of organ size, geometry, and density. For the example of an electron-emitting radionuclide in liver, AFs were, in decreasing order: liver, muscle, lungs, bone and GI tract, then the remainder over the range of most energies.

2.3.2. Sensitivity Analysis

A sensitivity analysis on both tissue composition and density was performed for the adult rabbit. For composition data, it was desired to determine the difference in self-AF (i.e. source and target are the same organ or tissue) values for the rabbit when realistic tissue compositions (i.e. the composition determined by EOA) were used as compared to using the most similar human tissue, e.g. striated muscle tissue for the heart. For density, it was desired to investigate the effects of variable density on the SAF values. Seven tissues were included in the sensitivity analysis: bone (including marrow), liver (including gallbladder), testes, lungs, kidneys, muscle tissue, and heart. Electron energies of 0.1, 0.5, 1.0, and 1.5 MeV and photon energies of 0.01, 0.1, 0.5, 1.0, 1.5, 2.0, and 4.0 MeV were used for the analysis. Table 2-2 details the human tissue reference sources used, and the

range of density values considered in the analysis. Tabular data for both composition and density is provided as electronic supplementary material.

Table 2-2: Human tissue equivalents

Organ/Tissue	Human Tissue	Measured	Range of	Increment¹³
	Equivalent¹²	density	density values	(g/cm³)
		(g/cm³)	(g/cm³)	
Bone and marrow	ICRP cortical bone	1.5	1.0 – 2.0	0.2
Liver and gallbladder	ICRU ¹⁴ 4-component	1.1	0.9 – 1.3	0.1
Testes	ICRP testes	1.1	0.9 – 1.3	0.1
Lungs	ICRP lung	0.9 ¹⁵	0.9 – 1.1	0.1
Kidneys	ICRU 4-component	1.1	0.9 – 1.3	0.1
Muscle tissue	ICRP skeletal muscle	1.1	0.9 – 1.3	0.1
Heart	ICRU striated muscle	1.2	0.9 - 1.4	0.1

¹² Data is from NIST 2010.

¹³ Increment used for sensitivity analysis on density (e.g. bone densities ranged from 1.0 – 2.0 g/cm³ in 0.2 g/cm³ increments).

¹⁴ ICRU is the International Commission on Radiation Units and Measurements.

¹⁵ ICRP given value of 1.05 used in model.

SAF ratios for measured rabbit tissues to the standard tissues (i.e. the human equivalent listed in Table 2-2) for photon and electron sources are calculated. A ratio of greater than one (e.g. above the measured=standard line on Figure 2-4) indicates that the SAF for the measured composition is greater than that for the human tissue equivalent. In general, the ratios are fairly close to one, indicating that mammalian tissue composition differences investigated in this study do not strongly influence SAF values. Bone is the only tissue in which the measured SAF value is slightly higher than the standard human value, possibly because rabbit bones have significantly more carbon and less oxygen than human bones. In general, rabbit tissues have a lower z-effective and a greater mean free path than their human equivalents. This is especially prominent at lower photon energies, where we see more of the initial energy escaping the organ composed of rabbit tissue (for energies < 0.5 Mev, Figure 2-4). Conversely, at higher energies, more photons traverse the tissue without interacting, and the SAF ratios diverge slightly from unity (Figure 2-4). Full energy absorption in the source volume is seen for low energy electrons, as expected due to their limited range. As incident electron energy is increased, more energy escapes the source organ and is deposited in adjacent tissues.

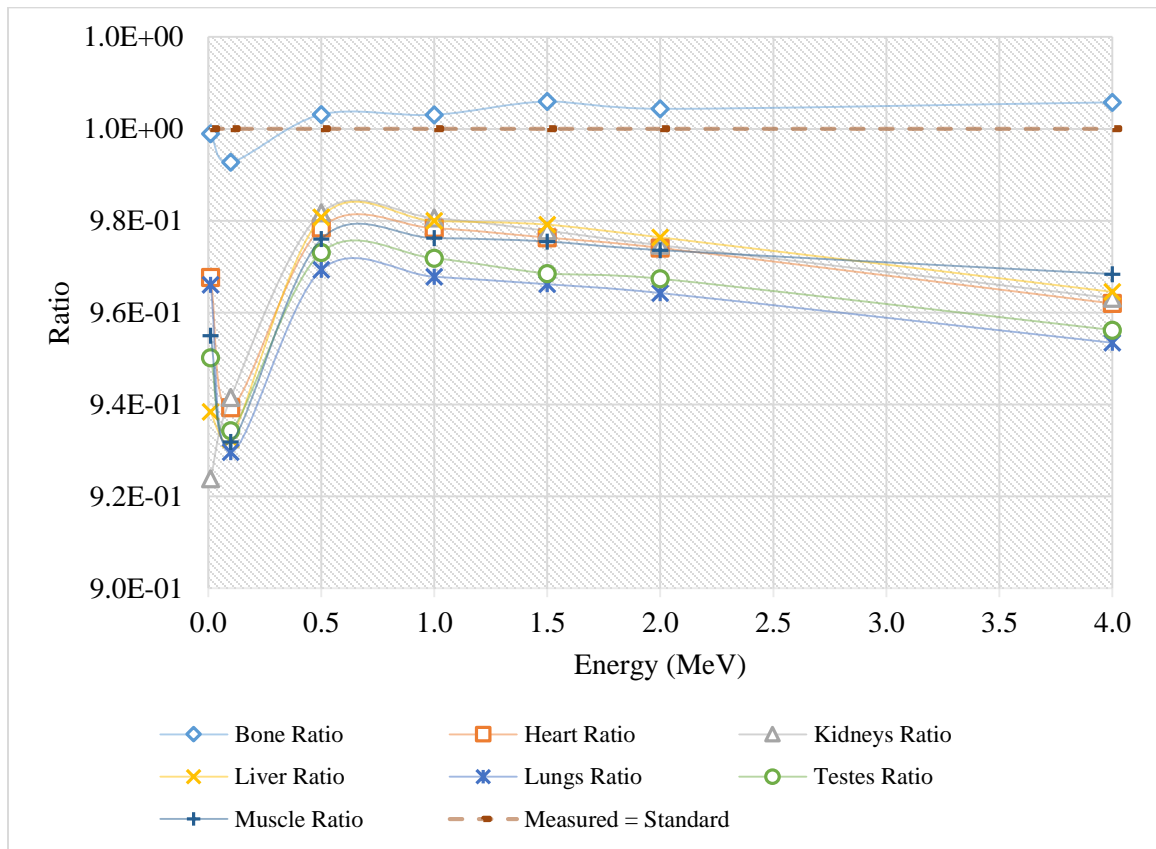


Figure 2-4: Ratio of photon SAFs for the sensitivity analysis on composition. Ratio is rabbit tissue SAF to human tissue SAF. A ratio of unity indicates measured value = standard value

Generally, as density increases, SAF values also increase as less energy is able to escape the source volume. This effect is seen more prominently in the electron SAF values, as electron range is strongly influenced by target material density (Figure 2-5). As juvenile rabbit bone density is lower than that of the adult rabbit (1.2 and 1.5 g/cm³ respectively), this pattern of energy deposition with density indicates that less energy is likely to be deposited in the bone of the juvenile rabbit, and more likely to irradiate the surrounding

tissues. This may also have implications in human bone dosimetry, as children's bones are significantly less dense than their adult counterparts.

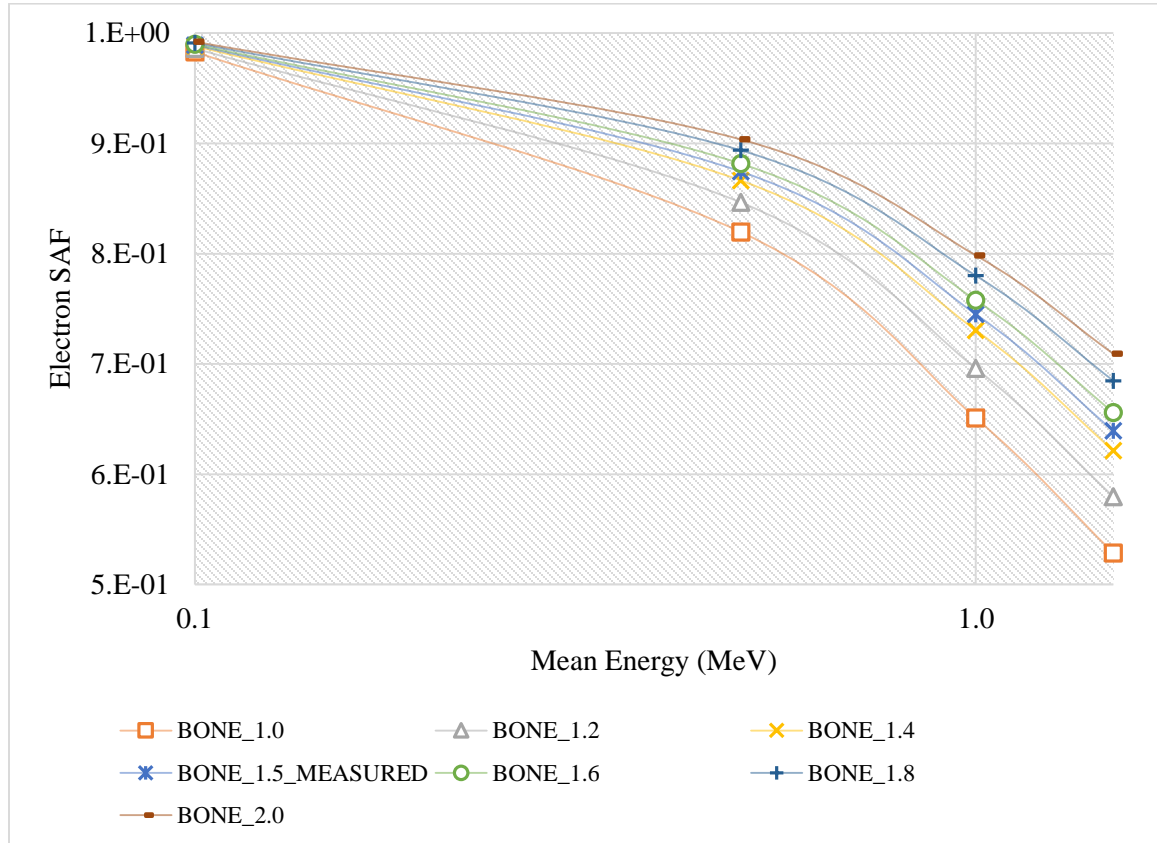


Figure 2-5: Electron SAF for the sensitivity analysis on density

2.3.3. Life-stage Comparisons

Photon and electron SAFs for the adult and juvenile rabbit were plotted to compare life-stages which reflect changes in organ/tissue sizes, densities, and to some degree their relative geometries. For photon SAFs, values were quite similar for all major organ systems, e.g., the liver, kidneys, lungs, heart, and GI tract (see electronic supplementary materials for tabular and graphical data). Adult SAF values were generally higher due to

the larger physical size and higher mass of the adult specimen. Major differences in SAF values were observed when comparing adult testes to the juvenile ovaries (see Figure 2-6). This is likely due to the small size of the juvenile ovaries.

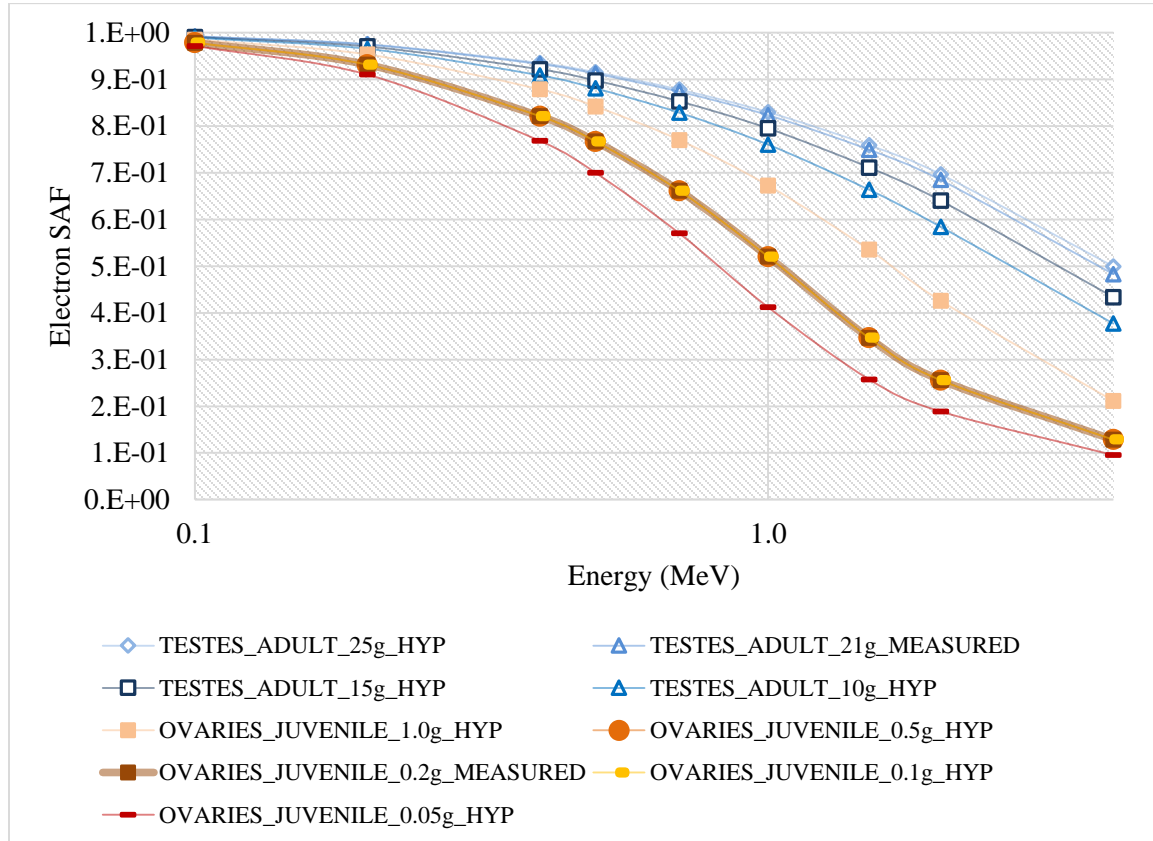


Figure 2-6: Electron SAFs for the adult and juvenile rabbit reproductive organs

While some studies have provided AFs for internal electron sources (e.g. [8], [9]), only one has specifically examined the effect of size. Martinez et al. [13] examined size effects in a freshwater organism, the rainbow trout, using ellipsoidal, stylized, and voxelized organism geometries. To explore this size effect for mammals for internal electron sources, a range of testis masses (adult rabbit), and ovary masses (juvenile rabbit) were

entered into the rabbit models to represent various life-stages. Testes were selected for detailed analysis because in general, reproductive organs are considered to be the most sensitive, and are the most relevant when considering the health of any given population. Testis size was altered in 3D Doctor Software to obtain specific volumes that were then correlated back to mass. Organs never overlapped, and all other organs were kept the same size. The juvenile rabbit ovaries were generally spherical, but the adult testes were contoured from the CT image. The measured mass of the adult testes was approximately 21 grams, and SAF values were calculated for testes of mass 25, 15, and 10 grams. The mass of the juvenile ovaries was determined to be 0.2 grams, and SAF values were additionally calculated for ovaries of mass 1.0, 0.5, 0.1, and 0.05 grams. SAF values generally increase with organ size, particularly through early growth ranges (Figure 2-6). This is due to more efficient capture of emission energies as the organ develops. The largest increases occur as the organ grows through its early (smaller) size increments (e.g. 0.05g – 0.1g ovaries). The SAF values reduce with increasing energies non-linearly (Figure 2-6). Over most energies, dose will increase with each stage of development for internal electron emitters located either within or proximally to the testes or ovaries, as more energy is deposited as the rabbit matures. Tabular data is provided as electronic supplementary material for adult verse juvenile SAFs.

Voxel models represent a significant improvement in realism over the traditional ellipsoidal model. This increase in complexity and realism comes at a cost, as voxel models are time consuming and laborious to construct. Readily available, user-friendly tools such as ERICA or RESRAD-BIOTA may prove to be sufficiently accurate given the uncertainties associated with environmental data. However, voxel models may prove

to be advantageous in dose-effect studies in illuminating underlying causes of radiation dose effects. Additionally, voxel models can account for organ-to-organ contributions to dose that may be significant in certain scenarios. A comparison of voxel verses ellipsoidal models has been completed for aquatic species [4], with the conclusion that the two models agree within a factor of two to three. No comparisons are yet available for mammalian species, though an assessment using the rabbit model presented here is currently underway.

2.4. Conclusions

In addressing long-standing questions about tissue composition and density effects on AF values, the dose results indicate that varying the composition between two mammalian tissue types (e.g. human vs rabbit bones) made little difference in SAF values (within 5% over most energy ranges). However, variable tissue density (e.g. bone vs liver) can significantly impact SAF values. As self-absorption can contribute greatly to total dose, accurate tissue densities should be used where practicable. Examining differences across life-stages revealed increasing SAFs with testis and ovary size of more than an order of magnitude for photons and several factors for electrons, indicating the potential for increasing dose rates to these sensitive organs as animals mature. The voxel models presented in this paper are intended to augment conventional ellipsoidal models for the purposes of testing underlying dose relationships (e.g. tissue density effects and age-specific differences). Generally, given the ubiquity of rabbits and other similar rodents, these results may be useful to those engaged in environmental radioprotection.

2.5. Supplementary Information

ElectronAF Adult: Electron absorbed fraction tables for adult rabbit.

ElectronAF Juvenile: Electron absorbed fraction tables for juvenile rabbit.

PhotonAF Adult: Photon absorbed fraction tables for adult rabbit.

PhotonAF Juvenile: Photon absorbed fraction tables for juvenile rabbit.

ElectronSAF Life stage comparison: Electron self-absorbed fractions compared for adult and juvenile rabbits.

PhotonSAF Life stage comparison: Photon self-absorbed fractions compared for adult and juvenile rabbits.

SAcomposition: Sensitivity analysis on rabbit tissue composition.

SAdensity Electron: Sensitivity analysis on rabbit tissue density for electron emitters.

SAdensity Photon: Sensitivity analysis on rabbit tissue density for photon emitters.

Rabbit tissue density and composition: Measured rabbit tissue densities and compositions.

2.6. References

See Chapter 6.

**3. ORGAN DOSE RATE CALCULATIONS FOR SMALL MAMMALS AT
MARALINGA, THE NEVADA TEST SITE, HANFORD, AND FUKUSHIMA:
A COMPARISON OF ELLIPSOIDAL AND VOXELIZED DOSIMETRIC
METHODOLOGIES**

Caffrey, E.A., Johansen, M.P., Higley, K.A.

Article and electronic supplementary information can be found online at:
<http://www.rjjournal.org/doi/abs/10.1667/RR14162.1>

and

https://www.dropbox.com/sh/2z8z88gx0fb1otg/AAAppfhRa8_Np2e4eQXKM5maa?dl=0

Caffrey E.A., Johansen M.P., Higley K.A., 2015. Organ Dose Rate Calculations for Small Mammals at Maralinga, the Nevada Test Site, Hanford, and Fukushima: A Comparison of Ellipsoidal and Voxelized Dosimetric Methodologies. *Radiation Research*; 184(4):433–41.

Abstract

Radiological dosimetry for nonhuman biota typically relies on calculations that utilize the Monte Carlo simulations of simple, ellipsoidal geometries with internal radioactivity distributed homogeneously throughout. In this manner it is quick and easy to estimate whole-body dose rates to biota. Voxel models are detailed anatomical phantoms that were first used for calculating radiation dose to humans, which are now being extended to nonhuman biota dose calculations. However, if simple ellipsoidal models provide conservative dose-rate estimates, then the additional labor involved in creating voxel models may be unnecessary for most scenarios. Here we show that the ellipsoidal method provides conservative estimates of organ dose rates to small mammals. Organ dose rates were calculated for environmental source terms from Maralinga, the Nevada Test Site, Hanford and Fukushima using both the ellipsoidal and voxel techniques, and in all cases the ellipsoidal method yielded more conservative dose rates by factors of 1.2–1.4 for photons and 5.3 for beta particles. Dose rates for alpha-emitting radionuclides are identical for each method as full energy absorption in source tissue is assumed. The voxel procedure includes contributions to dose from organ-to-organ irradiation (shown here to comprise 2–50% of total dose from photons and 0–93% of total dose from beta particles) that is not specifically quantified in the ellipsoidal approach. Overall, the voxel models provide robust dosimetry for the nonhuman mammals considered in this study, and though the level of detail is likely extraneous to demonstrating regulatory compliance today, voxel models may nevertheless be advantageous in resolving ongoing questions regarding the effects of ionizing radiation on wildlife.

3.1. Introduction

Techniques for calculating radiation doses to non-human biota from environmental source terms have recently evolved due to advances from the international community on improved dosimetric methods [2], [24], as well as increased data availability on radionuclide accumulation in wildlife [25]–[27]. Whole-body dose rates are assessed using dose conversion factors (DCFs), which are absorbed dose rates per unit activity concentration in the entire body or in a particular organ (units $\mu\text{Gy/day}$ per Bq/kg). The current process for calculating DCFs recommended by the International Commission on Radiological Protection (ICRP) and implemented in the ERICA Integrated Approach [1] makes use of a single ellipsoid to represent an organism of interest, with internal homogeneously distributed radionuclides [2]. This approach does not allow for the calculation of organ specific dose rates, and in the case of radionuclides that strongly partition into specific organs or tissues, dose rates to some sensitive tissues may be subsequently underestimated. Gomez-Ros et al. [28] devised a method for estimating organ specific dose rates from whole-body dose rates based on a ratio, R of said dose rates [4]. Gomez-Ros demonstrated that the maximum R value is a ratio of whole organism- to- organ mass. Organ specific dose rates are calculated by multiplying the whole-body dose rate by the ratio (R) of their relative masses. This method includes some uncertainty (negligible for alpha particles and low energy electrons; less than 30% for photons and high energy electrons), however the use of simplified shapes and mass-ratios provides for ease of use and consistent applicability to a wide range of organism types.

The voxel method relies on a three-dimensional representation of the organism, which is used to calculate absorbed fractions (AFs) and DCFs [5]–[7], [29]. This process provides

a hyper-realistic model of the organism, containing individual organs, and includes energy deposition from adjacent organs. It requires more input information and computation across multiple software platforms.

Radiation protection of wildlife aims to protect population levels of any given species, rather than individual organisms. Conservatism in dose rate calculations helps to ensure that the majority of a given population are protected from potential effects of ionizing radiation. A comparison of the two methodologies has been performed for one freshwater species, the trout, and two marine species, the flatfish and crab [4], with the conclusion that ellipsoidal models are conservative and therefore protective in most cases. An evaluation has not been completed for mammalian species to date. The purpose of this paper is therefore threefold:

- (1) Provide a comparison of dose calculation methodologies (mass-ratio/ellipsoidal and voxel) for a widely representative small mammal (a rabbit);
- (2) Calculate organ dose rates for small mammals from environmental data across four sites - the Nevada Test Site, Maralinga, Hanford, and Fukushima, for environmentally relevant concentrations of $^{134}, ^{137}\text{Cs}$, ^{137}Cs , $^{238,239}\text{Pu}$, ^{239}Pu , $^{239,240}\text{Pu}$, ^{90}Sr , and ^{241}Am ; and
- (3) Using the voxel model and the environmental data, quantify organ-to-organ (termed crossfire) contributions to dose which is included in voxel, but not ellipsoidal models.

3.2. Materials and Methods

Small mammals from the families *Leporidae*, *Muridae*, and *Cricetidae* were selected for this analysis as being representative of a broad array of mammals. Of these, most of the

modelling work in this study focused on rabbit (*Leporidae*) for several reasons. First, the general traits of rabbits (e.g. herbivorous, burrowing) are representative for many small mammals. Second, rabbits have been widely used in clinical trials and wildlife studies [30]–[35] and provide useful linkage to other rodent and mammalian data. Third, as they are ubiquitous across the globe, they are commonly present at many existing contamination sites. Fourth, there is a significant amount of high quality organ-specific activity concentration data available for rabbits and other similar rodents at the Nevada Test Site (NTS), the Maralinga site in Western Australia, the Hanford site, and from a contaminated forest near Fukushima [17], [35]–[40]. Finally, there is a robust set of dosimetric data available for the rabbit [29]. Radionuclides included in this study were selected based on available data, with the majority being nuclides commonly associated with weapons test sites and nuclear accidents. Selected radionuclides include: 134 , ^{137}Cs , ^{137}Cs , $^{238,239}\text{Pu}$, ^{239}Pu , $^{239,240}\text{Pu}$, ^{90}Sr , and ^{241}Am .

3.2.1. Organ dose rate comparison methodology

There is currently no process for summing individual organ dose rates to obtain a whole-body equivalent dose rate (there are no tissue weighting factors for non-human biota). It is therefore not possible to directly compare voxel and ellipsoidal DCFs. Instead, this paper will utilize a comparison methodology developed by Ruedig et al. [4]. Using the mass-ratio methodology of Gomez-Ros et al. [3], Ruedig illustrated that creating a ratio of the voxel dose rate to the ellipsoidal dose rate reduces to the following (termed K or K-ratio):

$$K = \frac{DR_{voxel}}{DR_{ellipsoidal}} = \frac{DCF_{voxel}}{DCF_{ellipsoidal}}$$

The K-ratio can then be used to compare ellipsoidal-based DCF for an organ which, in this study, are then compared with voxel DCFs where the source and target are the same organ (e.g., bone \leftarrow bone).

3.2.2. Rabbit voxel model DCFs

Voxel models have been developed by numerous researchers, and the process has been described in detail in [5]–[9], [41], [42]. These models are created using medical imaging techniques and contain detailed anatomical data. The models are used in Monte Carlo simulations to obtain AFs for each individual organ used as a source (emitting radiation) and target (absorbing radiation). AFs for the voxelized rabbit were obtained from a recently published study by Caffrey et al. [29]. From the AF data, dose conversion factors were calculated using the following:

$$DCF_{voxel} = X * \sum_j \bar{E} * (\varphi(\bar{E}, S \leftarrow S) * BR * Y)$$

Where:

- X is a conversion from keV to μJ , and from seconds to days
- $\varphi(\bar{E}, S \leftarrow S)$ is the absorbed fraction of energy for average energy E , for a source and target (S) that are the same organ
- BR is the branching ratio for the decay of interest
- Y is the yield for the decay of interest
- \bar{E} is the average energy of the emitted radiation in keV
- Summed over all radiations j
- DCF units are $\mu\text{Gy}/\text{day}$ per Bq/kg

DCFs are given as electronic supplementary material for each source-target combination for several commonly encountered radionuclides.

3.3.3. Ellipsoidal model DCFs

The ERICA Tool Version 1.2 [1] was used to obtain DCFs for an ellipsoidal figure with the same dimensions and mass as the voxelized rabbit. Using a tier 2 analysis and the “add organism” option within ERICA, an ellipsoid of mass 2.1 kg and dimensions of 35 x 24 x 0.7 cm was created. Using an ERICA-derived ellipsoid that correlates precisely to the voxelized rabbit eliminates discrepancies in the models due to size and mass. ERICA-derived DCFs are available as electronic supplementary material for ^{134}Cs , ^{137}Cs , ^{90}Sr , ^{238}Pu , ^{239}Pu , ^{240}Pu , ^{241}Am , $^{134,137}\text{Cs}$, $^{238,239}\text{Pu}$, and $^{239,240}\text{Pu}$.

Organ dose rates are calculated by multiplying the appropriate organ activity concentrations by the corresponding DCF. In cases where there is no organ activity concentration, appropriate concentration ratios may be used (see [14]). Whole body dose rates for the radionuclides considered in this study were summed using radiation weighting factors given in ERICA: 10 for alpha emitters ($^{239,240}\text{Pu}$ and ^{241}Am), 1 for beta/gamma emitters (^{137}Cs), and 3 for low beta emitters (^{90}Sr).

3.3.4. Sites and Data

The model methods were compared using real-world data summarized by location, radionuclide, and organism in Table 3-1. All data was collated in Excel, and is available as electronic supplementary material. All dose rate calculations used maximum values found at each site for each organ and radionuclide.

Table 3-1: Summary of data used in this study

Site	Maralinga	Nevada Test Site	Hanford	Fukushima
Radionuclide(s)	$^{239, 240}\text{Pu}$, ^{137}Cs , ^{90}Sr	^{90}Sr , ^{137}Cs , 238 , ^{239}Pu , ^{239}Pu , 239 , ^{240}Pu , ^{241}Am	^{90}Sr , ^{137}Cs	$^{134, 137}\text{Cs}$
Organisms	<i>Oryctolagus cuniculus</i>	<i>Lepus californicus</i> , <i>Sylvilagus audubonii</i>	<i>Lepus californicus</i> , <i>Sylvilagus nuttallii</i>	<i>Apodemus speciosus</i> , <i>Apodemus argenteus</i> , <i>Microtus montebelli</i>
References	[17], [35], [43]	[36]–[38]	[39]	[40]

3.3.4.1. Maralinga

Maralinga is a former British nuclear weapons test site located in South Australia, at the edge of the semiarid Great Victoria Desert. In addition to seven full nuclear detonations, conventional explosives were used to test components of the devices that had plutonium- or uranium- material [32], [35]. Most of the contamination present at Maralinga is from the device component testing, in particular the test series named Vixen B held at Taranaki. The Vixen B series resulted in the explosive dispersal of approximately 22 kg of plutonium [32]. The resultant deposition plumes radiate outward from the test site

[35], [44]. The primary radio-toxicant at Maralinga is plutonium, though there is residual cesium and strontium, among other radionuclides present at the site.

There are three sets of *O. cuniculus* data used in this analysis. Data for all specimens from the three surveys is available as supplementary material in Johansen et al. [17]. For Pu, data are from sampling completed in 1988, approximately 25 years post detonation [43], and from a sampling in 2010-2012, approximately 50 years post deposition events [17], [35]. Plutonium analysis was performed using the ANTARES-AMS system at the Australian Nuclear Science and Technology Organization (ANSTO). See Johansen et al. [35], Hotchkis et al. [45], and Harrison et al. [46] for sample processing details. $^{239,240}\text{Pu}$ concentrations are available for the following tissues: lungs, bone, liver and spleen, kidneys, muscle tissue, heart, fecal material, stomach contents, GI tract, and the pelt and feet. All specimen dissection segments matched model organ segments.

For ^{137}Cs and ^{90}Sr , data are from the 1988 sampling referenced above which examined biotic samples that were primary food sources for the Pitantatjara people to determine their possible radiation doses [43]. Muscle tissues of twelve *O. cuniculus* specimens were analyzed for ^{137}Cs and ^{90}Sr content. No radio-analysis was performed on any other organ segments. Cesium partitions strongly to muscle [14], [47], [48] and thus the muscle segment represents the majority of the contribution to dose. However, strontium is an analog of calcium, and is known to primarily partition into the skeleton [49]. In order to estimate the amount of strontium in the skeleton, an estimate of ^{90}Sr bone activity concentration was made using reference muscle-to-organ tissue ratios. As there are no such reference ratios for strontium in mammals, the highest value presented in Yankovich et al. was used (maximum bone/muscle ratio of 560 for freshwater fishes) [14]. In this

way, a skeletal activity concentration was calculated for strontium and bone was included in the organ dose rate calculations.

3.3.4.2. Nevada Test Site

The Nevada Test Site (NTS) was used for ~84 atmospheric and ~900 underground weapons tests [50], [51], and is located in an arid desert region of Nevada, USA.

Three separate sets of Nevada Test Site data were used in this study. The first set is from a 1976 animal investigation program annual report [36]. *L. californicus* specimens were hunted and necropsied immediately after death. Bone, muscle, skin, testicles (if male), fetus (if available), entire GI tract, and composited internal organs (liver, lungs, kidneys, and spleen) data were available [36]. Data were averaged across all samples for each site. Composited internal organs present in the rabbit voxel model were the kidneys, lungs, and liver. These segments were grouped in the dose rate calculations as internal organs to keep consistency with this set of data.

The second set of data is from the Nevada Applied Ecology Group from 1977 [38]. They examined ^{239}Pu and ^{241}Am contamination in *S. audubonii* living at areas 5, 11-C, and 13, clean slate 2, and double track. Additional Area 11-C samples taken from a variety of small rodents were also used in this study. Radionuclide analysis methods are detailed in White et al. 1977. The samples were generalized into the broad categories of pelt, GI tract, and carcass. Carcass values were assumed to be muscle, pelt values skin (mass-ratio calculations only), and the GI tract itself.

The third and final set of NTS data that was considered for analysis was a summary of the Nevada Applied Ecology Group and other Correlative Programs completed in 1992

[37]. This report contained $^{239}, ^{240}\text{Pu}$ concentration data for the skin, stomach contents, intestines and contents, muscle, lung, bone, and liver of three *Vulpes macrotis*, *Canis latrans*, *Lepus californicus*, and *Sylvilagus audubonii*. Only *L. californicus*, and *S. audubonii* dose rates are reported in this study, but dose rates for the *V. macrotis* and *C. latrans* can be found in the supplementary materials. The intestines and contents segment was treated as GI tract for the purposes for organ dose rate calculations.

3.3.4.3. Hanford

The Hanford site housed the first full-scale plutonium production reactor and three chemical separations plants, and is located in the semiarid southeastern portion of Washington State in the USA. Areas of the site are broken into three general categories: separations (200 areas), research (300 Areas), and reactor (100 Areas).

The Hanford data used in this analysis is from a Department of Energy Report examining radionuclide concentrations in wildlife from 1983-1992 [39]. *L. californicus* and *S. nuttallii* have been routinely sampled close to site facilities and waste management areas. Tissue samples were analyzed for ^{137}Cs , ^{90}Sr , ^{238}Pu , and $^{239,240}\text{Pu}$. Levels of plutonium were less than the minimum detectable activity, and were subsequently not reported. Only data for muscle (^{137}Cs) and bone (^{90}Sr) were available, thus organ dose rate calculations are based on this data.

3.3.4.4. Fukushima

In March 2011, a 6.6 magnitude earthquake and a large tsunami off the coast of Japan resulted in damage to the Fukushima Daiichi Nuclear Power Plant (FDNPP), releasing large quantities of radionuclides to the atmosphere, followed by subsequent deposition in

the Pacific Ocean and, to a lesser extent, on the landscape of Japan with most terrestrial deposition occurring in the nearby forests [47], [52]. A study conducted in the forest of Ottozawa, Okuma Town (~4km west of FDNPP) examined $^{134,137}\text{Cs}$ levels in various tissues of three rodent species (*Apodemus speciosus*, *Apodemus argenteus*, and *Microtus montebelli*). Rodents were trapped, with some sacrificed immediately and represent $^{134,137}\text{Cs}$ accumulation within the organism commensurate with field conditions. The remainder of the animals were depurated with clean feed, and sacrificed at either 5-7 days or 11-15 days [40]. This revealed changes in the internal activity concentrations allowing for dose rates to be calculated at each time interval. Dissection segments consisted of the liver, kidneys, digestive organ, a mixture of muscle and bone, lungs, reproductive organ, and the spleen. For the purposes of the organ dose rate calculations, the reproductive organ was assumed to be the testes, the digestive organ the GI tract, and mixed muscle and bone was considered to be muscle.

3.3. Results and Discussion

3.3.1. K-Ratios

For alpha radiation, full energy absorption in the source organ is assumed in both voxel and ellipsoidal methods, and thus the K-ratio is equal to 1 for $^{239,240}\text{Pu}$ and $^{238,239}\text{Pu}$ (see Figure 3-1). The same pattern is evident for ^{241}Am , which is predominantly an alpha emitter but also has a photon emission which lowered the K-ratio slightly, particularly in lung where the voxel model used realistic lung densities. The K-ratios of highly penetrating photon radiation, e.g. $^{134,137}\text{Cs}$, and ^{137}Cs , range from 0.42 – 0.64 indicating the ellipsoidal DCFs over-predict organ dose rates by a factor of 1.2-1.4 relative to the

voxel model. Greater disparity was evident in beta radiation (K-ratio of 0.17 for most segments) for which the ellipsoidal DCFs over-predicted organ dose rates by a mean factor of 5.3 (^{90}Sr). This is primarily due to the model differences in treatment of high energy beta particles in the absorbed fraction calculations (see section 3.5 for detailed discussion). These results indicate that the ellipsoidal dose rates are generally higher than voxelized dose rates for beta and gamma emitting radionuclides.

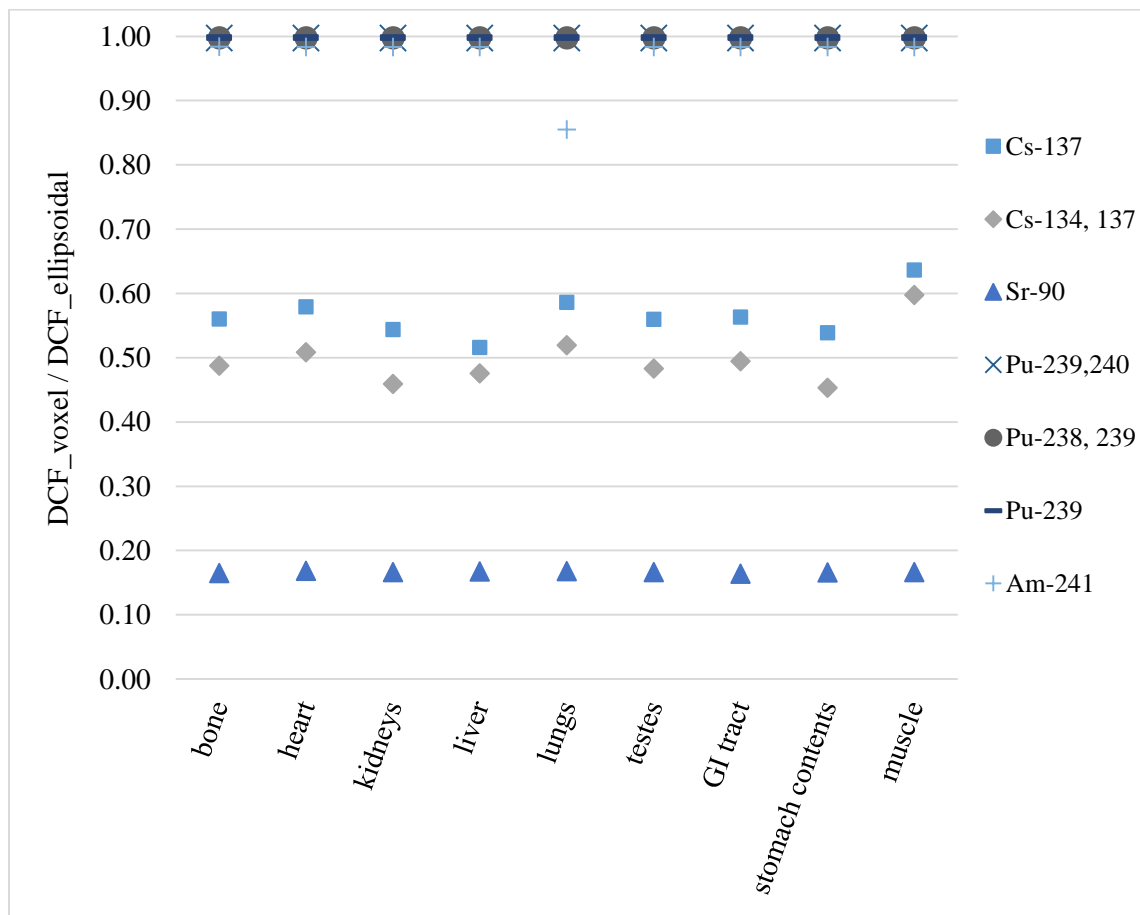


Figure 3-1: K-ratios for all radionuclides and segments considered. A K-ratio of 1 indicates that dose rates predicted by the voxel model are identical to those predicted by the ellipsoidal model. $K < 1$ indicates the ellipsoidal model is conservative.

3.3.2. Organ Dose Rates

The dose rates presented here were calculated for four sites, three particle types, and eleven organs. To elucidate differences in organ dose rate calculation methods, Figure 3-2 shows voxel dose rates versus mass-ratio dose rates for gamma emitters (134 , ^{137}Cs , ^{137}Cs) in black, a beta emitter (^{90}Sr) in speckled black, and alpha emitters (^{241}Am , 239 , ^{240}Pu , 238 , ^{239}Pu) in gray for each tissue. Alpha emitters align along the line of equality as both models assume full energy deposition in the source tissue. The gamma emitters considered here align parallel to, but above the line of equality, indicating that the mass-ratio dose rates are more conservative, in most cases, on average by a factor of approximately 1.3.

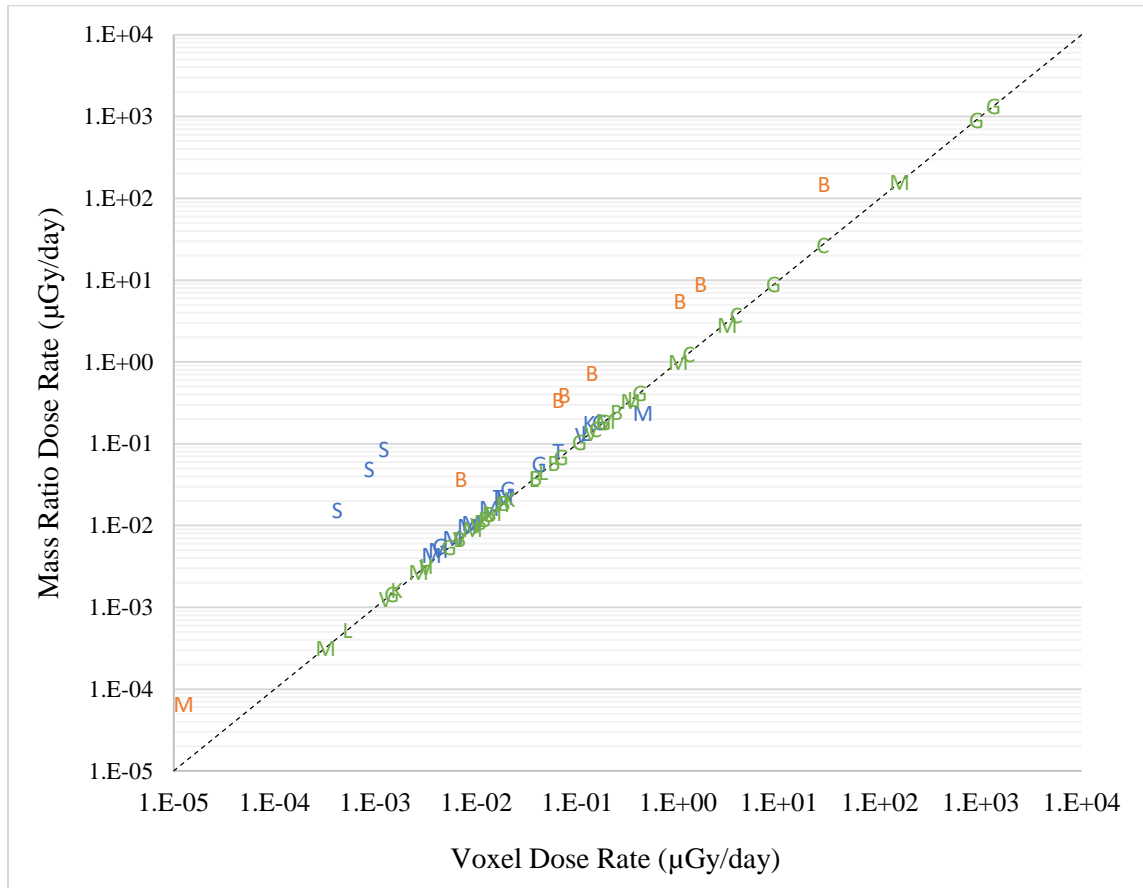


Figure 3-2: Voxel dose rate versus mass-ratio dose rate for: $^{134}, ^{137}\text{Cs}$, ^{137}Cs (blue); ^{90}Sr (orange); ^{241}Am , $^{239}, ^{240}\text{Pu}$, $^{238}, ^{239}\text{Pu}$ (green). Letters correspond to organs as follows: bone=B, heart=H, kidneys=K, liver=V, lungs=L, feces=F, testes=T, GI tract=G, stomach contents=C, skin=S, and muscle=M.

High energy beta emitters (e.g. ^{90}Sr) align above the line of equality in all cases, with the deviation equivalent to a factor of five (Figure 3-2). This is consistent with the feature in the voxel model whereby beta emissions are allowed to escape the source organ and impart energy to an adjacent organ, while the mass-ratio approach assumes an absorbed fraction of unity for all beta emissions. Although the travel lengths of beta particles in

tissue are short (up to ~0.23 cm for the maximum 0.5 MeV emissions of ^{90}Sr), the cumulative effect of escaping beta particles can be significant for smaller biota and depends on the physical factors that influence absorbed fraction values, specifically organ surface area to volume ratios, density, and shape. In the voxel model, the total surface area of the bone is large, allowing for a significant portion of the beta energy to escape the source volume and irradiate surrounding organs and thus adding, potentially significantly, to their dose rates. Muscle, which absorbs much of the beta energy from bone, also has a large surface area, allowing for further beta energy to escape. In numerous voxel model studies it has been demonstrated that high energy electrons should be treated as penetrating radiation for the purposes of organism dosimetry [5], [7]–[9], and that conclusion is supported here. This is potentially relevant for dose-effects studies, in which dose from radionuclides such as ^{90}Sr may dominate the total organism dose rates. The data suggests that organ-to-organ contributions to dose included in the voxel model do not overcome the conservatism incorporated into the mass-ratio dose rates.

The most extreme deviation in dose rates for gamma emitters spans about two orders of magnitude (skin dose rates for ^{137}Cs , Figure 3-2). Skin dose rates should be regarded carefully however, as the skin in both models does not include the rabbit's fur [29], and most data was for the rabbit pelt and feet.

The next sections present organ dose rates for each radionuclide considered at each site. Voxelized organ dose rate calculations are available for all organ segments. If no activity concentration data was available for a given segment, then dose to that segment is solely from adjacent segments. The mass-ratio method can only calculate individual organ dose rates that have activity concentration data, therefore, if there is no data for a given organ

segment, then no mass-ratio dose rate is reported. The only exception is ^{90}Sr in *O. cuniculus* at Maralinga, where a muscle-to-organ ratio was employed to obtain an estimate of skeletal activity concentration (see section 2.4.1).

The Maralinga *O. cuniculus* data [17] and the small rodent NTS data [38] have pelt and feet segments. These segments were not used in the voxel organ dose rate calculations, as no AF values for the skin were given [29]. Pelt and feet values were used to calculate skin dose rates using the mass-ratio method.

AFs taken from [29] for *L. californicus* were used for all organ dose rate calculations. Rat and mouse AFs exist in open literature for a select set of organs [8], but these do not include tissues such as muscle or testes (for the rat). A comparison of rabbit self-absorbed fraction (SAF; when source and target are the same organ/tissue) values to rat/mouse SAF values for a photon source in the liver revealed a maximum deviation of a factor of 4; with an average deviance of a factor of 2 over the energy range 0.02 – 1.0 MeV. For the same comparison for electrons in the energy range of 0.1 – 1.0 MeV, the maximum deviation was only a factor of 1.3, with an average of 1.08, indicating good agreement for electrons. The data available for organisms other than rabbit were ^{241}Am (at NTS), and $^{134}, ^{137}\text{Cs}$ (at Fukushima). For ^{241}Am , there is essentially no difference in SAF values, as the maximum deviation over the energy range of ^{241}Am photons is only a factor of 1.2 (rabbit to rat SAF values). For $^{134}, ^{137}\text{Cs}$, the deviation is higher at about a factor of 4, but even when taking that into account, individual organ dose rates are still low (see section 3.4).

Dose rates are presented and compared per radionuclide at each site in sections 3.3-3.7. As there are no dose effects benchmarks for individual organs in animals, primarily due to a lack of data on biological endpoints, no attempt is made to compare the organ dose rates calculated here to the existing dose effects benchmarks (e.g. the ICRP derived consideration reference levels (DCRLs), which indicate the potential for effects in whole-organisms and are intended for use in protecting populations). Such benchmark values are only valid when used to estimate the impact by comparison with the total exposure dose rate at the whole body level. Whole body dose rates calculated using the ERICA Tool [1] are given in section 3.8. All dose rates can be found as electronic supplementary material.

3.3.3. ^{137}Cs at NTS, Hanford, Maralinga

Dose rates were calculated for environmental levels of ^{137}Cs contamination at the Nevada Test Site, Hanford, and Maralinga. The highest dose rate was 8.8E-02 $\mu\text{Gy/day}$ to skin at the NTS Area 15 calculated using the mass-ratio method. In a study by Turner et al [53], muscular dose rates for *L. californicus* from ^{137}Cs were calculated to determine if levels of fallout from the Sedan test impacted wildlife in the area. Muscular dose rates calculated in that study were four orders of magnitude higher than those calculated here for the NTS at 2.7E+02 $\mu\text{Gy/day}$. The organ-to-organ contribution to dose for ^{137}Cs was low for the testes and GIT segments at about 2%; however about 33% of the total dose to the muscle was from crossfire contributions from other adjacent organs.

3.3.4. $^{134},^{137}\text{Cs}$ depuration at Fukushima

An examination of muscle tissue dose rates at capture showed that the mass-ratio and voxelized dose rates are similar (see Table 3-2). At time intervals 5-7 days and 11-15

days, the voxel method yields slightly higher dose rates. Mass-ratio organ dose rates are higher for all other tissues considered (see Figure 3-3).

Table 3-2: $^{134}, ^{137}\text{Cs}$ depuration at Fukushima demonstrated by muscle tissue dose rates at three time intervals at three time intervals in a contaminated forest outside Fukushima.

Time	Voxel Dose Rate ($\mu\text{Gy/day}$)	Mass-ratio Dose Rate ($\mu\text{Gy/day}$)
0 days	4.5E-01	2.4E-01
5-7 days	8.8E-02	6.5E-02
11-15 days	2.9E-02	2.5E-02

Muscle tissue dose rates are the maximum dose rates calculated in all cases, and about 50% of the dose can be attributed to organ crossfire. The maximum testicular dose rate is 8.2E-02 $\mu\text{Gy/day}$, calculated using the mass-ratio method for the day of capture. The organ-to-organ contribution to total testicular dose rate is about 7%, compared to that for kidneys at 2%, liver at 15%, lungs at 11%, and GIT at 17%. Kubota et al [40] calculated total body dose rates using ERICA, and found that the internal contribution to dose was fairly low, at a maximum of 100 $\mu\text{Gy/day}$.

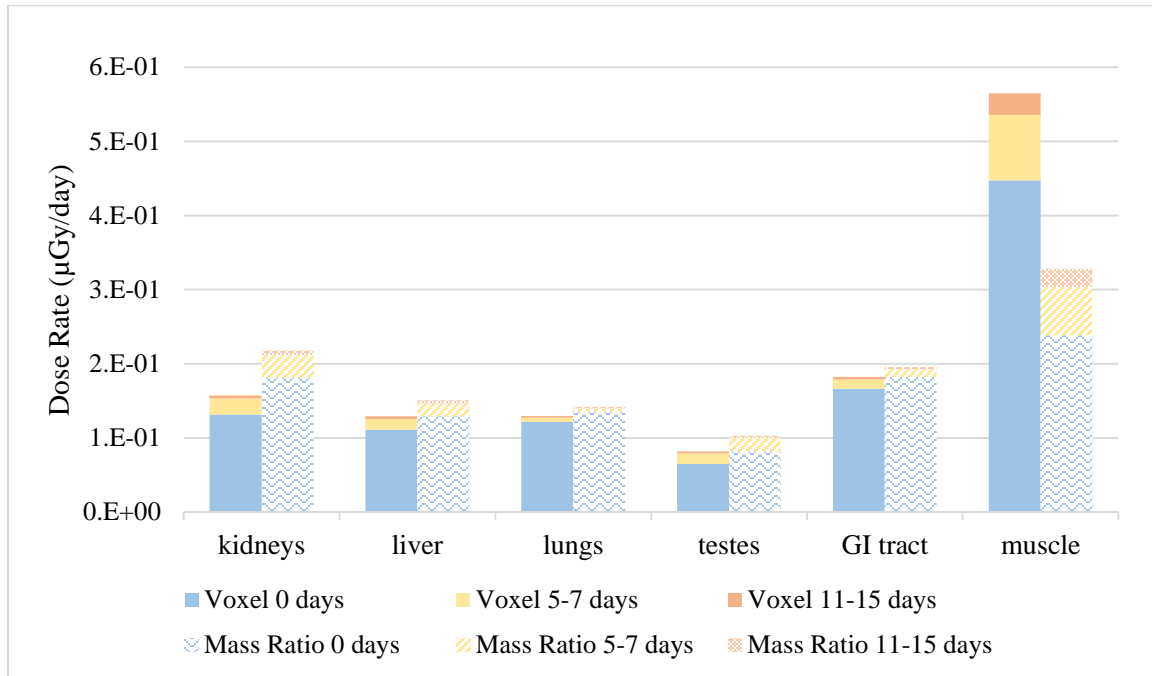


Figure 3-3: $^{134}, ^{137}\text{Cs}$ dose rates in various organ segments for small rodents at Fukushima calculated using voxel and mass-ratio methods.

3.3.5. ^{90}Sr at NTS, Hanford, and Maralinga

Dose rates for organs other than the bone were generally low, as the maximum range of ^{90}Sr in *L. californicus* bone (density 1.5g/cm^3) is about 0.2 cm [54], and thus most of the beta energy is deposited in the bone volume. However, a portion of the beta emissions escape the bone and are absorbed in adjacent tissues, primarily the muscle. The energy that escaped the bone contributed 94% of the muscular dose rates calculated in this study. It should be noted that aside from the Maralinga data (which had ^{90}Sr in muscle tissue), no activity concentration data was available for other organs/tissues at the other sites, and thus dose rates to organs other than the bone from the voxel model are from organ

crossfire contributions only. Bone dose rates calculated using each methodology for three NTS sites, three Hanford locations, and one Maralinga site are shown in Table 3-3. The Maralinga dose rates are significantly lower than dose rates at the other two sites. This may be an artifact of only the contributions from muscle and bone being included in the dose rate calculation.

Table 3-3: ^{90}Sr bone dose rates for NTS, Hanford, and Maralinga.

Location	Voxel Dose Rate ($\mu\text{Gy/day}$)	Mass-ratio Dose Rate ($\mu\text{Gy/day}$)
Area 18 NTS May 1976	7.5E-02	4.0E-01
Area 15 NTS March 1976	1.7E+00	8.9E+00
Area 15 NTS September 1976	1.4E-01	7.4E-01
200 Area Hanford	1.0E+00	5.6E+00
300 Area Hanford	6.5E-02	3.5E-01
100 Area Hanford	2.8E+01	1.5E+02
Maralinga	7.1E-03	3.8E-02

Bone dose rates calculated using the mass-ratio method are about a factor of five higher than those calculated using the voxel method. The Turner study [53] also considered ^{90}Sr dose rates to *L. californicus* bone, and the highest dose rate calculated for the NTS was 4.4E+02 $\mu\text{Gy/day}$, on the same order of magnitude as the highest dose rate calculated in this study (1.5E+02 $\mu\text{Gy/day}$ to bone).

3.3.6. $^{239, 240}\text{Pu}$ at NTS and Maralinga

Voxel and mass-ratio dose rates are equivalent for alpha particles, as total energy absorption in the source organ is assumed in both cases. Maximum dose rates for the 2010-2012 sampling at Maralinga were for voxel segments associated with the digestive system, GI tract dose rate was 1.1E-01 $\mu\text{Gy/day}$. The maximum dose rates for sampling completed in the 1980s were for the lungs at 3.5E-01 $\mu\text{Gy/day}$. For *L. californicus* at the NTS, the maximum dose rate was 4.8 $\mu\text{Gy/day}$ for the skin.

3.3.7. ^{241}Am at NTS

The highest organ specific dose rates across all sites and for all radionuclides was for ^{241}Am in the GI tract of small rodents at the NTS. Mass-ratio and voxelized dose rates are essentially identical, as the K-ratio for ^{241}Am nearly all segments is 0.98 (exception is the lung at 0.85, see section 3.1 for details). The maximum dose rate was 1.36E+03 $\mu\text{Gy/day}$ at Area 11-C.

3.3.8. Utility of organ-specific dose rates

Currently, dose screening levels for biota are based on a whole-body limit, predominantly because external photon exposures dominate the available effects data [4], [40], [55], [56]. It would be highly impractical to move to a system in which screening values and

limits are based on an organ specific dose rate, for several reasons: the lack of organ weighting factors for wildlife, the paucity of data on radionuclide distributions within biota, and the lack of appropriate risk factors [24]. Further, freshwater fish, marine fish, and with this study small terrestrial mammals have all been examined for differences in dose rate calculation methodologies, and in all cases considered, the simple ellipsoidal method provided conservative estimations that are consequently protective of the environment. In keeping with the current paradigm, the internal contributions to whole body dose rates from $^{239,240}\text{Pu}$, ^{137}Cs , ^{90}Sr , and ^{241}Am were assessed for rabbits at Maralinga, the NTS, and Hanford using the ERICA Tool [1], [57], [58] and assuming ellipsoidal organism geometry with activity concentration distributed homogeneously throughout. Whole body dose rates for average activity concentrations of all samples from each site are shown in Table 3-4.

Table 3-4: Internal whole body dose rates (in $\mu\text{Gy/day}$) for rabbits at Maralinga, NTS, and Hanford calculated using ERICA Version 1.2.

Radionuclide	Maralinga	NTS	Hanford
$^{239,240}\text{Pu}$	1.14E-01	6.51E+00	<MDA
^{241}Am	2.08E-01	No Data	No Data
^{137}Cs	1.64E-02	3.94E-02	3.30E-03
^{90}Sr	2.54E-03	9.26E-01	1.53E+01
TOTAL	3.24E+00	6.79E+01	4.60E+01

Maximum dose rates are low, indicating that there is unlikely to be any sort of deleterious effects [2]. However, these dose rates do not include dose from other radionuclides that may be of importance for internal dose rates (e.g. uranium and thorium series), or from external radiation sources, which may be significant for ground dwelling animals living in contaminated soils.

3.4. Conclusions

Upon examination the data for various decay modes, it was demonstrated that for alpha radiation the two methodologies yielded identical dose results. For photon and high energy electron radiation, the amount of energy deposited in organs from crossfire (originating from adjacent organs) ranged from 2-50%, and 0-93%, respectively. However, the conservatism in the mass-ratio approach (a factor of 1.3 for photons and 5.3 for electrons) appeared to dominate these contributions. As a consequence, dose rates to small mammals for the voxel and ellipsoidal modelling approaches were approximately the same for $^{239,240}\text{Pu}$ and ^{241}Am , but voxel dose rates were only about 50-60% of ellipsoidal rates for ^{137}Cs and only about 15% for ^{90}Sr .

A robust method for calculating organ dose-rates may prove useful in elucidating mechanisms by which radiation-induced effects arise in wildlife populations. There is good agreement between the more accurate voxel models and the ellipsoidal models created to date. Thus, the continued use of ellipsoidal models as the basis for the majority of regulatory dose assessments seems appropriate, though voxel models may resolve some of the controversy surrounding radiation effects seen in wildlife populations.

3.5. Supplementary Information

DCFvoxel Adult: Dose conversion factor spreadsheet for a variety of radionuclides for an adult rabbit voxel model.

Dose Rates: All dose rates calculated in this study.

ERICA-derived rabbit DCFs: DCFs for an adult rabbit for a variety of radionuclides calculated using the ERICA tool.

NTS, Hanford, Fukushima, Sr, Cs, Am, Pu Data: All raw data compiled for this study.

3.6. References

See Chapter 6.

4. COMPARISON OF HOMOGENEOUS AND PARTICULATE LUNG DOSE RATES FOR SMALL MAMMALS

Caffrey, E.A., Caffrey, J.A., Johansen, M.P., Higley, K.A.

Article can be found online at:

TBD

and

https://www.dropbox.com/sh/2z8z88gx0fb1otg/AAAppfhRa8_Np2e4eQXKM5maa?dl=0

Caffrey E.A., Caffrey J.A., Johansen M.P., Higley K.A., 2015. Comparison of Homogeneous and Particulate Lung Dose Rates for Small Mammals. *Health Physics*. Submitted.

Abstract

Small, highly radioactive fragments of material incorporated into metallic matrices are commonly found at nuclear weapons test and accident sites, and can be inhaled by wildlife. Inhaled particles often partition heterogeneously in the lungs, with aggregation occurring in the periphery of the lung, and are tenaciously retained. However, dose rates are typically calculated as if the material were homogeneously distributed throughout the entire organ. Here we quantify the variation in dose rates for alpha, beta, and gamma emitting radionuclides with particles sizes from 1-150 μm and considering three averaging volumes- the entire lung, a 10 cm^3 and a 1 cm^3 volume of tissue. Dose rates from beta-emitting particles (e.g. ^{90}Sr) were approximately one order of magnitude higher than those from gamma-emitting radionuclides (e.g. ^{137}Cs). Self-shielding within the particle was negligible for gammas and minor for betas. For alpha-emitting particles (e.g. ^{239}Pu) it was found that particles in the respirable size range of less than 5 μm are not greatly self-shielded, but rather deposit a significant amount of energy into the surrounding tissue. As such particles may remain lodged deep in the lung, they represent a considerable contribution to long term lung dose rates. For practical dose rate calculation purposes, a graph of particle size versus dose rate for plutonium containing hot particles is given. This study demonstrates one possible approach to dose assessments for biota in environments contaminated by radioactive particles, which may prove useful for those engaged in environmental radioprotection.

4.1. Introduction

Hot particles are small, typically highly radioactive fragments of material that have a diameter of less than one millimeter [59]–[62]. When hot particles are inhaled and lodged in the lung they cause non-uniform distribution of dose, with particle track images indicating potentially high dose rates to the immediately surrounding tissues. There is substantial uncertainty in the effects of such localized dose [63]. However, the literature suggests that the non-uniform exposure from an inhaled hot particle is likely less carcinogenic than that from a spatially uniform exposure for the same average dose [62], [64]–[68]. The National Commission on Radiological Protection (NCRP) and the International Commission on Radiological Protection (ICRP) have provided guidance on the limitation of hot particle exposures to skin, lungs, and other organs [68]–[71]. There are few studies that directly compare the dose rates from homogeneous irradiation of tissues with the heterogeneous irradiation from hot particles.

Recently, the International Atomic Energy Agency (IAEA) announced a coordinated research activity that will enhance capabilities in assessing the long-term environmental impact on ecosystems contaminated with hot particles. Particular interest for this research is in improving the approach for dose assessments to biota for environments contaminated by radioactive particles, and assessing the role of such particles in the lungs of prey animals. Numerous animal studies have shown that inhaled insoluble particulate matter accumulates heterogeneously in the lungs, with aggregation in the periphery of the lung [15], [34], [72]–[74]. Improved dosimetric models for biota have also been called for by the International Commission on Radiological Protection (ICRP) to improve the understanding of radiation dose and effects [2].

This study examines dose rates from alpha- (^{239}Pu), beta- (^{90}Sr), and gamma- (^{137}Cs) emitting hot particles in the lungs of small mammals represented by the rabbit family (*Leporidae*). The rabbit family was selected for numerous reasons. Firstly, it is representative of other rodents and small mammals. Secondly, rabbits are commonly used in clinical trials and wildlife studies [30]–[35], and provide useful linkage to other rodent and mammal data. They are also present at many sites contaminated with hot particles (e.g. Maralinga, the Nevada Test Site), and there is a robust set of dosimetric data available for the rabbit [29]. The radionuclides considered in this study were chosen as representing alpha, beta, and gamma emitters typical of contamination at many nuclear waste sites and for their ubiquity in the environment.

Plutonium oxide ($^{239}\text{PuO}_2$) is found as a friable particulate at the Maralinga test site in South Australia [17], [35], [75]–[77]. PuO_2 has been found to be insoluble in simulated lung fluid [77]. Plutonium oxides are considered to be avidly retained, and inhaled particles represent a long-term dose contributor [15], [78]. However, the deposition of energy into the surrounding tissue may be decreased by the self-shielding within the particle itself. Our literature search did not find previously published studies that quantified the amount of self-shielding versus energy deposited for particles in mammalian lung tissue.

Cesium and strontium hot particles are present in the environment as a result of nuclear weapons testing (e.g. at Nevada Test Site, USA, and Maralinga, Australia) and of reactor accidents such as Chernobyl. They are generally considered to be incorporated into metallic matrices, for which strontium has been shown to be tenaciously retained in the lungs [78]. Cesium compounds are generally found to be more soluble; this is consistent

with ICRP recommendations that cesium is assumed to be uniformly distributed throughout the body [78].

Conventional methods for calculating radiation dose are unsuitable when the inhaled activity is in the form of hot particles. Previously, the calculation of dose rates from particulate radionuclides assumed that particles were broken down or dissolved with activity distributed homogeneously throughout each organism [29], [40], [47], [79]. These doses are likely not representative of the actual doses received, as the dose will not be uniformly distributed over the entire mass of the organ, but rather highly localized around the particle. As the dose is confined to a small tissue volume, averaging the dose over the entire organ or tissue volume seems erroneous. Recent advances in wildlife modeling allow dose rates to be determined to an accuracy not feasible when many past studies on particle dose rates were undertaken [5], [29]. Here we will determine dose rates from localized alpha, beta, and gamma emitting hot particles on small mammal lung tissue; examine the effects of self-shielding on the dose rate; and compare homogeneous and particulate dose rates to determine the extent to which traditional models may misrepresent dose from particles.

4.2. Materials and Methods

A voxel model of an adult rabbit was used for the localized dose rate calculations [29]. Highly localized doses are difficult to measure directly. For each case detailed below, a Monte Carlo transport code (MCNP6) was used [80]. For each emission type, a particle of diameter 1-150 μm (1-10 and then by tens to 150) was used as the source. Potential differences in dose based on particle location were accounted for by placing particles at

three distinct locations in the lung: the periphery of the deep lung, the center of the lung, and the top of the lung near the trachea. Figure 4-1 shows approximate location of a deep lung particle.

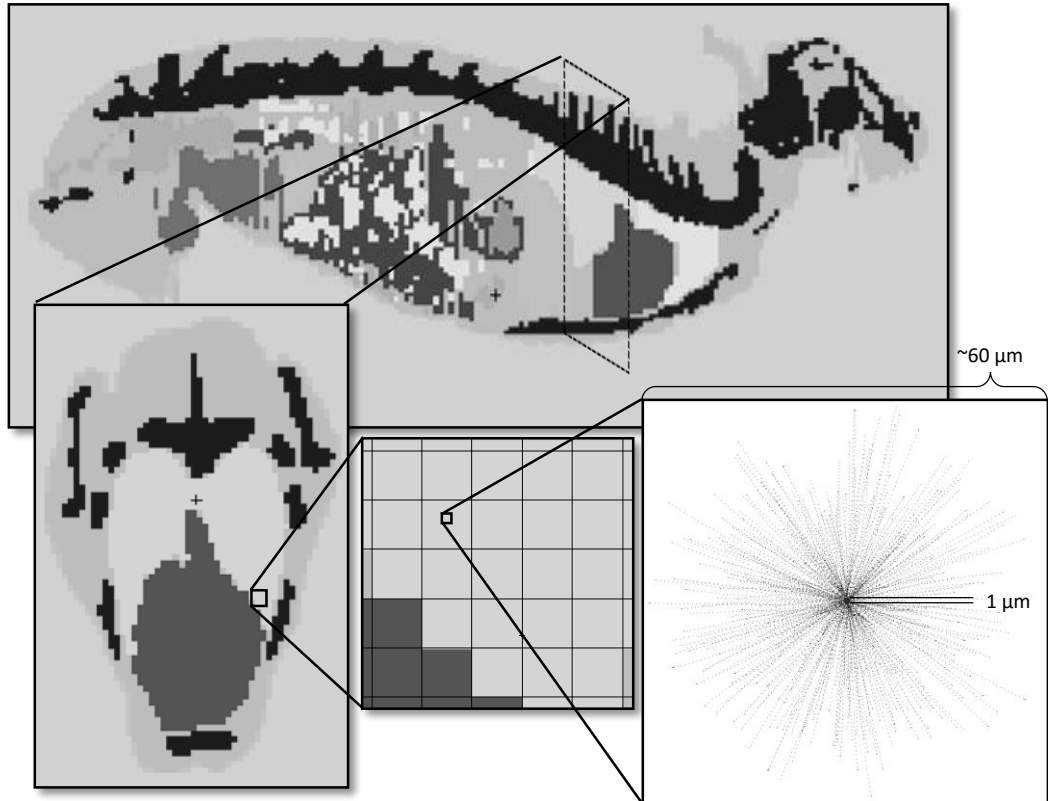


Figure 4-1: Rabbit voxel model with alpha particle tracks in lung tissue shown to approximately scale.

MCNP6 was used to obtain energy deposition in the lungs (using the *F8 volumetric tally) for particles of each size in each location of the lung, and for the same activity distributed homogeneously throughout the lung. The absorbed fraction of emitted energy

was determined across multiple averaging volumes selected for analysis: the entire lung, a 10 cm³, and a 1 cm³ tissue volume. Dose rates were calculated as follows:

$$DR = AC * \sum_j \bar{E} * (\phi(\bar{E}, S \leftarrow S) * BR * Y)$$

Where:

$\phi(\bar{E}, S \leftarrow S)$ is the absorbed fraction of energy for average energy E, for a source and target (S) that are the same organ (lungs in this case)

BR is the branching ratio for the decay of interest

Y is the yield for the decay of interest

\bar{E} is the average energy of the emitted radiation

AC is the activity concentration

Summed over all radiations j

Any radiation occurring in less than 1% of decays was omitted, but otherwise all decay emissions were included.

²³⁹Pu was used as the alpha emitting radionuclide. It was assumed to be in the form of plutonium oxide (PuO₂, density 11.46 g cm⁻³), consistent with the chemical composition found in the environment at Maralinga, the Nevada Test Site, and Chernobyl [17], [36], [60], [81]. The average energy of ²³⁹Pu alpha emissions is 5.15 MeV, with a maximum range in tissue or water of about 40 μm [82]. This range is significantly smaller than the size of the voxels used in the rabbit model, which span 700 μm x 700 μm x 2000 μm (Figure 4-1) [29]. In the case of homogeneously distributed alpha emitters, a practically

negligible quantity of alpha energy crosses between voxels within a given organ, and even less so at the organ boundary. Furthermore, the very short range of alpha particles means that the precise quantity of organ-to-organ contributions to dose at the organ boundary is driven by the surface area of the organ itself, which is poorly represented by voxel models. The same is true for hot-particle emitters with a strong dependence upon the precise placement of the particle and very low probability of placement at the thin boundary of an organ. MCNP analysis of ^{239}Pu particles was thus performed using simple concentric sphere models. A sphere of ICRP soft tissue with unit density contained an embedded sphere of PuO_2 of varying sizes. Tissue sphere size was also considered as a variable, although its effects only demonstrate the relationship between dose and the size of the volume selected for use in the denominator of such calculations. A tissue dose volume of 1 cm^3 was thus selected as a reference value for this analysis.

The gamma emitter selected for this analysis was ^{137}Cs and the beta emitter ^{90}Sr , both found in the environment as particulates at both the Maralinga site and at Fukushima [32], [43], [83]. Both cesium and strontium were assumed to be in an insoluble matrix with iron (density 7.874 g cm^{-3}). As the range of cesium and strontium particles in tissue is larger than the size of the voxels in the rabbit model, and thus organ-to-organ contributions to dose become relevant, the entire model was employed.

This paper examines dose rates from a single particle placed within three averaging volume alternatives: the whole rabbit lung, and 1.0 cm^3 and 10.0 cm^3 spherical volumes within the lung. These sizes were selected as being representative of localized volumes within lung tissues and have been selected to show differences in dose rates as the volume considered is scaled. These volume sizes also fit within the lungs of most

mammals and our results will therefore have relevance to a wide range of mammals including humans. For short ranged particles in which the energy does not escape the dose averaging volume, calculated dose rates increase proportionally as dose averaging volumes are reduced. Dose rates from these particulate configurations are compared with that which assumes the same activity is homogenously spread throughout the rabbit lung.

4.3. Results and Discussion

4.3.1. Photon Emitters

Photons have a relatively long average distance between interactions, and increasing particle size did not significantly change the dose rates, indicating that very little self-shielding occurred for the gamma emissions over all particle sizes tested (Figure 4-2).

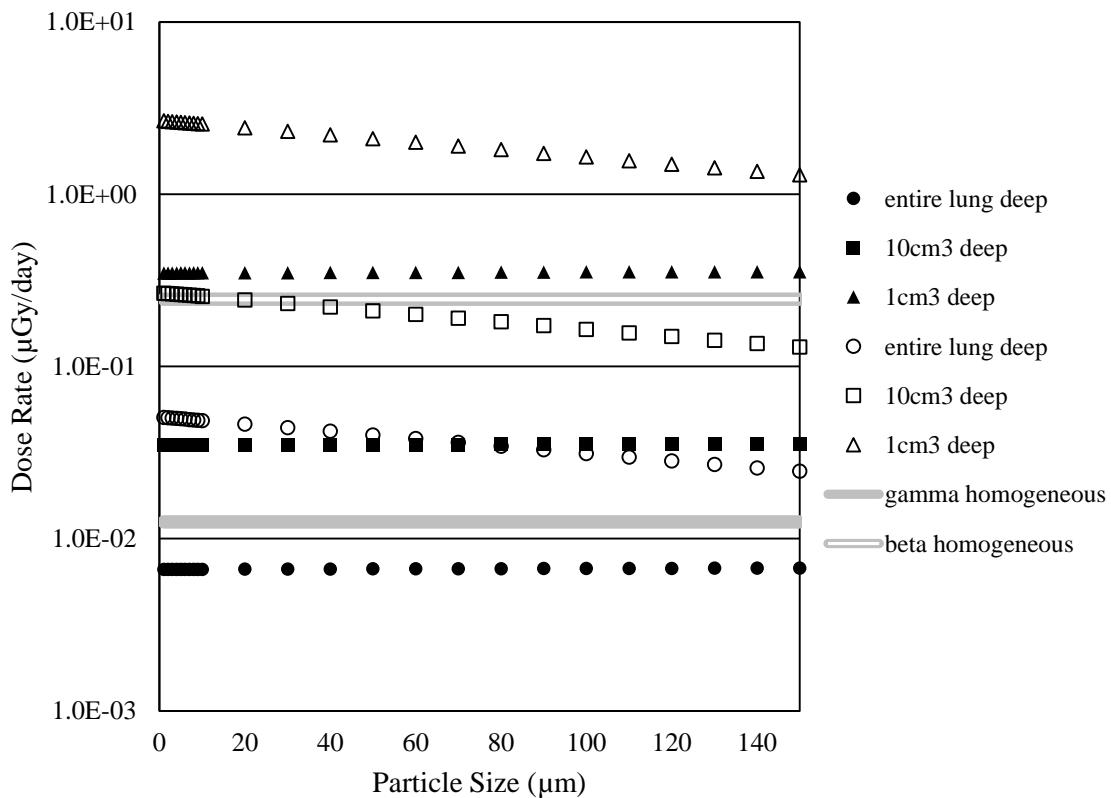


Figure 4-2: Lung dose rates for various particle sizes assuming placement of the particle deep within the lung. Closed symbols are for ^{137}Cs , open symbols for ^{90}Sr . The models compare the same activity in the lung, either distributed homogeneously or contained within a single particle.

Lung dose was the highest when particles were placed in the mid lung (1.7 times the deep lung dose). The models compare the same activity in the lung, either distributed

homogeneously or contained within a single particle. Using an averaging volume of 10 cm³ yielded a particulate dose rate 4.6 times higher than that calculated for the homogeneous case (mid-lung dose). In the mid-lung case, when the entire lung is used as the averaging volume, the homogeneous and particulate dose rates are essentially identical. For the deep and top lung cases using the entire lung as the averaging volume, the particulate dose rates are 1.5 and 1.9 times lower, respectively, than the homogeneous dose rate.

4.3.2. Electron Emitters

Electrons have a short range in tissue, and thus less energy escapes the organ/volume resulting in order-of-magnitude higher dose rates (Figure 4-2). The dose rate decreases by a factor of two over the particle size range considered here indicating a relative increase in self-shielding with particle size (Figure 4-2). Due to their limited range in tissue, translocating the particle from the deep lung to the mid or top of the lung did not change the dose rates. For electrons, the homogeneous dose rate is generally higher than the particulate dose rate for the averaging volumes of the entire organ and 10 cm³. Using an averaging volume of 1 cm³ yields a dose rate that is higher than that calculated for the homogeneous case by factors of 11 and 5.3 for 1 µm particles and 150 µm particles, respectively.

4.3.3. Alpha Emitters

Alpha particles have a very short range in tissue. When alpha radioactivity is incorporated into particulate form, it is often assumed that much of the source energy is locked within the particle due to self-shielding effects and does not contribute to the

organ dose rate. This is the case for plutonium particles of about $20\text{ }\mu\text{m}$ and larger in which more than 90% of the alpha emission energy is self-shielded (Figure 4-3).

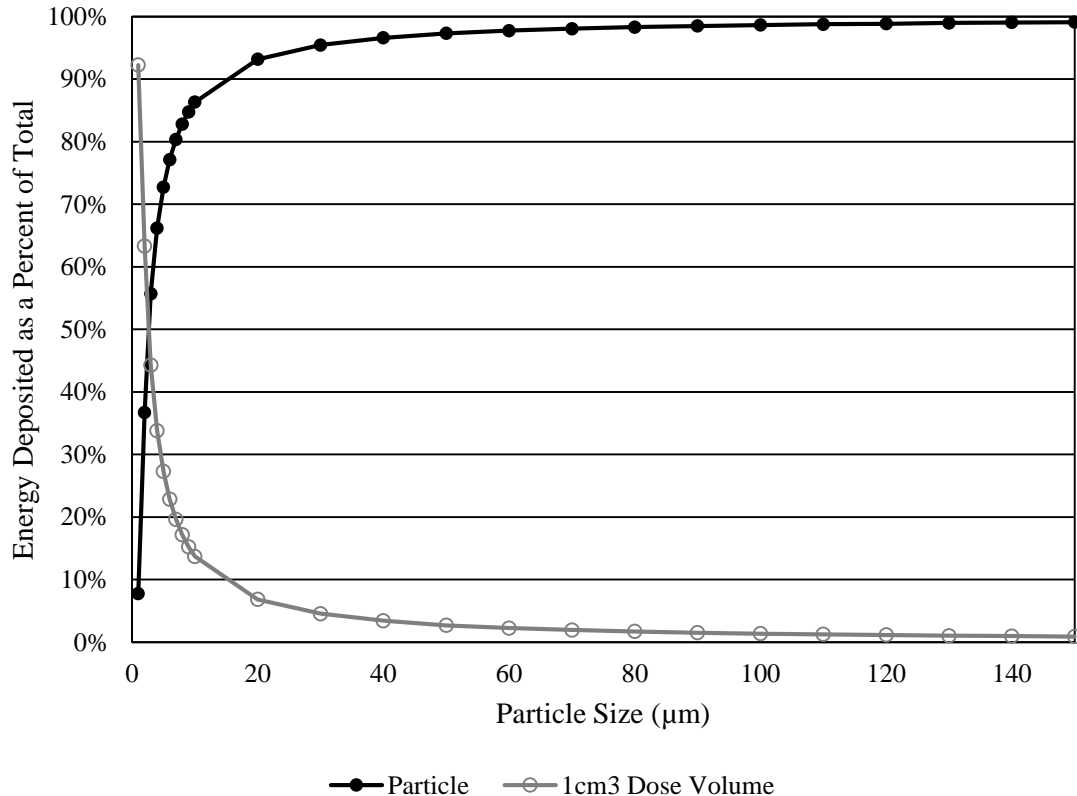


Figure 4-3: ^{239}Pu energy deposition in the source particle and a 1 cm^3 dose volume as a percent of initial energy.

However, for particles in the respirable range of less than $5\text{ }\mu\text{m}$, an average of 52% of the energy escapes the particle and irradiates the surrounding tissue. The majority of these emissions are not self-shielded but rather deposit energy into the tissue. This result has important implications as it is particles less than $5\text{ }\mu\text{m}$ in diameter that penetrate deep into the lung and can remain there for extended periods imparting energy and contributing to

long term dose rates. As most plutonium accumulates on the fine fraction of soil particles, when such particles are inhaled, they may represent a significant contributor to the internal dose rates of wildlife. The self-shielding effect is clearly seen in Figure 4-3, which shows the energy deposited in the particle itself verses energy deposited in a 1 cm³ tissue dose volume as a percent of the total energy.

To consider a more realistic exposure scenario in which the concentration of plutonium found in individual particles in a given location is static, dose rates were calculated for the same quantity of plutonium in each particle, over a wide range of particle sizes, and a range of plutonium contents (1%, 10%, and 50% plutonium as $^{239}\text{PuO}_2$) using dose averaging volumes of 1 cm³ (Figure 4-4 closed symbols) and 100 μm^3 (Figure 4-4 open symbols).

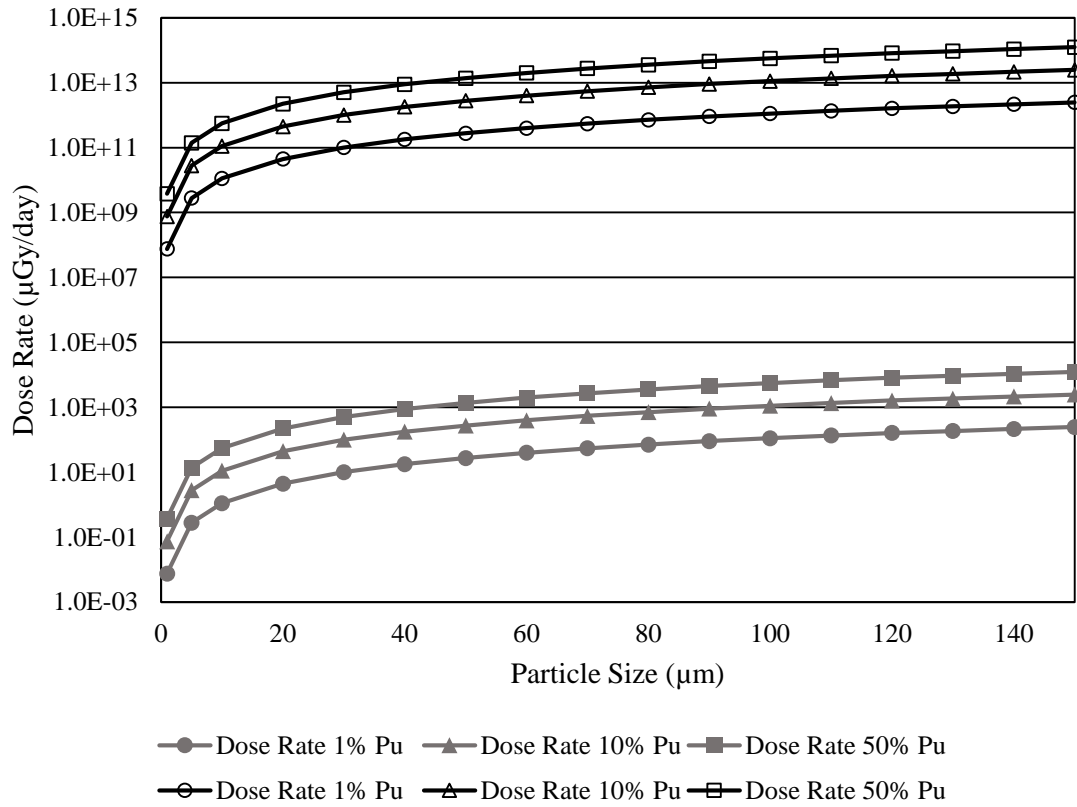


Figure 4-4: Dose rates for 1 cm³ (closed symbols) and 100 μm³ (open symbols) dose volumes assuming 1%, 10%, and 50% of the particle is plutonium. Here the amount of plutonium in each particle is no longer a constant, but increases with particle size.

These ranges are generally representative of particles at former weapons testing sites such as those found at the Maralinga site [32], [43], [75]. Results indicate the dose rate increases over several orders of magnitude with increasing particle size (Figure 4-4). Dose rates are a factor of 1.0E+10 higher for the smaller 100 μm³ dose averaging volume (Figure 4-4). Figure 4-4 illustrates two competing effects: the increase in self-shielding due to particle size is diminished by the increasing amount of plutonium present in the particle itself. The steep increase in dose rate with particle size drops off between 10 and

20 μm , and dose rates level out as particle size is increased. Additionally, Figure 4-4 allows for a quick estimation of lung dose rate for small mammals given a known particle size and percentage of plutonium, which may be of use to those engaged in environmental radioprotection at sites where there is plutonium contamination.

The implications of these high, localized dose rates are difficult to quantify, particularly for biota in uncontrolled (natural) environments such as the one studied here. Previous laboratory studies have demonstrated a reduction in carcinogenesis in animals exposed to particulate radiation vs. soluble forms [62], [63], [66]. However, there is a paucity of information on biological effects of inhaled hot particles in mammals in the environmental exposure conditions. Our results on dose rates and particle self-shielding provide a useful basis for future assessment of dose effects to biota living in environments contaminated by hot particles.

4.4. Conclusions

Lung dose rates were examined for alpha, beta, and gamma emitting radionuclides with the same activity distributed both heterogeneously in hot particle form and homogeneously throughout the entire lung. For photons, there is minimal change in dose rate with particle size. When the entire organ is used as the dose averaging volume, particulate dose rates for photons are slightly lower than their homogeneous counterparts. However, for electron emitters, particulate dose rates are significantly lower than those calculated for the homogeneous case when the entire lung is used as the dose averaging volume. Overall particulate dose rates decrease slightly with particle size, indicating that there is a perceptible self-shielding effect for electron emitters. This self-shielding effect

is stronger in alpha particles which have a size threshold at a diameter of approximately 5 μm . Above this size, most of the emissions are shielded. Below this size, more than 50% of the initial alpha particle energy escapes the particle and irradiates the surrounding tissue. The significance of this result is that it is these small particles which may lodge deep in the lungs and contribute significantly to long term dose rates. Additionally, dose rates for particles containing various amounts of plutonium were calculated, and it was determined that dose rates increase with greater particle size. This is driven by the increased quantity of plutonium present in larger particles that dominates the self-shielding effect. Given the wide range of dose rates calculated here, in ecosystems where particulate contamination is present, it is suggested that analysis methods capable of determining particulate size are employed to allow for more accurate determinations of dose rate.

4.5. References

See Chapter 6.

5. CONCLUSIONS

The research sought to characterize the uncertainty introduced in wildlife radiation dose rate calculations from tissue composition and density, geometry, and homogeneity, and to comment on the applicability of ellipsoidal models in a regulatory context. In a comparison of four-part tissue composition versus complex, realistic tissue composition, the maximum potential uncertainty introduced is a factor of 1.1 for photon emitters, and no difference for electron emitters. In comparing a tissue density of unity with a measured value of tissue density, the maximum potential uncertainty was a factor of 1.5 for photon emitters and 1.1 for electron emitters. For both tissue composition and density, the assumption is not conservative, meaning that the predicted dose rate using simplistic tissue composition and unit density will under predict wildlife dose rates. Next, dose rates calculated from a simple ellipsoidal representation of the rabbit were compared to dose rates calculated from a more complex anatomical phantom of the rabbit. The maximum potential uncertainty introduced was found to be a factor of 1.4 for photon emitters and 5.3 for electron emitters. In this case the simplified model is conservative, meaning that predicted dose rates using the simple ellipsoidal model will be greater than those predicted by the voxel model. This work examined the effects of homogeneity for the specific case of hot particle exposures. For inhaled hot particles (e.g. embedded deep in the lung of a mammal), dose rates are entirely dependent on the averaging volume selected for analysis. When the entire organ is used as the dose averaging volume, particulate dose rates for photons are slightly lower than their homogeneous counterparts. However, for electron emitters, particulate dose rates are significantly lower than those calculated for the homogeneous case when the entire lung is used as the dose averaging

volume. In cases where the radionuclide(s) of interest is (are) known to partition heterogeneously (e.g. radioiodine, bone seeking radionuclides such as $^{226,228}\text{Ra}$ or ^{90}Sr , and radionuclides bound to sediments within the GI tract) should be evaluated on a site-specific and case-by-case basis as the dose to the critical organ (i.e., the organ into which a radionuclide is heterogeneously partitioned) may be considerably higher than that calculated using the homogeneous assumption. Such dose rates may be several orders of magnitude higher than the whole-body, homogeneous distribution dose rate.

A robust method for calculating organ dose-rates may prove useful in elucidating mechanisms by which radiation-induced effects arise in wildlife populations. The continued use of ellipsoidal models as the basis for the majority of regulatory dose assessments seems appropriate. Voxel models may be more useful than geometric models in scenarios where accurate, rather than conservative estimates of dose rates are desired, such as aiding in the interpretation of effects studies, in assessing limits on routine discharges, or in interpreting dose measurement data gathered at a single point on the body (e.g. a TLD on an animal collar) which may receive dose from internal organs.

6. REFERENCES

- [1] J. E. Brown, B. Alfonso, R. Avila, N. a. Beresford, D. Copplestone, G. Pröhle, and A. Ulanovsky, “The ERICA Tool,” *J. Environ. Radioact.*, vol. 99, no. 9, pp. 1371–1383, Sep. 2008.
- [2] ICRP, “Environmental Protection: The Concept and Use of Reference Animals and Plants. ICRP Publication 108.,” *Ann. ICRP*, vol. 38, no. 4–6, 2008.
- [3] J. M. Gómez-Ros, G. Pröhle, A. Ulanovsky, and M. Lis, “Uncertainties of internal dose assessment for animals and plants due to non-homogeneously distributed radionuclides.,” *J. Environ. Radioact.*, vol. 99, no. 9, pp. 1449–55, Sep. 2008.
- [4] E. Ruedig, N. A. Beresford, M. E. Gomez Fernandez, and K. Higley, “A comparison of the ellipsoidal and voxelized dosimetric methodologies for internal, heterogeneous radionuclide sources.,” *J. Environ. Radioact.*, vol. 140, pp. 70–77, Nov. 2014.
- [5] E. A. Caffrey and K. A. Higley, “Creation of a voxel phantom of the ICRP reference crab,” *J. Environ. Radioact.*, vol. 120, pp. 14–18, 2013.
- [6] E. A. Caffrey, “Improvements in the Dosimetric Models of Selected Benthic Organisms. Oregon State University Master’s Thesis.,” Oregon State University, 2012.
- [7] E. Ruedig, E. A. Caffrey, C. Hess, and K. A. Higley, “Monte Carlo Derived Absorbed Fractions for a Voxelized Model of *Oncorhynchus Mykiss*, a Rainbow Trout,” *Radiat. Environ. Biophys.*, vol. 53, no. 3, pp. 581–587, 2014.
- [8] M. G. Stabin, T. E. Peterson, G. E. Holburn, and M. A. Emmons, “Voxel-Based Mouse and Rat Models for Internal Dose Calculations,” *J. Nucl. Med.*, vol. 47, pp. 655–659, 2006.
- [9] S. Kinase, “Voxel-Based Frog Phantom for Internal Dose Evaluation,” *J. Nucl. Sci. Technol.*, vol. 45, no. 10, pp. 1049–1052, 2008.
- [10] B. Dogdas, D. Stout, A. F. Chatzioannou, and R. M. Leahy, “Digimouse: a 3D whole body mouse atlas from CT and cryosection data.,” *Phys. Med. Biol.*, vol. 52, no. 3, pp. 577–587, 2007.
- [11] L. Padilla, C. Lee, R. Milner, A. Shahlaee, and W. E. Bolch, “Canine anatomic phantom for preclinical dosimetry in internal emitter therapy.,” *J. Nucl. Med.*, vol. 49, no. 3, pp. 446–52, Mar. 2008.
- [12] G. H. Kramer, K. Capello, S. Strocchi, B. Bearrs, K. Leung, and N. Martinez, “The HML’s New Voxel Phantoms,” *Health Phys.*, vol. 103, no. 6, pp. 802–807, 2012.
- [13] N. E. Martinez, T. E. Johnson, K. Capello, J. E. P. Iii, and M. Carlo, “Development and comparison of computational models for estimation of absorbed organ radiation dose in rainbow trout (*Oncorhynchus mykiss*) from uptake of iodine-131,” *J. Environ. Radioact.*, vol. 138, pp. 50–59, 2014.

- [14] T. L. Yankovich, N. a Beresford, M. D. Wood, T. Aono, P. Andersson, C. L. Barnett, P. Bennett, J. E. Brown, S. Fesenko, J. Fesenko, A. Hosseini, B. J. Howard, M. P. Johansen, M. M. Phaneuf, K. Tagami, H. Takata, J. R. Twining, and S. Uchida, “Whole-body to tissue concentration ratios for use in biota dose assessments for animals.,” *Radiat. Environ. Biophys.*, vol. 49, no. 4, pp. 549–65, 2010.
- [15] ICRP, “The Metabolism of Plutonium and Related Elements. ICRP Publication 48.,” *Ann. ICRP*, vol. 16, no. 2–3, 1986.
- [16] ICRP, “Age-dependent Doses to Members of the Public from Intake of Radionuclides - Part 2 Ingestion Dose Coefficients. ICRP Publication 67.,” *Ann. ICRP*, vol. 23, no. 3–4, 1993.
- [17] M. P. Johansen, D. P. Child, E. A. Caffrey, E. Davis, J. J. Harrison, M. A. C. Hotchkis, T. E. Payne, A. Ikeda-Ohno, S. Thiruvoth, J. R. Twining, and N. A. Beresford, “Accumulation of plutonium in mammalian wildlife tissues following dispersal by accidental-release tests,” *J. Environ. Radioact.*, vol. In press., 2015.
- [18] G. H. Kramer, K. Capello, A. Chiang, E. Cardenas-Mendez, and T. Sabourin, “Tools for Creating and Manipulating Voxel Phantoms,” *Health Phys.*, vol. 98, no. 3, pp. 542–548, 2010.
- [19] X-5 Monte Carlo Team, “MCNP5 Manual Volume 1,” Los Alamos National Laboratory, Report No. LA-UR-03-1987., 2008.
- [20] A. Ulanovsky and G. Pröhl, “A practical method for assessment of dose conversion coefficients for aquatic biota.,” *Radiat. Environ. Biophys.*, vol. 45, no. 3, pp. 203–14, Sep. 2006.
- [21] P. W. Webb, “How does benthic living affect body volume, tissue composition, and density of fishes?,” *Can. J. Zool.*, vol. 68, pp. 1250–1255, 1990.
- [22] E. Pella, “Elemental Organic Analysis. Part 1. Historical Developments,” *Am. Lab.*, vol. 22, no. 3, pp. 116–125, 1990.
- [23] E. Pella, “Elemental Organic Analysis. Part 2. State of the Art,” *Am. Lab.*, vol. 22, no. 12, pp. 28–32, 1990.
- [24] T. G. Hinton, J. S. Bedford, J. C. Congdon, and F. W. Whicker, “Effects of radiation on the environment: a need to question old paradigms and enhance collaboration among radiation biologists and radiation ecologists.,” *Radiat. Res.*, vol. 162, no. 3, pp. 332–338, 2004.
- [25] A. Beresford, N.A., Copplestone, D., Hosseini, J. E. Brown, M. P. Johansen, G. Hirth, S. Sheppard, E. Dagher, T. Yankovich, S. Uchida, J. Napier, I. Outola, C. Wells, B. J. Howard, C. L. Barnett, and M. D. Wood, “An international database of radionuclide concentration ratios for wildlife: development and uses,” in *3rd International Conference on Radioecology and Environmental Radioactivity*, 2014.

- [26] C. Howard, B.J., Beresford, N.A., Copplestone, D., Telleria, D., Proehl, G., Fesenko, S., Jeffree, R.A., Yankovich, T.L., Brown, J.E., Higley, K., Johansen, M.P., Mulye, H., Vandenhove, H., Gashchak, S., Wood, M.D., Takata, H., Andersson, P., Dale, P., Ryan, "The IAEA handbook on radionuclide transfer to wildlife," *J. Environ. Radioact.*, vol. 121, pp. 55–74, 2013.
- [27] M. D. Wood, N. A. Beresford, B. J. Howard, and D. Copplestone, "Evaluating summarised radionuclide concentration ratio datasets for wildlife.,," *J. Environ. Radioact.*, vol. 126, pp. 314–25, Dec. 2013.
- [28] J. M. Gomez-Ros, G. Prohl, A. Ulanovsky, and M. Lis, "Uncertainties of internal dose assessment for animals and plants due to non-homogeneously distributed radionuclides," *J. Environ. Radioact.*, vol. 99, pp. 1449–1455, 2008.
- [29] E. A. Caffrey, M. P. Johansen, and K. A. Higley, "Voxel Modeling of Rabbits for Use in Radiological Dose Rate Calculations," *J. Environ. Radioact.*, vol. 151, no. 2, pp. 480–486, 2016.
- [30] A. Real, S. Sundell-Bergman, J. F. Knowles, D. S. Woodhead, and I. Zinger, "Effects of ionising radiation exposure on plants, fish and mammals: relevant data for environmental radiation protection," *J. Radiol. Prot.*, vol. 24, no. 4A, pp. A123–A137, Dec. 2004.
- [31] J. F. Park, "Inhaled plutonium oxide in dogs, Pacific Northwest Laboratory Annual Report for 1985 to the DOE Office of Energy Research, Part I. Biomedical Sciences. PNL-5750.,," Springfield, Virginia, 1986.
- [32] B. W. Church, J. M. Costello, D. R. Davy, K. H. Lokan, L. J. Morris, and T. A. Vaeth, "Rehabilitation of Former Nuclear Test Sites at Emu and Maralinga," Canberra, Australia, 2003.
- [33] S. M. Haywood and J. G. Smith, "Assessment of potential doses at the Maralinga and Emu test sites.,," *Health Phys.*, vol. 63, no. 6, pp. 624–30, Dec. 1992.
- [34] P. W. Durbin, "Plutonium in Mammals: Influence of Plutonium Chemistry, Route of Administration, and Physiological Status of the Animal on Initial Distribution and Long-Term Metabolism," *Health Phys.*, vol. 29, pp. 495–510, 1975.
- [35] M. P. Johansen, D. P. Child, E. Davis, C. Doering, J. J. Harrison, M. a C. Hotchkis, T. E. Payne, S. Thiruvoth, J. R. Twining, and M. D. Wood, "Plutonium in wildlife and soils at the Maralinga legacy site: persistence over decadal time scales.,," *J. Environ. Radioact.*, pp. 1–9, Nov. 2013.
- [36] D. D. Smith, K. R. Giles, D. E. Bernhardt, and K. W. Brown, "Animal Investigation Program 1976 Annual Report: Nevada Test Site and Vicinity," Las Vegas, NV, 1978.
- [37] H. N. Friesen, "Summary of the Nevada Applied Ecology Group and Correlative Programs," Las Vegas, NV, 1992.
- [38] M. White, P. Dunaway, and W. Howard, "Environmental Plutonium on the

- Nevada Test and Environs," Las Vegas, NV, 1977.
- [39] T. M. Poston and A. T. Cooper, "A Qualitative Evaluation of Radionuclide Concentrations in Hanford Site Wildlife, 1983 Through 1992," Richland, WA., 1994.
- [40] Y. Kubota, H. Takahashi, Y. Watanabe, S. Fuma, I. Kawaguchi, M. Aoki, M. Kubota, Y. Furuhata, Y. Shigemura, F. Yamada, T. Ishikawa, S. Obara, and S. Yoshida, "Estimation of absorbed radiation dose rates in wild rodents inhabiting a site severely contaminated by the Fukushima Dai-ichi nuclear power plant accident," *J. Environ. Radioact.*, vol. 142, pp. 124–131, 2015.
- [41] A. Mohammadi, S. Kinase, and K. Saito, "Evaluation of absorbed doses in voxel-based and simplified models for small animals.," *Radiat. Prot. Dosimetry*, vol. 150, no. 3, pp. 283–91, Jan. 2012.
- [42] A. Mohammadi, S. Kinase, and K. Saito, "Comparison of Photon and Electron Absorbed Fractions in Voxel-Based and Simplified Phantoms for Small Animals," *Prog. Nucl. Sci. Technol.*, vol. 2, pp. 365–368, 2011.
- [43] ANSTO, "Final Report to the Technical Assessment Group for the Maralinga Rehabilitation Project," Lucas Heights, NSW Australia, 1990.
- [44] P. A. Burns, M. B. Cooper, P. N. Johnston, L. J. Martin, and G. A. Williams, "Determination of the Ratios of ^{239}Pu and ^{240}Pu to ^{241}Am for Nuclear Weapons Test Sites in Australia," *Health Phys.*, vol. 67, no. 3, pp. 226–232, 1994.
- [45] M. a. C. Hotchkis, D. P. Child, and B. Zorko, "Actinides AMS for nuclear safeguards and related applications," *Nucl. Instruments Methods Phys. Res. Sect. B Beam Interact. with Mater. Atoms*, vol. 268, no. 7–8, pp. 1257–1260, Apr. 2010.
- [46] J. J. Harrison, A. Zawadzki, R. Chisari, and H. K. Y. Wong, "Separation and measurement of thorium, plutonium, americium, uranium and strontium in environmental matrices.," *J. Environ. Radioact.*, vol. 102, no. 10, pp. 896–900, Oct. 2011.
- [47] M. P. Johansen, E. Ruedig, K. Tagami, S. Uchida, K. Higley, and N. a. Beresford, "Radiological Dose Rates to Marine Fish from the Fukushima Daiichi Accident: The First Three Years Across the North Pacific," *Environ. Sci. Technol.*, vol. 49, no. 3, pp. 1277–1285, 2015.
- [48] N. a. Beresford, B. J. Howard, R. W. Mayes, and C. S. Lamb, "The transfer of radionuclides from saltmarsh vegetation to sheep tissues and milk," *J. Environ. Radioact.*, vol. 98, no. 1–2, pp. 36–49, 2007.
- [49] ICRP, "Age-dependent Doses to Members of the Public from Intake of Radionuclides - Part 1. ICRP Publication 56.," *Ann. ICRP*, vol. 20, no. 2, 1990.
- [50] B. Salbu, "Actinides associated with Particles," in *Plutonium in the Environment*, 2001, pp. 121–138.
- [51] A. B. Kersting, "Plutonium transport in the environment," *Inorg. Chem.*, vol. 52,

- no. 7, pp. 3533–46, May 2013.
- [52] S. Hashimoto, S. Ugawa, K. Nanko, and K. Shichi, “The total amounts of radioactively contaminated materials in forests in Fukushima, Japan.,” *Sci. Rep.*, vol. 2, p. 416, Jan. 2012.
- [53] F. B. Turner, R. H. Rowland, and R. a Wood, “Radioactivity in Jackrabbits After the Sedan Test,” *J. Wildl. Manage.*, vol. 30, no. 2, pp. 433–443, 1966.
- [54] M. J. Berger, J. S. Coursey, M. A. Zucker, and J. Chang, “ESTAR, PSTAR, and ASTAR: Computer Programs for Calculating Stopping-Power and Range Tables for Electrons, Protons, and Helium Ions,” *National Institute of Standards and Technology*. NIST, Gaithersburg, MD, 2005.
- [55] P. Andersson, J. Garnier-Laplace, N. a. Beresford, D. Copplestone, B. J. Howard, P. Howe, D. Oughton, and P. Whitehouse, “Protection of the environment from ionising radiation in a regulatory context (protect): proposed numerical benchmark values,” *J. Environ. Radioact.*, vol. 100, no. 12, pp. 1100–1108, 2009.
- [56] L. J. Dallas, M. Keith-Roach, B. P. Lyons, and A. N. Jha, “Assessing the Impact of Ionizing Radiation on Aquatic Invertebrates: A Critical Review,” *Radiat. Res.*, vol. 177, no. 5, pp. 693–716, 2012.
- [57] C. M. Larsson, “An overview of the ERICA Integrated Approach to the assessment and management of environmental risks from ionising contaminants,” *J. Environ. Radioact.*, vol. 99, no. 9, pp. 1364–1370, Sep. 2008.
- [58] A. Ulanovsky, G. Pröhl, and J. . M. Gómez-Ros, “Methods for calculating dose conversion coefficients for terrestrial and aquatic biota.,” *J. Environ. Radioact.*, vol. 99, no. 9, pp. 1440–8, Sep. 2008.
- [59] M. W. Charles, “The Hot Particle Problem,” *Radiat. Prot. Dosimetry*, vol. 39, no. 1–3, pp. 39–47, 1991.
- [60] F. J. Sandalls, “Hot particles from Chernobyl,” *J. Environ. Radioact.*, vol. 18, no. 1, pp. 5–22, 1993.
- [61] P. J. Darley, M. W. Charles, I. E. Othman, A. S. Al-Aydarous, and A. J. Mill, “Origins and Dosimetry of ‘Hot Particles’ from Nuclear Plant Operation,” *Radiat. Prot. Dosimetry*, vol. 92, no. 1–3, pp. 131–137, 2000.
- [62] M. W. Charles and J. D. Harrison, “Hot particle dosimetry and radiobiology—past and present,” *J. Radiol. Prot.*, vol. 27, pp. A97–A109, 2007.
- [63] J. D. Harrison and J. W. Stather, “The assessment of doses and effects from intakes of radioactive particles,” *J. Anat.*, vol. 189, no. 3, pp. 521–30, Dec. 1996.
- [64] C. R. Richmond, J. Langham, and R. S. Stone, “Biological Response to Small Discrete Highly Radioactive Sources. II. Morphogenesis of Microlesions in Rat Lungs From Intravenously Injected $^{238}\text{PuO}_2$ Microspheres,” *Health Phys.*, vol. 18, pp. 401–408, 1970.

- [65] C. L. Sanders, “Effects of PuO₂ Particles Deposited in the Lung Following Intraperitoneal Injection,” *Health Phys.*, vol. 28, pp. 84–86, 1975.
- [66] C. L. Sanders, G. E. Dagle, W. C. Cannon, G. J. Powers, and D. M. Meier, “Inhalation Carcinogenesis of High-Fired 238-PuO₂ in Rats,” *Radiat. Res.*, vol. 71, no. 3, pp. 528–546, 1977.
- [67] B. E. Lambert, M. L. Phipps, P. J. Lindop, A. Black, and S. R. Moores, “Induction of Lung tumors in mice following the inhalation of 239-PuO₂,” in *Proc. 3rd Int. Symp. on SRP Inverness*, 1982, pp. 370–375.
- [68] M. W. Charles, A. J. Mill, and P. J. Darley, “Carcinogenic risk of hot-particle exposures.,” *J. Radiol. Prot.*, vol. 23, no. 1, pp. 5–28, Mar. 2003.
- [69] NCRP, “Alpha-emitting particles in Lungs. NCRP Report No 46.,” Bethesda, MD, 1975.
- [70] ICRP, “The Biological Basis for Dose Limitation in the Skin. ICRP Publication 59.,” *Ann. ICRP*, vol. 22, no. 2, 1992.
- [71] NCRP, “Biological effects and exposure limits for ‘hot particles’. NCRP Report No 130.,” Bethesda, MD, 1999.
- [72] C. L. Sanders, “Deposition patterns and toxicity of transuranium elements in lung,” *Health Phys.*, vol. 22, pp. 607–615, 1972.
- [73] J. H. Diel, J. A. Mewhinney, and M. B. Snipes, “Distribution of inhaled 238PuO₂ particles in Syrian hamster lungs,” *Radiat. Res.*, vol. 88, pp. 299–312, 1981.
- [74] D. L. Lundgren, D. L. Damon, J. H. Diel, and F. F. Hahn, “The deposition, distribution and retention of inhaled 239PuO₂ in the lungs of rats with pulmonary emphysema,” *Health Phys.*, vol. 40, pp. 231–235, 1981.
- [75] P. A. Burns, M. B. Cooper, C. J. Duggleby, F. Mika, Joachim, and G. A. Williams, “Plutonium-contaminated fragments at the Taranaki site at Maralinga.” Australian Radiation Laboratory, Yallambie, Victoria, 1986.
- [76] ARL, “Inhalation Hazard Assessment at Maralinga and Emu. Technical Report ARL/TR087.,” Yallambie, Victoria, 1990.
- [77] M. B. Cooper, P. A. Burns, B. L. Tracy, M. J. Wilks, and G. A. Williams, “Characterization of plutonium contamination at the former nuclear weapons testing range at Maralinga in South Australia,” *J. Radioanal. Nucl. Chem.*, vol. 177, no. 1, pp. 161–184, 1994.
- [78] ICRP, “Limits for Intakes of Radionuclides by Workers. ICRP Publication 30.,” *Ann. ICRP*, vol. 2, no. 3–4, 1979.
- [79] N. A. Beresford, “The transfer of radionuclides to wildlife,” *Radiat. Environ. Biophys.*, vol. 49, no. 4, pp. 505–8, Nov. 2010.
- [80] D. B. Pelowitz, J. T. Goorley, M. R. James, T. E. Booth, F. B. Brown, J. S. Bull, L. J. Cox, J. W. Durkee, J. S. Elson, M. L. Fensin, R. A. Forster, J. S. Hendricks, H.

- G. Hughes, R. C. Johns, B. C. Kiedrowski, and S. G. Mashnik, “MCNP6 User’s Manual,” Los Alamos National Laboratory, Report No. LA-CP-13-00634, Rev. 0., 2013.
- [81] A. Ikeda-Ohno, M. P. Johansen, T. E. Payne, M. A. C. Hotchkis, and D. P. Child, “XFM Studies of Plutonium Dispersed in an Arid Environment,” in *12th International Conference on X-Ray Microscopy*, 2014.
 - [82] NIST, “NIST Standard Reference Databases,” 2010. [Online]. Available: <http://www.nist.gov/srd/onlinelist.cfm>.
 - [83] K. Adachi, M. Kajino, Y. Zaizen, and Y. Igarashi, “Emission of spherical cesium-bearing particles from an early stage of the Fukushima nuclear accident.,” *Sci. Rep.*, vol. 3, no. 2554, pp. 1–5, 2013.
 - [84] H. Q. Woodard and D. R. White, “The composition of body tissues,” *Br. J. Radiol.*, vol. 59, no. 708, pp. 1209–18, 1986.

7. APPENDICES

7.1. APPENDIX A – Rabbit tissue density and composition data

Rabbit tissues with measured tissue composition and density

The ratio is a measure of the difference between the adult rabbit tissue composition and the human tissue composition. If Ratio = 1, rabbit tissue is identical to human tissue for that element. If Ratio > 1, rabbit tissue has MORE of that element than human tissue. If Ratio < 1, rabbit tissue has LESS of that element than human tissue.

Element	Juvenile Rabbit BONE	Adult Rabbit BONE	Human BONE*	Ratio
density (g/cc)	1.3	1.5	1.85	--
H (Z=1)	0.036706	0.050682	0.047234	1.07
C (Z=6)	0.240115	0.318947	0.144330	2.21
N (Z=7)	0.064589	0.046877	0.041990	1.12
O (Z=8)	0.338241	0.263144	0.446096	0.59
Mg (Z=12)	0.002200	0.002200	0.002200	1.00
P (Z=15)	0.104970	0.104970	0.104970	1.00
S (Z=16)	0.003150	0.003150	0.003150	1.00
Ca (Z=20)	0.209930	0.209930	0.209930	1.00
Zn (Z=30)	0.000100	0.000100	0.000100	1.00

*ICRP cortical bone; fraction by weight

Element	Adult Rabbit TESTES	Human TESTES [^]	Ratio
density (g/cc)	1.1	1.04	--
H (Z=1)	0.074912	0.104166	0.72
C (Z=6)	0.483130	0.092270	5.24
N (Z=7)	0.114906	0.019940	5.76
O (Z=8)	0.317312	0.773884	0.41
Na (Z=11)	0.002260	0.002260	1.00
Mg (Z=12)	0.000110	0.000110	1.00
P (Z=15)	0.001250	0.001250	1.00
S (Z=16)	0.001460	0.001460	1.00
Cl(Z=17)	0.002440	0.002440	1.00
K (Z=19)	0.002080	0.002080	1.00
Ca (Z=20)	0.000100	0.000100	1.00
Fe (Z=26)	0.000020	0.000020	1.00
Zn (Z=30)	0.000020	0.000020	1.00

[^]ICRP testes; fraction by weight

Element	Juvenile Rabbit KIDNEYS	Adult Rabbit KIDNEYS	Human KIDNEYS**	Ratio
density (g/cc)	1.1	1.1	1.0	--
H (Z=1)	0.075666	0.082061	0.101172	0.81
C (Z=6)	0.490600	0.508575	0.111000	4.58
N (Z=7)	0.115463	0.117520	0.026000	4.52
O (Z=8)	0.318271	0.291845	0.761828	0.38

**ICRU 4 component; fraction by weight

Element	Juvenile Rabbit HEART	Adult Rabbit HEART	Human HEART#	Ratio
density (g/cc)	1.2	1.2	1.04	--
H (Z=1)	0.052072	0.079254	0.101997	0.78
C (Z=6)	0.382275	0.502299	0.123000	4.08
N (Z=7)	0.102919	0.125030	0.035000	3.57
O (Z=8)	0.451734	0.282417	0.729003	0.39
Na (Z=11)	0.000800	0.000800	0.000800	1.00
Mg (Z=12)	0.000200	0.000200	0.000200	1.00
P (Z=15)	0.002000	0.002000	0.002000	1.00
S (Z=16)	0.005000	0.005000	0.005000	1.00
K (Z=19)	0.003000	0.003000	0.003000	1.00

#ICRU striated muscle; fraction by weight

Element	Juvenile Rabbit LIVER	Adult Rabbit LIVER	Human LIVER**	Ratio
density (g/cc)	1.1	1.1	1.0	--
H (Z=1)	0.073712	0.080397	0.101172	0.79
C (Z=6)	0.489518	0.535814	0.111000	4.83
N (Z=7)	0.114291	0.118292	0.026000	4.55
O (Z=8)	0.322479	0.265497	0.761828	0.35

**ICRU 4 component; fraction by weight

Rabbit tissues with measured tissue composition only

Element	Juvenile Rabbit GI TRACT	Adult Rabbit GI TRACT
density (g/cc)	1.0	1.0
H (Z=1)	0.069476	0.079400
C (Z=6)	0.466503	0.556927
N (Z=7)	0.087918	0.075165
O (Z=8)	0.376103	0.288509

Element	Juvenile Rabbit STOMACH CONTENTS	Adult Rabbit STOMACH CONTENTS
density (g/cc)	1.0	1.0
H (Z=1)	0.067930	0.061135
C (Z=6)	0.445294	0.453564
N (Z=7)	0.047660	0.086743
O (Z=8)	0.439116	0.398559

Element	Juvenile Rabbit FECES	Adult Rabbit FECES
density (g/cc)	1.0	1.0
H (Z=1)	0.066356	0.067841
C (Z=6)	0.437624	0.482342
N (Z=7)	0.047685	0.012695
O (Z=8)	0.448335	0.437122

Element	Juvenile Rabbit FAT	Adult Rabbit FAT
density (g/cc)*	0.92	
H (Z=1)	0.102967	0.102967
C (Z=6)	0.738839	0.738839
N (Z=7)	0.007732	0.007732
O (Z=8)	0.150461	0.150461

*ICRP adipose tissue

Element	Adult Rabbit URINARY BLADDER
density (g/cc)	1.0
H (Z=1)	0.071858
C (Z=6)	0.498235
N (Z=7)	0.088858
O (Z=8)	0.341049

Rabbit tissues using human data

Element	Juvenile Rabbit BRAIN	Adult Rabbit BRAIN
density (g/cc)	ICRP brain, 1.03	ICRP brain, 1.03
H (Z=1)	0.110667	0.110667
C (Z=6)	0.125420	0.125420
N (Z=7)	0.013280	0.013280
O (Z=8)	0.737723	0.737723
Na (Z=11)	0.001840	0.001840
Mg (Z=12)	0.000150	0.000150
P (Z=15)	0.003540	0.003540
S (Z=16)	0.001770	0.001770
Cl (Z=17)	0.002360	0.002360
K (Z=19)	0.003100	0.003100
Ca (Z=20)	0.000090	0.000090
Fe (Z=26)	0.000050	0.000050
Zn (Z=30)	0.000010	0.000010

*fraction by weight

Element	Juvenile Rabbit SKIN	Adult Rabbit SKIN
density (g/cc)	ICRP human skin, 1.1	ICRP human skin, 1.1
H (Z=1)	0.100588	0.100588
C (Z=6)	0.228250	0.228250
N (Z=7)	0.046420	0.046420
O (Z=8)	0.619002	0.619002
Na (Z=11)	0.000070	0.000070
Mg (Z=12)	0.000060	0.000060
P (Z=15)	0.000330	0.000330
S (Z=16)	0.001590	0.001590
Cl (Z=17)	0.002670	0.002670
K (Z=19)	0.000850	0.000850
Ca (Z=20)	0.000150	0.000150
Fe (Z=26)	0.000010	0.000010
Zn (Z=30)	0.000010	0.000010

*fraction by weight

7.2. APPENDIX B – Photon absorbed fractions for adult *Lepus californicus*

TARGET	PHOTON ABSORBED FRACTIONS												
	Source = BONE												
	Energy (MeV)												
	0.01	0.015	0.02	0.03	0.05	0.1	0.2	0.5	1.0	1.5	2.0	4.0	
BONE	9.57E-01	8.86E-01	7.90E-01	5.78E-01	2.66E-01	7.27E-02	4.37E-02	4.14E-02	3.68E-02	3.19E-02	2.78E-02	1.87E-02	
HEART	1.43E-04	6.30E-04	1.39E-03	2.00E-03	1.47E-03	1.13E-03	1.23E-03	1.33E-03	1.27E-03	1.17E-03	1.10E-03	8.91E-04	
KIDNEYS	--	8.62E-05	2.47E-04	4.12E-04	3.61E-04	3.06E-04	3.45E-04	3.69E-04	3.59E-04	3.37E-04	3.16E-04	2.63E-04	
GALLBLADDER	--	<u>1.51E-05</u>	<u>3.38E-05</u>	4.64E-05	<u>3.90E-05</u>	3.03E-05	3.37E-05	3.88E-05	<u>3.65E-05</u>	<u>3.87E-05</u>	<u>3.28E-05</u>	2.60E-05	
LIVER	1.66E-04	9.16E-04	1.99E-03	2.72E-03	2.01E-03	1.67E-03	1.90E-03	2.05E-03	1.95E-03	1.81E-03	1.70E-03	1.36E-03	
URINARY BLADDER	0.00E+00	--	5.33E-05	1.35E-04	1.28E-04	1.09E-04	1.18E-04	1.20E-04	1.16E-04	1.12E-04	1.02E-04	8.71E-05	
LUNGS	6.77E-04	2.45E-03	4.59E-03	5.96E-03	4.26E-03	3.17E-03	3.47E-03	3.69E-03	3.53E-03	3.27E-03	3.06E-03	2.42E-03	
BLOOD	4.41E-04	1.68E-03	3.36E-03	4.89E-03	3.62E-03	2.44E-03	2.57E-03	2.73E-03	2.60E-03	2.43E-03	2.26E-03	1.83E-03	
FECES	<u>1.48E-05</u>	8.32E-05	2.24E-04	4.54E-04	4.04E-04	3.27E-04	3.61E-04	3.95E-04	3.90E-04	3.79E-04	3.42E-04	2.85E-04	
FAT	3.42E-04	8.29E-04	1.34E-03	1.68E-03	1.45E-03	1.39E-03	1.62E-03	1.75E-03	1.67E-03	1.54E-03	1.43E-03	1.13E-03	
TESTES	--	1.34E-04	5.88E-04	1.31E-03	1.12E-03	8.38E-04	8.96E-04	9.50E-04	8.94E-04	8.31E-04	7.80E-04	6.35E-04	
BRAIN	8.33E-04	1.95E-03	2.81E-03	2.80E-03	1.67E-03	1.15E-03	1.26E-03	1.35E-03	1.28E-03	1.17E-03	1.08E-03	8.00E-04	
GI TRACT	1.77E-04	7.88E-04	1.81E-03	3.03E-03	2.60E-03	2.25E-03	2.55E-03	2.84E-03	2.76E-03	2.56E-03	2.43E-03	1.96E-03	
STOMACH CONTENTS	--	7.01E-05	2.24E-04	3.80E-04	2.80E-04	2.21E-04	2.38E-04	2.63E-04	2.59E-04	2.40E-04	2.22E-04	1.81E-04	
BONE MARROW	3.76E-03	1.01E-02	1.58E-02	1.72E-02	8.99E-03	2.58E-03	1.53E-03	1.47E-03	1.36E-03	1.22E-03	1.09E-03	7.00E-04	
SKIN	3.61E-03	6.59E-03	8.05E-03	7.88E-03	5.15E-03	3.95E-03	4.51E-03	4.96E-03	4.54E-03	4.03E-03	3.66E-03	2.72E-03	
MUSCLE	2.89E-02	5.92E-02	8.15E-02	8.84E-02	6.29E-02	5.04E-02	5.67E-02	6.18E-02	5.87E-02	5.40E-02	4.98E-02	3.79E-02	
EXTERNAL	3.99E-04	8.06E-04	1.00E-03	9.79E-04	6.15E-04	4.31E-04	4.77E-04	4.63E-04	4.01E-04	3.63E-04	3.36E-04	2.74E-04	

TARGET	PHOTON ABSORBED FRACTIONS												
	Source = MUSCLE												
	Energy (MeV)												
	0.01	0.015	0.02	0.03	0.05	0.1	0.2	0.5	1.0	1.5	2.0	4.0	
BONE	7.18E-02	1.59E-01	2.28E-01	2.49E-01	1.39E-01	4.02E-02	2.26E-02	2.09E-02	1.95E-02	1.79E-02	1.65E-02	1.26E-02	
HEART	1.33E-03	2.40E-03	2.98E-03	2.64E-03	1.52E-03	1.06E-03	1.16E-03	1.24E-03	1.17E-03	1.09E-03	1.02E-03	8.16E-04	
KIDNEYS	6.62E-04	1.73E-03	2.12E-03	1.67E-03	8.91E-04	6.49E-04	7.05E-04	7.59E-04	7.10E-04	6.61E-04	6.17E-04	4.95E-04	
GALLBLADDER	1.32E-04	1.82E-04	1.67E-04	1.11E-04	5.95E-05	3.90E-05	4.77E-05	5.01E-05	4.65E-05	4.39E-05	4.18E-05	3.10E-05	
LIVER	3.77E-03	6.29E-03	6.72E-03	4.99E-03	2.75E-03	2.06E-03	2.32E-03	2.52E-03	2.40E-03	2.21E-03	2.04E-03	1.63E-03	
URINARY BLADDER	5.32E-04	9.54E-04	1.05E-03	7.75E-04	3.85E-04	2.73E-04	2.89E-04	3.06E-04	2.85E-04	2.65E-04	2.48E-04	1.93E-04	
LUNGS	2.98E-03	4.94E-03	6.13E-03	5.97E-03	3.72E-03	2.63E-03	2.84E-03	3.07E-03	2.92E-03	2.70E-03	2.52E-03	2.02E-03	
BLOOD	8.55E-03	1.47E-02	1.65E-02	1.28E-02	6.39E-03	3.63E-03	3.73E-03	4.00E-03	3.78E-03	3.48E-03	3.24E-03	2.53E-03	
FECES	7.55E-04	1.81E-03	2.28E-03	1.93E-03	1.03E-03	7.14E-04	7.75E-04	8.32E-04	7.90E-04	7.46E-04	6.81E-04	5.40E-04	
FAT	6.74E-03	8.39E-03	7.64E-03	5.08E-03	2.84E-03	2.42E-03	2.77E-03	3.00E-03	2.83E-03	2.60E-03	2.40E-03	1.83E-03	
TESTES	3.38E-03	7.31E-03	9.14E-03	6.88E-03	3.28E-03	2.08E-03	2.20E-03	2.34E-03	2.18E-03	2.01E-03	1.85E-03	1.45E-03	
BRAIN	4.23E-05	8.23E-05	2.16E-04	4.85E-04	4.15E-04	3.24E-04	3.61E-04	4.05E-04	3.85E-04	3.55E-04	3.40E-04	2.74E-04	
GI TRACT	9.44E-03	1.43E-02	1.52E-02	1.14E-02	6.09E-03	4.52E-03	5.01E-03	5.44E-03	5.16E-03	4.77E-03	4.46E-03	3.50E-03	
STOMACH CONTENTS	3.41E-04	9.97E-04	1.21E-03	9.17E-04	4.75E-04	3.24E-04	3.42E-04	3.67E-04	3.60E-04	3.37E-04	3.06E-04	2.48E-04	
BONE MARROW	7.84E-05	3.08E-04	1.91E-03	6.54E-03	5.33E-03	1.66E-03	9.27E-04	8.31E-04	7.93E-04	7.27E-04	6.88E-04	5.39E-04	
SKIN	3.03E-02	3.13E-02	2.46E-02	1.38E-02	6.22E-03	4.17E-03	4.73E-03	5.16E-03	4.70E-03	4.15E-03	3.74E-03	2.77E-03	
MUSCLE	8.24E-01	6.25E-01	4.44E-01	2.32E-01	1.04E-01	7.21E-02	8.03E-02	8.65E-02	8.01E-02	7.19E-02	6.49E-02	4.70E-02	
EXTERNAL	3.46E-03	3.51E-03	2.74E-03	1.58E-03	7.15E-04	4.34E-04	4.76E-04	4.72E-04	4.03E-04	3.62E-04	3.33E-04	2.69E-04	

TARGET	PHOTON ABSORBED FRACTIONS												
	Source = LIVER												
	Energy (MeV)												
	0.01	0.015	0.02	0.03	0.05	0.1	0.2	0.5	1.0	1.5	2.0	4.0	
BONE	1.20E-02	7.00E-02	1.58E-01	2.15E-01	1.21E-01	3.46E-02	1.83E-02	1.63E-02	1.52E-02	1.40E-02	1.31E-02	1.05E-02	
HEART	<u>2.93E-05</u>	2.69E-03	8.42E-03	9.50E-03	4.90E-03	3.05E-03	3.15E-03	3.26E-03	3.05E-03	2.83E-03	2.61E-03	2.12E-03	
KIDNEYS	8.90E-04	3.72E-03	4.49E-03	3.43E-03	1.70E-03	1.15E-03	1.23E-03	1.30E-03	1.23E-03	1.13E-03	1.05E-03	8.18E-04	
GALLBLADDER	3.65E-03	6.17E-03	5.00E-03	2.38E-03	8.90E-04	6.15E-04	6.73E-04	7.10E-04	6.59E-04	6.01E-04	5.44E-04	3.67E-04	
LIVER	8.18E-01	5.68E-01	3.53E-01	1.46E-01	5.28E-02	3.70E-02	4.17E-02	4.41E-02	3.93E-02	3.38E-02	2.92E-02	1.79E-02	
URINARY BLADDER	0.00E+00	--	<u>1.24E-05</u>	8.38E-05	8.09E-05	6.41E-05	7.47E-05	8.33E-05	8.02E-05	7.86E-05	7.18E-05	6.13E-05	
LUNGS	3.95E-02	9.16E-02	1.06E-01	6.83E-02	2.82E-02	1.68E-02	1.75E-02	1.83E-02	1.70E-02	1.55E-02	1.43E-02	1.09E-02	
BLOOD	3.78E-03	1.30E-02	2.18E-02	2.16E-02	1.07E-02	5.70E-03	5.59E-03	5.84E-03	5.46E-03	5.03E-03	4.68E-03	3.75E-03	
FECES	--	2.53E-04	1.25E-03	2.10E-03	1.30E-03	8.43E-04	8.87E-04	9.49E-04	8.96E-04	8.23E-04	7.67E-04	6.36E-04	
FAT	2.05E-03	4.15E-03	4.83E-03	3.81E-03	2.13E-03	1.73E-03	1.95E-03	2.11E-03	2.01E-03	1.85E-03	1.72E-03	1.38E-03	
TESTES	0.00E+00	--	<u>1.87E-05</u>	2.04E-04	2.67E-04	2.16E-04	2.39E-04	2.85E-04	2.98E-04	2.89E-04	2.72E-04	2.34E-04	
BRAIN	0.00E+00	0.00E+00	--	<u>2.10E-05</u>	7.03E-05	8.47E-05	1.01E-04	1.26E-04	1.28E-04	1.26E-04	1.23E-04	1.07E-04	
GI TRACT	7.80E-03	2.30E-02	3.31E-02	2.85E-02	1.44E-02	9.94E-03	1.07E-02	1.13E-02	1.06E-02	9.72E-03	9.02E-03	7.20E-03	
STOMACH CONTENTS	5.45E-03	1.81E-02	2.05E-02	1.21E-02	4.75E-03	2.92E-03	3.07E-03	3.22E-03	2.98E-03	2.70E-03	2.51E-03	1.90E-03	
BONE MARROW	0.00E+00	--	1.79E-04	1.74E-03	2.19E-03	8.06E-04	4.16E-04	3.63E-04	3.43E-04	3.27E-04	3.07E-04	2.58E-04	
SKIN	3.54E-04	3.11E-03	6.18E-03	7.99E-03	5.05E-03	3.45E-03	3.79E-03	4.19E-03	3.88E-03	3.52E-03	3.21E-03	2.60E-03	
MUSCLE	1.06E-01	1.79E-01	1.91E-01	1.41E-01	7.32E-02	4.94E-02	5.35E-02	5.78E-02	5.50E-02	5.09E-02	4.72E-02	3.69E-02	
EXTERNAL	5.77E-05	5.80E-04	1.14E-03	1.34E-03	7.58E-04	4.59E-04	4.80E-04	4.54E-04	3.95E-04	3.60E-04	3.37E-04	2.97E-04	

TARGET	PHOTON ABSORBED FRACTIONS												
	Source = TESTES												
	Energy (MeV)												
	0.01	0.015	0.02	0.03	0.05	0.1	0.2	0.5	1.0	1.5	2.0	4.0	
BONE	2.88E-04	1.48E-02	6.77E-02	1.47E-01	1.04E-01	3.11E-02	1.57E-02	1.35E-02	1.24E-02	1.14E-02	1.07E-02	8.81E-03	
HEART	0.00E+00	0.00E+00	--	<u>2.95E-05</u>	6.38E-05	6.22E-05	7.58E-05	1.05E-04	1.24E-04	1.24E-04	1.24E-04	1.12E-04	
KIDNEYS	0.00E+00	4.34E-05	4.03E-04	8.96E-04	6.34E-04	4.65E-04	4.94E-04	5.28E-04	5.00E-04	4.69E-04	4.34E-04	3.61E-04	
GALLBLADDER	0.00E+00	0.00E+00	--	--	--	<u>5.29E-06</u>	<u>7.50E-06</u>	<u>9.81E-06</u>	<u>8.73E-06</u>	--	--	<u>7.99E-06</u>	
LIVER	0.00E+00	--	<u>2.88E-05</u>	2.94E-04	3.99E-04	3.68E-04	4.22E-04	5.11E-04	5.26E-04	5.17E-04	4.85E-04	4.20E-04	
URINARY BLADDER	4.20E-03	9.71E-03	1.01E-02	5.88E-03	2.40E-03	1.54E-03	1.66E-03	1.75E-03	1.62E-03	1.48E-03	1.34E-03	9.98E-04	
LUNGS	0.00E+00	--	--	1.87E-04	3.09E-04	2.84E-04	3.25E-04	4.14E-04	4.46E-04	4.36E-04	4.28E-04	3.73E-04	
BLOOD	1.29E-04	2.52E-03	7.57E-03	1.00E-02	5.47E-03	2.94E-03	2.89E-03	3.06E-03	2.89E-03	2.68E-03	2.52E-03	2.04E-03	
FECES	4.95E-04	2.68E-03	4.60E-03	4.26E-03	2.12E-03	1.34E-03	1.42E-03	1.50E-03	1.39E-03	1.29E-03	1.20E-03	9.44E-04	
FAT	2.30E-02	3.58E-02	3.34E-02	1.96E-02	9.18E-03	7.20E-03	8.03E-03	8.50E-03	7.98E-03	7.26E-03	6.64E-03	4.87E-03	
TESTES	8.20E-01	5.82E-01	3.69E-01	1.52E-01	5.14E-02	3.20E-02	3.55E-02	3.74E-02	3.31E-02	2.82E-02	2.41E-02	1.42E-02	
BRAIN	0.00E+00	0.00E+00	0.00E+00	--	--	<u>8.63E-06</u>	<u>1.16E-05</u>	<u>1.88E-05</u>	<u>2.24E-05</u>	<u>2.49E-05</u>	<u>2.43E-05</u>	<u>2.17E-05</u>	
GI TRACT	6.10E-03	1.62E-02	2.14E-02	1.76E-02	9.10E-03	6.33E-03	6.84E-03	7.26E-03	6.87E-03	6.39E-03	5.90E-03	4.66E-03	
STOMACH CONTENTS	0.00E+00	--	--	7.10E-05	8.76E-05	6.73E-05	7.62E-05	8.83E-05	8.74E-05	8.65E-05	8.35E-05	6.67E-05	
BONE MARROW	--	<u>3.19E-05</u>	1.19E-03	7.90E-03	7.35E-03	2.32E-03	1.16E-03	9.96E-04	9.20E-04	8.61E-04	7.87E-04	6.39E-04	
SKIN	5.39E-03	1.49E-02	1.88E-02	1.46E-02	7.08E-03	4.35E-03	4.60E-03	4.93E-03	4.55E-03	4.15E-03	3.82E-03	3.02E-03	
MUSCLE	1.39E-01	3.03E-01	3.76E-01	2.82E-01	1.35E-01	8.60E-02	9.11E-02	9.61E-02	9.02E-02	8.29E-02	7.66E-02	5.98E-02	
EXTERNAL	1.94E-04	6.77E-04	1.24E-03	1.30E-03	7.13E-04	4.24E-04	4.37E-04	4.15E-04	3.60E-04	3.23E-04	3.05E-04	2.68E-04	

TARGET	PHOTON ABSORBED FRACTIONS												
	Source = LUNGS												
	Energy (MeV)												
	0.01	0.015	0.02	0.03	0.05	0.1	0.2	0.5	1.0	1.5	2.0	4.0	
BONE	2.99E-02	1.18E-01	2.29E-01	2.97E-01	1.70E-01	4.90E-02	2.62E-02	2.33E-02	2.17E-02	1.99E-02	1.84E-02	1.46E-02	
HEART	1.05E-02	2.69E-02	3.43E-02	2.42E-02	1.06E-02	6.47E-03	6.82E-03	7.13E-03	6.65E-03	6.09E-03	5.60E-03	4.31E-03	
KIDNEYS	0.00E+00	<u>3.49E-05</u>	3.48E-04	8.19E-04	6.20E-04	4.57E-04	4.90E-04	5.27E-04	5.07E-04	4.76E-04	4.44E-04	3.71E-04	
GALLBLADDER	<u>1.53E-05</u>	3.58E-04	6.75E-04	5.79E-04	2.74E-04	1.84E-04	1.96E-04	2.04E-04	1.92E-04	1.78E-04	1.62E-04	1.30E-04	
LIVER	2.54E-02	5.77E-02	6.58E-02	4.26E-02	1.87E-02	1.28E-02	1.39E-02	1.45E-02	1.35E-02	1.24E-02	1.14E-02	8.65E-03	
URINARY BLADDER	0.00E+00	0.00E+00	--	<u>3.40E-05</u>	<u>4.16E-05</u>	3.54E-05	4.43E-05	5.12E-05	5.41E-05	5.21E-05	4.91E-05	4.25E-05	
LUNGS	8.72E-01	6.72E-01	4.60E-01	2.06E-01	7.35E-02	4.52E-02	4.92E-02	5.17E-02	4.63E-02	4.01E-02	3.52E-02	2.24E-02	
BLOOD	7.38E-03	1.72E-02	2.38E-02	2.12E-02	1.05E-02	5.76E-03	5.72E-03	5.97E-03	5.57E-03	5.13E-03	4.76E-03	3.76E-03	
FECES	0.00E+00	--	1.91E-04	6.81E-04	5.59E-04	4.00E-04	4.28E-04	4.79E-04	4.57E-04	4.31E-04	4.03E-04	3.32E-04	
FAT	<u>1.20E-05</u>	2.13E-04	6.60E-04	1.14E-03	8.81E-04	7.62E-04	8.61E-04	9.61E-04	9.39E-04	8.90E-04	8.42E-04	6.95E-04	
TESTES	0.00E+00	0.00E+00	--	7.98E-05	1.42E-04	1.29E-04	1.46E-04	1.87E-04	1.99E-04	1.98E-04	1.92E-04	1.71E-04	
BRAIN	0.00E+00	--	--	<u>3.69E-05</u>	1.27E-04	1.47E-04	1.82E-04	2.16E-04	2.23E-04	2.05E-04	1.98E-04	1.72E-04	
GI TRACT	2.81E-04	3.20E-03	8.11E-03	1.07E-02	6.74E-03	4.84E-03	5.22E-03	5.56E-03	5.27E-03	4.87E-03	4.60E-03	3.74E-03	
STOMACH CONTENTS	6.19E-05	1.96E-03	4.63E-03	4.26E-03	2.05E-03	1.27E-03	1.30E-03	1.33E-03	1.24E-03	1.14E-03	1.06E-03	8.68E-04	
BONE MARROW	--	8.00E-05	9.85E-04	4.26E-03	3.88E-03	1.28E-03	6.93E-04	6.09E-04	5.70E-04	5.25E-04	4.90E-04	4.03E-04	
SKIN	2.57E-04	1.98E-03	4.26E-03	6.58E-03	<u>4.77E-03</u>	3.43E-03	3.81E-03	4.14E-03	3.86E-03	3.49E-03	3.21E-03	2.59E-03	
MUSCLE	5.36E-02	8.86E-02	1.09E-01	1.06E-01	6.63E-02	4.81E-02	5.21E-02	5.61E-02	5.34E-02	4.95E-02	4.59E-02	3.66E-02	
EXTERNAL	4.33E-05	3.69E-04	7.54E-04	1.09E-03	7.10E-04	4.50E-04	4.77E-04	4.56E-04	3.80E-04	3.52E-04	3.30E-04	2.89E-04	

TARGET	PHOTON ABSORBED FRACTIONS												
	Source = KIDNEYS												
	Energy (MeV)												
	0.01	0.015	0.02	0.03	0.05	0.1	0.2	0.5	1.0	1.5	2.0	4.0	
BONE	1.72E-03	2.50E-02	7.41E-02	1.27E-01	8.52E-02	2.61E-02	1.35E-02	1.18E-02	1.11E-02	1.03E-02	9.65E-03	7.96E-03	
HEART	0.00E+00	--	6.29E-05	4.64E-04	4.88E-04	3.73E-04	4.05E-04	4.57E-04	4.54E-04	4.26E-04	4.09E-04	3.40E-04	
KIDNEYS	7.74E-01	4.72E-01	2.60E-01	9.43E-02	3.19E-02	2.25E-02	2.59E-02	2.74E-02	2.37E-02	1.96E-02	1.62E-02	8.34E-03	
GALLBLADDER	0.00E+00	--	<u>2.63E-05</u>	7.14E-05	5.50E-05	4.25E-05	4.33E-05	4.57E-05	4.68E-05	4.13E-05	3.93E-05	3.02E-05	
LIVER	3.39E-03	1.44E-02	1.73E-02	1.32E-02	6.67E-03	4.58E-03	4.94E-03	5.21E-03	4.90E-03	4.54E-03	4.21E-03	3.28E-03	
URINARY BLADDER	--	6.02E-04	1.64E-03	1.61E-03	8.13E-04	5.35E-04	5.52E-04	5.86E-04	5.41E-04	4.92E-04	4.56E-04	3.74E-04	
LUNGS	--	2.16E-04	2.16E-03	5.17E-03	3.66E-03	2.41E-03	2.47E-03	2.62E-03	2.52E-03	2.32E-03	2.19E-03	1.82E-03	
BLOOD	1.83E-02	6.54E-02	8.73E-02	6.14E-02	2.45E-02	1.25E-02	1.24E-02	1.28E-02	1.20E-02	1.10E-02	1.02E-02	7.96E-03	
FECES	8.75E-03	2.18E-02	2.39E-02	1.49E-02	6.12E-03	3.81E-03	4.06E-03	4.26E-03	3.95E-03	3.63E-03	3.35E-03	2.53E-03	
FAT	9.83E-02	1.07E-01	7.53E-02	3.41E-02	1.40E-02	1.10E-02	1.26E-02	1.35E-02	1.26E-02	1.13E-02	1.02E-02	6.58E-03	
TESTES	0.00E+00	1.08E-04	1.05E-03	2.41E-03	1.65E-03	1.06E-03	1.10E-03	1.16E-03	1.11E-03	1.02E-03	9.59E-04	7.84E-04	
BRAIN	0.00E+00	0.00E+00	--	<u>1.57E-05</u>	<u>4.34E-05</u>	5.24E-05	6.42E-05	7.89E-05	9.01E-05	8.62E-05	8.38E-05	7.04E-05	
GI TRACT	2.17E-02	6.23E-02	8.10E-02	5.92E-02	2.73E-02	1.83E-02	1.96E-02	2.05E-02	1.92E-02	1.76E-02	1.62E-02	1.27E-02	
STOMACH CONTENTS	--	3.56E-04	1.56E-03	2.10E-03	1.12E-03	6.95E-04	7.19E-04	7.42E-04	6.82E-04	6.42E-04	5.96E-04	4.87E-04	
BONE MARROW	0.00E+00	--	2.35E-04	2.64E-03	3.33E-03	1.18E-03	6.26E-04	5.32E-04	4.99E-04	4.73E-04	4.34E-04	3.64E-04	
SKIN	6.94E-04	6.42E-03	1.02E-02	9.77E-03	5.32E-03	3.46E-03	3.74E-03	4.08E-03	3.81E-03	3.44E-03	3.18E-03	2.56E-03	
MUSCLE	7.19E-02	1.90E-01	2.36E-01	1.84E-01	9.34E-02	6.11E-02	6.52E-02	6.96E-02	6.60E-02	6.10E-02	5.68E-02	4.50E-02	
EXTERNAL	1.16E-04	1.08E-03	1.67E-03	1.52E-03	8.00E-04	4.53E-04	4.66E-04	4.37E-04	3.75E-04	3.44E-04	3.24E-04	2.85E-04	

TARGET	PHOTON ABSORBED FRACTIONS												
	Source = HEART												
	Energy (MeV)												
	0.01	0.015	0.02	0.03	0.05	0.1	0.2	0.5	1.0	1.5	2.0	4.0	
BONE	1.53E-02	7.59E-02	1.73E-01	2.49E-01	1.47E-01	4.26E-02	2.27E-02	2.02E-02	1.89E-02	1.74E-02	1.62E-02	1.30E-02	
HEART	8.81E-01	6.75E-01	4.46E-01	1.87E-01	6.37E-02	3.99E-02	4.42E-02	4.67E-02	4.17E-02	3.60E-02	3.11E-02	1.88E-02	
KIDNEYS	0.00E+00	--	<u>2.53E-05</u>	1.81E-04	2.15E-04	1.74E-04	2.00E-04	2.25E-04	2.27E-04	2.11E-04	2.02E-04	1.74E-04	
GALLBLADDER	--	9.63E-05	3.64E-04	4.22E-04	2.19E-04	1.51E-04	1.61E-04	1.66E-04	1.53E-04	1.43E-04	1.34E-04	1.09E-04	
LIVER	4.82E-05	4.17E-03	1.32E-02	1.49E-02	8.17E-03	5.65E-03	6.06E-03	6.35E-03	5.97E-03	5.50E-03	5.10E-03	4.12E-03	
URINARY BLADDER	0.00E+00	0.00E+00	--	<u>1.13E-05</u>	<u>1.90E-05</u>	<u>1.99E-05</u>	2.40E-05	<u>2.88E-05</u>	<u>3.12E-05</u>	<u>3.07E-05</u>	<u>3.00E-05</u>	<u>2.80E-05</u>	
LUNGS	2.63E-02	6.76E-02	8.57E-02	6.07E-02	2.62E-02	1.57E-02	1.65E-02	1.72E-02	1.61E-02	1.48E-02	1.36E-02	1.05E-02	
BLOOD	1.70E-02	4.79E-02	5.90E-02	3.96E-02	1.62E-02	8.67E-03	8.77E-03	9.21E-03	8.69E-03	7.97E-03	7.33E-03	5.61E-03	
FECES	0.00E+00	--	4.65E-05	2.60E-04	2.71E-04	2.10E-04	2.39E-04	2.81E-04	2.81E-04	2.68E-04	2.53E-04	2.15E-04	
FAT	0.00E+00	<u>9.97E-06</u>	1.23E-04	3.68E-04	3.79E-04	3.53E-04	4.20E-04	4.91E-04	5.01E-04	4.89E-04	4.70E-04	3.94E-04	
TESTES	0.00E+00	--	--	<u>2.85E-05</u>	7.22E-05	6.82E-05	8.85E-05	1.19E-04	1.31E-04	1.27E-04	1.29E-04	1.15E-04	
BRAIN	0.00E+00	0.00E+00	0.00E+00	--	6.56E-05	1.04E-04	1.30E-04	1.66E-04	1.75E-04	1.68E-04	1.62E-04	1.43E-04	
GI TRACT	0.00E+00	5.43E-05	8.50E-04	2.95E-03	2.56E-03	2.05E-03	2.29E-03	2.59E-03	2.54E-03	2.40E-03	2.27E-03	1.89E-03	
STOMACH CONTENTS	0.00E+00	7.00E-05	6.89E-04	1.30E-03	8.12E-04	5.26E-04	5.42E-04	5.73E-04	5.26E-04	4.89E-04	4.61E-04	3.77E-04	
BONE MARROW	--	5.49E-05	4.41E-04	2.51E-03	2.72E-03	9.18E-04	5.09E-04	4.43E-04	4.25E-04	3.95E-04	3.70E-04	3.01E-04	
SKIN	4.77E-04	3.72E-03	7.55E-03	9.16E-03	5.71E-03	3.96E-03	4.33E-03	4.72E-03	4.39E-03	3.97E-03	3.65E-03	2.94E-03	
MUSCLE	5.95E-02	1.08E-01	1.32E-01	1.16E-01	6.69E-02	4.73E-02	5.15E-02	5.56E-02	5.31E-02	4.91E-02	4.55E-02	3.62E-02	
EXTERNAL	6.53E-05	5.52E-04	1.10E-03	1.27E-03	7.41E-04	4.56E-04	4.83E-04	4.61E-04	3.97E-04	3.65E-04	3.44E-04	3.00E-04	

TARGET	PHOTON ABSORBED FRACTIONS												
	Source = GI TRACT												
	Energy (MeV)												
	0.01	0.015	0.02	0.03	0.05	0.1	0.2	0.5	1.0	1.5	2.0	4.0	
BONE	5.75E-03	2.84E-02	6.81E-02	1.12E-01	7.40E-02	2.26E-02	1.19E-02	1.06E-02	1.01E-02	9.34E-03	8.72E-03	7.16E-03	
HEART	0.00E+00	<u>1.45E-05</u>	2.50E-04	8.78E-04	7.47E-04	5.31E-04	5.77E-04	6.38E-04	6.26E-04	5.96E-04	5.65E-04	4.65E-04	
KIDNEYS	2.67E-03	7.66E-03	9.95E-03	7.26E-03	3.32E-03	2.20E-03	2.34E-03	2.45E-03	2.26E-03	2.08E-03	1.93E-03	1.48E-03	
GALLBLADDER	1.51E-04	2.54E-04	3.00E-04	2.49E-04	1.32E-04	8.84E-05	9.26E-05	9.82E-05	9.43E-05	8.38E-05	8.08E-05	6.19E-05	
LIVER	3.67E-03	1.08E-02	1.57E-02	1.35E-02	6.90E-03	4.74E-03	5.10E-03	5.36E-03	5.01E-03	4.63E-03	4.30E-03	3.40E-03	
URINARY BLADDER	1.40E-03	3.69E-03	3.97E-03	2.46E-03	1.05E-03	6.89E-04	7.34E-04	7.77E-04	7.32E-04	6.73E-04	6.21E-04	4.63E-04	
LUNGS	2.04E-04	2.40E-03	6.15E-03	8.07E-03	4.81E-03	3.05E-03	3.15E-03	3.34E-03	3.16E-03	2.93E-03	2.76E-03	2.25E-03	
BLOOD	8.78E-02	1.27E-01	1.19E-01	6.88E-02	2.58E-02	1.34E-02	1.37E-02	1.43E-02	1.33E-02	1.21E-02	1.10E-02	7.91E-03	
FECES	4.33E-02	5.23E-02	4.27E-02	2.19E-02	8.27E-03	5.27E-03	5.75E-03	6.09E-03	5.63E-03	5.07E-03	4.57E-03	3.16E-03	
FAT	9.30E-03	1.38E-02	1.45E-02	9.90E-03	4.97E-03	3.90E-03	4.36E-03	4.67E-03	4.40E-03	4.03E-03	3.70E-03	2.85E-03	
TESTES	1.98E-03	5.26E-03	7.02E-03	5.81E-03	2.84E-03	1.76E-03	1.85E-03	1.97E-03	1.85E-03	1.70E-03	1.58E-03	1.25E-03	
BRAIN	0.00E+00	0.00E+00	--	<u>1.10E-05</u>	<u>3.48E-05</u>	3.47E-05	5.17E-05	6.65E-05	7.22E-05	7.60E-05	7.02E-05	6.37E-05	
GI TRACT	7.04E-01	4.84E-01	3.20E-01	1.45E-01	5.54E-02	3.86E-02	4.33E-02	4.56E-02	4.09E-02	3.57E-02	3.13E-02	2.07E-02	
STOMACH CONTENTS	8.76E-03	1.00E-02	8.59E-03	5.06E-03	2.12E-03	1.33E-03	1.41E-03	1.50E-03	1.39E-03	1.25E-03	1.14E-03	8.26E-04	
BONE MARROW	--	<u>3.92E-05</u>	3.74E-04	2.47E-03	2.79E-03	1.02E-03	5.31E-04	4.55E-04	4.30E-04	4.08E-04	3.87E-04	3.22E-04	
SKIN	2.84E-03	1.06E-02	1.43E-02	1.18E-02	5.90E-03	3.79E-03	4.14E-03	4.49E-03	4.17E-03	3.75E-03	3.44E-03	2.71E-03	
MUSCLE	1.25E-01	1.94E-01	2.06E-01	1.54E-01	7.74E-02	5.13E-02	5.54E-02	5.98E-02	5.69E-02	5.25E-02	4.86E-02	3.79E-02	
EXTERNAL	3.77E-04	1.67E-03	2.22E-03	1.75E-03	8.38E-04	4.65E-04	4.94E-04	4.75E-04	4.03E-04	3.68E-04	3.47E-04	2.97E-04	

TARGET	PHOTON ABSORBED FRACTIONS												
	Source = STOMACH CONTENTS												
	Energy (MeV)												
	0.01	0.015	0.02	0.03	0.05	0.1	0.2	0.5	1.0	1.5	2.0	4.0	
BONE	1.56E-03	3.23E-02	1.07E-01	1.77E-01	1.07E-01	3.11E-02	1.61E-02	1.41E-02	1.31E-02	1.22E-02	1.14E-02	9.37E-03	
HEART	0.00E+00	2.89E-04	2.64E-03	4.97E-03	3.07E-03	1.94E-03	2.00E-03	2.07E-03	1.93E-03	1.78E-03	1.65E-03	1.37E-03	
KIDNEYS	--	5.32E-04	2.42E-03	3.23E-03	1.82E-03	1.22E-03	1.29E-03	1.32E-03	1.23E-03	1.13E-03	1.05E-03	8.41E-04	
GALLBLADDER	1.06E-03	3.66E-03	3.83E-03	2.11E-03	8.42E-04	5.67E-04	6.27E-04	6.52E-04	6.11E-04	5.45E-04	4.96E-04	3.61E-04	
LIVER	3.27E-02	1.08E-01	1.23E-01	7.29E-02	2.98E-02	1.99E-02	2.16E-02	2.26E-02	2.10E-02	1.93E-02	1.77E-02	1.34E-02	
URINARY BLADDER	0.00E+00	--	<u>1.76E-05</u>	1.18E-04	1.18E-04	8.49E-05	9.46E-05	1.05E-04	1.00E-04	9.83E-05	8.91E-05	7.50E-05	
LUNGS	6.01E-04	1.85E-02	4.42E-02	4.12E-02	1.94E-02	1.13E-02	1.16E-02	1.18E-02	1.10E-02	1.01E-02	9.38E-03	7.57E-03	
BLOOD	5.98E-03	2.76E-02	4.22E-02	3.49E-02	1.56E-02	8.04E-03	7.91E-03	8.18E-03	7.65E-03	6.99E-03	6.49E-03	5.15E-03	
FECES	--	7.13E-04	2.82E-03	3.77E-03	2.08E-03	1.31E-03	1.37E-03	1.42E-03	1.34E-03	1.24E-03	1.16E-03	9.34E-04	
FAT	4.43E-03	8.17E-03	8.31E-03	5.91E-03	3.14E-03	2.48E-03	2.75E-03	2.96E-03	2.79E-03	2.59E-03	2.38E-03	1.82E-03	
TESTES	0.00E+00	--	<u>2.51E-05</u>	2.83E-04	3.43E-04	2.80E-04	3.00E-04	3.43E-04	3.52E-04	3.35E-04	3.25E-04	2.71E-04	
BRAIN	0.00E+00	0.00E+00	--	<u>1.97E-05</u>	6.13E-05	7.64E-05	9.24E-05	1.17E-04	1.24E-04	1.20E-04	1.16E-04	1.04E-04	
GI TRACT	1.11E-01	1.27E-01	1.09E-01	6.40E-02	2.81E-02	1.91E-02	2.08E-02	2.20E-02	2.05E-02	1.85E-02	1.67E-02	1.20E-02	
STOMACH CONTENTS	7.85E-01	4.92E-01	2.75E-01	9.91E-02	3.18E-02	2.10E-02	2.39E-02	2.52E-02	2.17E-02	1.78E-02	1.46E-02	7.26E-03	
BONE MARROW	0.00E+00	--	9.65E-05	1.35E-03	1.91E-03	7.29E-04	3.76E-04	3.40E-04	3.20E-04	2.99E-04	2.81E-04	2.33E-04	
SKIN	<u>2.92E-05</u>	1.37E-03	4.63E-03	7.45E-03	4.91E-03	3.30E-03	3.61E-03	3.93E-03	3.65E-03	3.31E-03	3.05E-03	2.46E-03	
MUSCLE	5.75E-02	1.70E-01	2.06E-01	1.56E-01	7.90E-02	5.21E-02	5.58E-02	5.99E-02	5.70E-02	5.27E-02	4.90E-02	3.86E-02	
EXTERNAL	--	2.82E-04	9.08E-04	1.32E-03	7.80E-04	4.56E-04	4.76E-04	4.46E-04	3.78E-04	3.46E-04	3.28E-04	2.86E-04	

TARGET	PHOTON ABSORBED FRACTIONS												
	Source = FECES												
	Energy (MeV)												
	0.01	0.015	0.02	0.03	0.05	0.1	0.2	0.5	1.0	1.5	2.0	4.0	
BONE	2.18E-03	1.63E-02	4.75E-02	9.39E-02	6.79E-02	2.13E-02	1.11E-02	9.86E-03	9.29E-03	8.65E-03	8.08E-03	6.71E-03	
HEART	0.00E+00	--	8.35E-05	4.61E-04	4.64E-04	3.49E-04	3.76E-04	4.34E-04	4.41E-04	4.18E-04	3.93E-04	3.43E-04	
KIDNEYS	5.97E-03	1.50E-02	1.63E-02	1.03E-02	4.39E-03	2.90E-03	3.13E-03	3.30E-03	3.09E-03	2.84E-03	2.59E-03	1.96E-03	
GALLBLADDER	0.00E+00	<u>9.97E-06</u>	5.92E-05	1.11E-04	6.86E-05	5.09E-05	5.50E-05	5.64E-05	5.32E-05	4.62E-05	4.44E-05	3.90E-05	
LIVER	--	6.63E-04	3.28E-03	5.56E-03	3.59E-03	2.56E-03	2.74E-03	2.93E-03	2.77E-03	2.58E-03	2.41E-03	1.96E-03	
URINARY BLADDER	1.26E-03	6.08E-03	7.33E-03	4.53E-03	1.82E-03	1.19E-03	1.27E-03	1.33E-03	1.23E-03	1.13E-03	1.04E-03	8.11E-04	
LUNGS	0.00E+00	<u>3.70E-05</u>	8.26E-04	2.92E-03	2.39E-03	1.62E-03	1.70E-03	1.86E-03	1.80E-03	1.70E-03	1.62E-03	1.34E-03	
BLOOD	6.66E-02	1.19E-01	1.21E-01	7.30E-02	2.74E-02	1.42E-02	1.44E-02	1.51E-02	1.41E-02	1.28E-02	1.17E-02	8.50E-03	
FECES	6.06E-01	3.33E-01	1.87E-01	7.09E-02	2.36E-02	1.55E-02	1.75E-02	1.83E-02	1.53E-02	1.24E-02	1.03E-02	5.91E-03	
FAT	1.26E-02	1.93E-02	1.94E-02	1.26E-02	6.19E-03	4.84E-03	5.42E-03	5.78E-03	5.45E-03	5.01E-03	4.56E-03	3.44E-03	
TESTES	9.25E-04	4.93E-03	8.53E-03	7.94E-03	3.92E-03	2.40E-03	2.48E-03	2.59E-03	2.44E-03	2.25E-03	2.09E-03	1.66E-03	
BRAIN	0.00E+00	0.00E+00	--	--	<u>1.80E-05</u>	2.64E-05	3.58E-05	4.96E-05	5.25E-05	5.52E-05	5.00E-05	4.55E-05	
GI TRACT	2.43E-01	2.93E-01	2.40E-01	1.24E-01	4.91E-02	3.36E-02	3.73E-02	3.97E-02	3.69E-02	3.32E-02	2.98E-02	2.07E-02	
STOMACH CONTENTS	--	3.15E-04	1.24E-03	1.66E-03	9.07E-04	5.80E-04	5.99E-04	6.30E-04	5.93E-04	5.51E-04	4.98E-04	4.04E-04	
BONE MARROW	--	4.79E-05	4.90E-04	3.01E-03	3.38E-03	1.17E-03	6.12E-04	5.42E-04	5.04E-04	4.72E-04	4.36E-04	3.63E-04	
SKIN	2.49E-03	1.22E-02	1.67E-02	1.33E-02	6.41E-03	4.04E-03	4.39E-03	4.73E-03	4.38E-03	3.95E-03	3.62E-03	2.86E-03	
MUSCLE	5.68E-02	1.36E-01	1.76E-01	1.48E-01	7.77E-02	5.11E-02	5.48E-02	5.90E-02	5.60E-02	5.19E-02	4.82E-02	3.82E-02	
EXTERNAL	3.03E-04	1.57E-03	2.22E-03	1.78E-03	8.33E-04	4.71E-04	4.93E-04	4.75E-04	4.05E-04	3.69E-04	3.46E-04	2.94E-04	

TARGET	PHOTON ABSORBED FRACTIONS											
	Source = SKIN											
	Energy (MeV)											
	0.01	0.015	0.02	0.03	0.05	0.1	0.2	0.5	1.0	1.5	2.0	4.0
BONE	7.50E-02	1.48E-01	1.91E-01	1.90E-01	1.01E-01	2.89E-02	1.73E-02	1.67E-02	1.57E-02	1.44E-02	1.32E-02	9.85E-03
HEART	8.85E-05	6.92E-04	1.44E-03	1.79E-03	1.18E-03	8.60E-04	9.62E-04	1.06E-03	1.02E-03	9.59E-04	9.14E-04	7.62E-04
KIDNEYS	5.33E-05	4.86E-04	7.74E-04	7.60E-04	4.37E-04	3.49E-04	4.04E-04	4.50E-04	4.35E-04	4.09E-04	3.71E-04	3.06E-04
GALLBLADDER	--	<u>1.82E-05</u>	4.18E-05	5.49E-05	<u>3.51E-05</u>	2.87E-05	3.33E-05	3.95E-05	<u>3.80E-05</u>	<u>3.39E-05</u>	<u>3.10E-05</u>	2.67E-05
LIVER	1.08E-04	8.98E-04	1.82E-03	2.45E-03	1.72E-03	1.40E-03	1.62E-03	1.82E-03	1.78E-03	1.66E-03	1.56E-03	1.27E-03
URINARY BLADDER	<u>1.23E-05</u>	1.84E-04	3.59E-04	3.48E-04	1.87E-04	1.45E-04	1.62E-04	1.76E-04	1.70E-04	1.60E-04	1.43E-04	1.14E-04
LUNGS	1.23E-04	9.23E-04	2.05E-03	3.26E-03	2.43E-03	1.86E-03	2.05E-03	2.28E-03	2.20E-03	2.05E-03	1.93E-03	1.58E-03
BLOOD	9.68E-04	4.08E-03	6.34E-03	6.29E-03	3.55E-03	2.15E-03	2.28E-03	2.52E-03	2.45E-03	2.30E-03	2.14E-03	1.72E-03
FECES	2.80E-04	1.34E-03	1.86E-03	1.50E-03	7.78E-04	5.40E-04	6.04E-04	6.65E-04	6.40E-04	6.06E-04	5.62E-04	4.57E-04
FAT	1.25E-03	2.49E-03	2.64E-03	2.07E-03	1.30E-03	1.17E-03	1.37E-03	1.52E-03	1.47E-03	1.38E-03	1.27E-03	1.01E-03
TESTES	1.08E-03	3.00E-03	3.80E-03	3.01E-03	1.54E-03	1.03E-03	1.11E-03	1.20E-03	1.15E-03	1.06E-03	9.93E-04	7.78E-04
BRAIN	--	6.33E-05	2.78E-04	5.75E-04	4.65E-04	3.44E-04	3.86E-04	4.35E-04	4.22E-04	4.00E-04	3.76E-04	2.93E-04
GI TRACT	1.76E-03	6.55E-03	8.85E-03	7.41E-03	4.15E-03	3.19E-03	3.67E-03	4.09E-03	3.97E-03	3.71E-03	3.48E-03	2.79E-03
STOMACH CONTENTS	--	7.09E-05	2.31E-04	3.69E-04	2.60E-04	1.96E-04	2.16E-04	2.38E-04	2.34E-04	2.22E-04	2.09E-04	1.78E-04
BONE MARROW	5.28E-05	3.99E-04	1.85E-03	4.74E-03	3.42E-03	1.04E-03	6.22E-04	5.92E-04	5.62E-04	5.19E-04	4.90E-04	3.77E-04
SKIN	4.27E-01	1.90E-01	9.56E-02	3.45E-02	1.16E-02	7.54E-03	8.63E-03	8.75E-03	6.70E-03	5.22E-03	4.34E-03	2.71E-03
MUSCLE	2.51E-01	2.60E-01	2.06E-01	1.17E-01	5.59E-02	4.05E-02	4.64E-02	5.16E-02	4.91E-02	4.47E-02	4.07E-02	3.03E-02
EXTERNAL	2.47E-02	1.16E-02	5.94E-03	2.30E-03	8.16E-04	4.88E-04	5.55E-04	5.94E-04	4.74E-04	3.79E-04	3.24E-04	2.19E-04

7.3. APPENDIX C - Electron absorbed fractions for adult *Lepus californicus*

TARGET	ELECTRON ABSORBED FRACTIONS									
	Source = BONE									
	Energy (MeV)									
	0.1	0.2	0.4	0.5	0.7	1.0	1.5	2.0	4.0	
BONE	9.89E-01	9.64E-01	9.04E-01	8.75E-01	8.19E-01	7.45E-01	6.39E-01	5.59E-01	3.77E-01	
HEART	<u>1.84E-05</u>	6.11E-05	1.65E-04	2.24E-04	3.63E-04	6.34E-04	1.18E-03	1.71E-03	3.05E-03	
KIDNEYS	--	--	--	--	--	<u>2.02E-06</u>	<u>1.25E-05</u>	4.97E-05	3.52E-04	
GALLBLADDER	--	--	--	--	--	--	--	<u>5.64E-06</u>	7.22E-05	
LIVER	<u>1.41E-05</u>	<u>4.56E-05</u>	1.46E-04	1.99E-04	3.53E-04	7.02E-04	1.54E-03	2.50E-03	5.17E-03	
URINARY BLADDER	--	--	--	--	--	--	--	--	--	3.64E-05
LUNGS	8.97E-05	2.93E-04	8.08E-04	1.13E-03	1.85E-03	3.33E-03	6.15E-03	8.70E-03	1.42E-02	
BLOOD	6.09E-05	2.17E-04	5.90E-04	7.96E-04	1.26E-03	2.10E-03	3.61E-03	4.95E-03	8.15E-03	
FECES	--	--	--	<u>1.46E-05</u>	<u>2.31E-05</u>	3.96E-05	9.39E-05	1.48E-04	4.05E-04	
FAT	9.26E-05	3.14E-04	8.46E-04	1.11E-03	1.63E-03	2.36E-03	3.47E-03	4.33E-03	6.76E-03	
TESTES	--	--	<u>2.18E-06</u>	<u>2.57E-06</u>	<u>5.18E-06</u>	<u>7.50E-06</u>	<u>1.75E-05</u>	4.23E-05	4.85E-04	
BRAIN	2.06E-04	6.86E-04	1.82E-03	2.40E-03	3.48E-03	4.89E-03	6.94E-03	8.42E-03	1.06E-02	
GI TRACT	<u>2.67E-05</u>	9.86E-05	2.55E-04	3.41E-04	5.18E-04	8.43E-04	1.47E-03	2.09E-03	4.08E-03	
STOMACH CONTENTS	--	--	--	--	--	--	<u>8.73E-06</u>	3.66E-05	3.12E-04	
BONE MARROW	7.67E-04	2.51E-03	6.73E-03	8.88E-03	1.28E-02	1.73E-02	2.15E-02	2.19E-02	1.47E-02	
SKIN	8.83E-04	3.01E-03	8.10E-03	1.07E-02	1.54E-02	2.07E-02	2.59E-02	2.83E-02	2.85E-02	
MUSCLE	8.17E-03	2.69E-02	7.17E-02	9.36E-02	1.33E-01	1.79E-01	2.40E-01	2.80E-01	3.35E-01	
EXTERNAL	2.00E-04	4.30E-04	6.22E-04	6.92E-04	1.04E-03	1.59E-03	2.23E-03	2.60E-03	2.94E-03	

ELECTRON ABSORBED FRACTIONS

Source = MUSCLE

Energy (MeV)

TARGET	0.1	0.2	0.4	0.5	0.7	1.0	1.5	2.0	4.0
BONE	2.73E-03	8.75E-03	2.31E-02	3.01E-02	4.25E-02	5.77E-02	7.70E-02	9.00E-02	1.08E-01
HEART	7.13E-05	2.24E-04	5.70E-04	7.39E-04	1.04E-03	1.38E-03	1.84E-03	2.24E-03	3.56E-03
KIDNEYS	<u>1.95E-05</u>	6.25E-05	1.67E-04	2.18E-04	3.22E-04	4.75E-04	7.64E-04	1.11E-03	2.32E-03
GALLBLADDER	--	<u>2.53E-05</u>	7.09E-05	9.23E-05	1.24E-04	1.55E-04	1.86E-04	1.92E-04	2.31E-04
LIVER	1.87E-04	5.93E-04	1.57E-03	2.07E-03	2.95E-03	4.02E-03	5.30E-03	6.32E-03	8.82E-03
URINARY BLADDER	<u>2.56E-05</u>	8.19E-05	2.16E-04	2.82E-04	4.03E-04	5.45E-04	7.37E-04	8.91E-04	1.23E-03
LUNGS	1.66E-04	5.35E-04	1.39E-03	1.81E-03	2.46E-03	3.25E-03	4.19E-03	4.99E-03	7.62E-03
BLOOD	4.09E-04	1.31E-03	3.40E-03	4.37E-03	6.11E-03	8.11E-03	1.05E-02	1.20E-02	1.54E-02
FECES	<u>1.51E-05</u>	<u>5.27E-05</u>	1.54E-04	2.11E-04	3.54E-04	5.93E-04	1.04E-03	1.40E-03	2.19E-03
FAT	4.70E-04	1.49E-03	3.89E-03	5.00E-03	6.87E-03	8.99E-03	1.12E-02	1.25E-02	1.40E-02
TESTES	1.43E-04	4.64E-04	1.24E-03	1.65E-03	2.33E-03	3.22E-03	4.40E-03	5.45E-03	8.75E-03
BRAIN	--	--	<u>1.83E-05</u>	<u>2.51E-05</u>	<u>3.78E-05</u>	6.62E-05	1.48E-04	2.83E-04	1.10E-03
GI TRACT	5.29E-04	1.70E-03	4.42E-03	5.74E-03	8.01E-03	1.06E-02	1.35E-02	1.54E-02	1.93E-02
STOMACH CONTENTS	--	<u>1.39E-05</u>	<u>4.09E-05</u>	5.70E-05	1.07E-04	2.09E-04	4.42E-04	6.78E-04	1.36E-03
BONE MARROW	--	<u>1.48E-05</u>	<u>3.60E-05</u>	<u>4.72E-05</u>	6.94E-05	1.34E-04	4.16E-04	1.05E-03	3.52E-03
SKIN	2.22E-03	7.06E-03	1.77E-02	2.21E-02	2.79E-02	3.11E-02	3.19E-02	3.11E-02	2.80E-02
MUSCLE	9.92E-01	9.75E-01	9.34E-01	9.14E-01	8.79E-01	8.35E-01	7.75E-01	7.27E-01	5.97E-01
EXTERNAL	6.97E-04	1.42E-03	1.77E-03	1.86E-03	2.21E-03	2.56E-03	2.75E-03	2.79E-03	2.71E-03

ELECTRON ABSORBED FRACTIONS
Source = LIVER
Energy (MeV)

TARGET	0.1	0.2	0.4	0.5	0.7	1.0	1.5	2.0	4.0
BONE	1.66E-04	4.67E-04	1.21E-03	1.62E-03	2.73E-03	5.27E-03	1.15E-02	1.87E-02	3.86E-02
HEART	--	<u>3.88E-06</u>	<u>5.87E-06</u>	8.07E-06	9.55E-06	1.30E-05	1.87E-05	2.65E-05	1.52E-03
KIDNEYS	--	--	<u>2.84E-06</u>	<u>3.24E-06</u>	<u>1.16E-05</u>	2.14E-04	1.11E-03	2.23E-03	5.56E-03
GALLBLADDER	8.89E-05	2.67E-04	7.60E-04	1.03E-03	1.64E-03	2.80E-03	4.83E-03	6.56E-03	8.08E-03
LIVER	9.94E-01	9.80E-01	9.47E-01	9.30E-01	8.98E-01	8.54E-01	7.87E-01	7.25E-01	5.29E-01
URINARY BLADDER	--	--	--	--	--	--	--	--	--
LUNGS	1.06E-03	3.66E-03	1.01E-02	1.35E-02	2.00E-02	2.98E-02	4.61E-02	6.08E-02	1.02E-01
BLOOD	7.73E-05	2.35E-04	6.36E-04	8.58E-04	1.35E-03	2.25E-03	4.04E-03	5.77E-03	1.14E-02
FECES	--	--	--	<u>1.83E-06</u>	<u>2.81E-06</u>	<u>3.38E-06</u>	<u>4.96E-06</u>	6.47E-06	8.25E-05
FAT	7.62E-05	2.45E-04	6.72E-04	8.96E-04	1.33E-03	2.09E-03	3.33E-03	4.28E-03	6.61E-03
TESTES	--	--	--	--	--	--	--	--	<u>3.95E-06</u>
BRAIN	--	--	--	--	--	--	--	--	--
GI TRACT	1.99E-04	5.82E-04	1.61E-03	2.18E-03	3.39E-03	5.61E-03	9.95E-03	1.42E-02	2.84E-02
STOMACH CONTENTS	9.53E-05	2.73E-04	7.65E-04	1.03E-03	1.63E-03	2.84E-03	5.71E-03	9.35E-03	2.28E-02
BONE MARROW	--	--	--	--	<u>2.18E-06</u>	<u>2.57E-06</u>	<u>3.38E-06</u>	4.19E-06	4.08E-05
SKIN	--	3.71E-06	6.44E-06	7.81E-06	1.08E-05	3.17E-05	2.42E-04	9.75E-04	5.98E-03
MUSCLE	4.34E-03	1.38E-02	3.67E-02	4.79E-02	6.84E-02	9.29E-02	1.23E-01	1.46E-01	2.04E-01
EXTERNAL	--	--	--	--	<u>1.22E-06</u>	<u>2.05E-06</u>	1.56E-05	8.20E-05	7.69E-04

ELECTRON ABSORBED FRACTIONS
Source = TESTES
Energy (MeV)

TARGET	0.1	0.2	0.4	0.5	0.7	1.0	1.5	2.0	4.0
BONE	3.39E-05	5.60E-05	8.71E-05	9.79E-05	1.18E-04	1.67E-04	3.08E-04	6.33E-04	6.47E-03
HEART	0.00E+00	--	--	--	--	--	--	--	--
KIDNEYS	--	--	--	--	--	--	<u>2.85E-06</u>	<u>3.63E-06</u>	<u>7.01E-06</u>
GALLBLADDER	--	--	--	--	--	--	--	--	--
LIVER	--	--	--	--	--	--	--	<u>2.95E-06</u>	<u>6.51E-06</u>
URINARY BLADDER	9.57E-05	3.60E-04	1.04E-03	1.40E-03	2.20E-03	3.55E-03	6.12E-03	8.48E-03	1.41E-02
LUNGS	--	--	--	--	--	--	<u>1.65E-06</u>	<u>2.44E-06</u>	<u>6.72E-06</u>
BLOOD	--	<u>4.12E-06</u>	<u>6.32E-06</u>	7.97E-06	1.08E-05	1.80E-05	7.01E-05	1.86E-04	1.56E-03
FECES	--	--	<u>2.90E-05</u>	<u>4.19E-05</u>	7.32E-05	1.87E-04	5.82E-04	1.11E-03	3.28E-03
FAT	1.20E-03	3.87E-03	1.02E-02	1.33E-02	1.94E-02	2.79E-02	3.98E-02	4.85E-02	6.22E-02
TESTES	9.92E-01	9.75E-01	9.33E-01	9.12E-01	8.74E-01	8.23E-01	7.49E-01	6.85E-01	4.83E-01
BRAIN	0.00E+00	0.00E+00	--	--	--	--	--	--	--
GI TRACT	1.96E-04	6.51E-04	1.76E-03	2.32E-03	3.46E-03	5.35E-03	8.98E-03	1.25E-02	2.32E-02
STOMACH CONTENTS	--	--	--	--	--	--	--	--	--
BONE MARROW	--	--	<u>5.48E-06</u>	<u>5.54E-06</u>	7.42E-06	8.15E-06	1.10E-05	1.59E-05	2.60E-04
SKIN	1.27E-04	4.17E-04	1.18E-03	1.56E-03	2.45E-03	3.93E-03	6.71E-03	9.37E-03	1.65E-02
MUSCLE	6.06E-03	1.95E-02	5.18E-02	6.75E-02	9.64E-02	1.32E-01	1.82E-01	2.26E-01	3.62E-01
EXTERNAL	<u>3.05E-05</u>	4.99E-05	6.68E-05	7.17E-05	8.59E-05	1.27E-04	2.05E-04	2.75E-04	5.41E-04

ELECTRON ABSORBED FRACTIONS
Source = LUNGS
Energy (MeV)

TARGET	0.1	0.2	0.4	0.5	0.7	1.0	1.5	2.0	4.0
BONE	5.85E-04	1.80E-03	4.99E-03	6.77E-03	1.11E-02	1.96E-02	3.62E-02	5.11E-02	8.39E-02
HEART	3.52E-04	1.15E-03	3.12E-03	4.15E-03	6.21E-03	9.50E-03	1.49E-02	2.00E-02	3.56E-02
KIDNEYS	--	--	--	--	--	<u>1.75E-06</u>	<u>2.62E-06</u>	<u>4.24E-06</u>	<u>7.79E-06</u>
GALLBLADDER	--	--	--	--	--	<u>7.58E-07</u>	<u>1.39E-06</u>	<u>3.33E-06</u>	3.77E-04
LIVER	1.04E-03	3.15E-03	8.36E-03	1.10E-02	1.63E-02	2.41E-02	3.71E-02	4.87E-02	8.17E-02
URINARY BLADDER	0.00E+00	--	--	--	--	--	--	--	--
LUNGS	9.95E-01	9.83E-01	9.55E-01	9.41E-01	9.15E-01	8.78E-01	8.20E-01	7.67E-01	5.94E-01
BLOOD	2.13E-04	7.48E-04	2.16E-03	2.94E-03	4.54E-03	6.81E-03	1.02E-02	1.29E-02	1.87E-02
FECES	--	--	--	--	--	<u>1.37E-06</u>	<u>2.30E-06</u>	<u>3.06E-06</u>	<u>6.18E-06</u>
FAT	--	--	--	--	<u>2.05E-06</u>	<u>3.10E-06</u>	<u>6.27E-06</u>	2.41E-05	2.44E-04
TESTES	0.00E+00	--	--	--	--	--	--	--	<u>2.65E-06</u>
BRAIN	--	--	--	--	--	--	--	--	<u>2.87E-06</u>
GI TRACT	--	<u>5.36E-06</u>	8.32E-06	1.09E-05	1.47E-05	5.19E-05	2.42E-04	6.33E-04	3.51E-03
STOMACH CONTENTS	--	--	<u>2.65E-06</u>	<u>3.44E-06</u>	<u>4.25E-06</u>	5.73E-06	1.25E-05	4.91E-05	1.35E-03
BONE MARROW	--	--	<u>2.35E-06</u>	<u>3.19E-06</u>	<u>3.84E-06</u>	<u>6.37E-06</u>	4.64E-05	2.28E-04	1.82E-03
SKIN	--	<u>3.48E-06</u>	<u>5.97E-06</u>	7.26E-06	1.14E-05	3.70E-05	3.31E-04	1.11E-03	5.10E-03
MUSCLE	3.04E-03	9.76E-03	2.54E-02	3.28E-02	4.53E-02	5.93E-02	7.71E-02	9.21E-02	1.39E-01
EXTERNAL	--	--	--	--	<u>1.33E-06</u>	<u>2.41E-06</u>	2.28E-05	1.01E-04	6.63E-04

ELECTRON ABSORBED FRACTIONS
Source = KIDNEYS
Energy (MeV)

TARGET	0.1	0.2	0.4	0.5	0.7	1.0	1.5	2.0	4.0
BONE	2.73E-05	4.71E-05	7.03E-05	7.97E-05	9.50E-05	1.16E-04	4.12E-04	1.53E-03	1.03E-02
HEART	--	--	--	--	--	--	--	<u>2.79E-06</u>	<u>6.81E-06</u>
KIDNEYS	9.92E-01	9.74E-01	9.31E-01	9.10E-01	8.70E-01	8.13E-01	7.24E-01	6.42E-01	3.88E-01
GALLBLADDER	--	--	--	--	--	--	--	--	--
LIVER	<u>4.88E-06</u>	<u>7.88E-06</u>	1.14E-05	1.27E-05	3.85E-05	8.28E-04	4.28E-03	8.68E-03	2.21E-02
URINARY BLADDER	--	--	--	<u>1.27E-06</u>	<u>1.68E-06</u>	<u>1.93E-06</u>	<u>3.60E-06</u>	<u>3.77E-06</u>	4.01E-04
LUNGS	--	--	<u>3.88E-06</u>	<u>4.75E-06</u>	<u>6.14E-06</u>	9.10E-06	1.37E-05	1.75E-05	3.60E-05
BLOOD	2.77E-04	8.49E-04	2.41E-03	3.29E-03	5.30E-03	9.23E-03	1.75E-02	2.67E-02	6.13E-02
FECES	2.17E-04	6.32E-04	1.68E-03	2.18E-03	3.31E-03	5.37E-03	9.65E-03	1.39E-02	2.60E-02
FAT	5.14E-03	1.67E-02	4.38E-02	5.67E-02	8.04E-02	1.10E-01	1.45E-01	1.63E-01	1.58E-01
TESTES	--	--	--	<u>2.08E-06</u>	<u>2.95E-06</u>	<u>3.82E-06</u>	<u>5.97E-06</u>	7.77E-06	1.62E-05
BRAIN	--	--	--	--	--	--	--	--	--
GI TRACT	6.01E-04	1.87E-03	4.94E-03	6.55E-03	9.93E-03	1.55E-02	2.58E-02	3.74E-02	8.07E-02
STOMACH CONTENTS	--	--	--	--	<u>2.22E-06</u>	<u>2.76E-06</u>	<u>4.07E-06</u>	<u>5.57E-06</u>	2.12E-05
BONE MARROW	--	--	--	<u>2.51E-06</u>	<u>2.77E-06</u>	<u>4.20E-06</u>	5.04E-06	6.05E-06	1.10E-05
SKIN	--	<u>4.48E-06</u>	7.24E-06	8.89E-06	1.18E-05	1.60E-05	7.25E-05	5.39E-04	6.58E-03
MUSCLE	1.83E-03	5.84E-03	1.55E-02	2.03E-02	2.96E-02	4.34E-02	7.00E-02	1.01E-01	2.13E-01
EXTERNAL	--	--	--	<u>1.11E-06</u>	<u>1.58E-06</u>	<u>1.93E-06</u>	4.58E-06	4.17E-05	7.63E-04

ELECTRON ABSORBED FRACTIONS
Source = HEART
Energy (MeV)

TARGET	0.1	0.2	0.4	0.5	0.7	1.0	1.5	2.0	4.0
BONE	3.24E-04	9.24E-04	2.45E-03	3.28E-03	5.28E-03	9.14E-03	1.70E-02	2.46E-02	4.41E-02
HEART	9.95E-01	9.85E-01	9.59E-01	9.47E-01	9.23E-01	8.90E-01	8.37E-01	7.86E-01	6.04E-01
KIDNEYS	--	--	--	--	--	--	--	--	<u>3.22E-06</u>
GALLBLADDER	--	--	--	--	--	--	--	--	<u>3.19E-06</u>
LIVER	--	<u>6.79E-06</u>	1.08E-05	1.27E-05	1.82E-05	2.39E-05	3.53E-05	4.66E-05	2.97E-03
URINARY BLADDER	--	--	--	--	--	--	--	--	--
LUNGS	8.68E-04	2.80E-03	7.63E-03	1.01E-02	1.52E-02	2.31E-02	3.65E-02	4.88E-02	8.70E-02
BLOOD	4.22E-04	1.46E-03	4.05E-03	5.39E-03	8.25E-03	1.32E-02	2.26E-02	3.19E-02	5.77E-02
FECES	--	--	--	--	--	--	--	<u>1.61E-06</u>	<u>4.11E-06</u>
FAT	--	--	--	--	--	--	<u>1.91E-06</u>	<u>2.76E-06</u>	<u>7.04E-06</u>
TESTES	--	--	--	--	--	--	--	--	--
BRAIN	--	--	--	--	--	--	--	--	<u>1.71E-06</u>
GI TRACT	--	--	<u>3.28E-06</u>	<u>3.95E-06</u>	<u>5.00E-06</u>	7.44E-06	1.26E-05	1.60E-05	3.70E-05
STOMACH CONTENTS	--	--	--	--	--	<u>1.79E-06</u>	<u>2.83E-06</u>	<u>4.07E-06</u>	8.06E-06
BONE MARROW	--	--	--	<u>2.38E-06</u>	<u>3.12E-06</u>	<u>7.08E-06</u>	2.46E-05	4.27E-05	1.19E-04
SKIN	--	<u>3.84E-06</u>	7.52E-06	9.74E-06	2.37E-05	1.10E-04	5.85E-04	1.57E-03	7.74E-03
MUSCLE	3.00E-03	9.74E-03	2.56E-02	3.32E-02	4.64E-02	6.21E-02	8.24E-02	9.99E-02	1.58E-01
EXTERNAL	--	--	--	--	<u>1.81E-06</u>	6.92E-06	4.14E-05	1.28E-04	8.06E-04

ELECTRON ABSORBED FRACTIONS
Source = GI TRACT
Energy (MeV)

TARGET	0.1	0.2	0.4	0.5	0.7	1.0	1.5	2.0	4.0
BONE	1.23E-04	3.61E-04	9.61E-04	1.26E-03	1.89E-03	3.01E-03	5.11E-03	7.36E-03	1.45E-02
HEART	--	--	--	--	<u>1.34E-06</u>	<u>2.03E-06</u>	<u>2.71E-06</u>	<u>3.92E-06</u>	8.32E-06
KIDNEYS	7.09E-05	2.18E-04	5.83E-04	7.71E-04	1.19E-03	1.85E-03	3.06E-03	4.41E-03	9.59E-03
GALLBLADDER	--	<u>1.58E-05</u>	<u>4.67E-05</u>	6.11E-05	8.81E-05	1.31E-04	1.87E-04	2.25E-04	2.99E-04
LIVER	7.45E-05	2.65E-04	7.50E-04	1.00E-03	1.59E-03	2.64E-03	4.71E-03	6.77E-03	1.35E-02
URINARY BLADDER	<u>2.54E-05</u>	8.26E-05	2.41E-04	3.22E-04	5.11E-04	9.08E-04	1.77E-03	2.67E-03	5.06E-03
LUNGS	--	<u>3.42E-06</u>	<u>5.97E-06</u>	6.40E-06	9.55E-06	3.25E-05	1.47E-04	3.83E-04	2.08E-03
BLOOD	3.93E-03	1.26E-02	3.26E-02	4.19E-02	5.72E-02	7.32E-02	8.90E-02	9.76E-02	1.07E-01
FECES	2.27E-03	7.22E-03	1.87E-02	2.41E-02	3.33E-02	4.28E-02	5.20E-02	5.60E-02	5.47E-02
FAT	5.26E-04	1.70E-03	4.43E-03	5.72E-03	8.03E-03	1.09E-02	1.43E-02	1.65E-02	2.14E-02
TESTES	5.68E-05	1.82E-04	4.83E-04	6.34E-04	9.44E-04	1.43E-03	2.40E-03	3.33E-03	6.16E-03
BRAIN	--	--	--	--	--	--	--	--	--
GI TRACT	9.86E-01	9.57E-01	8.88E-01	8.55E-01	7.98E-01	7.35E-01	6.60E-01	6.07E-01	4.69E-01
STOMACH CONTENTS	4.78E-04	1.54E-03	4.03E-03	5.19E-03	7.15E-03	8.98E-03	1.05E-02	1.11E-02	1.02E-02
BONE MARROW	--	--	--	<u>1.95E-06</u>	<u>2.64E-06</u>	<u>4.06E-06</u>	<u>6.63E-06</u>	<u>1.31E-05</u>	1.63E-04
SKIN	<u>1.75E-05</u>	<u>4.70E-05</u>	1.35E-04	1.90E-04	4.17E-04	1.16E-03	3.29E-03	5.55E-03	1.16E-02
MUSCLE	5.85E-03	1.86E-02	4.84E-02	6.26E-02	8.76E-02	1.16E-01	1.47E-01	1.69E-01	2.09E-01
EXTERNAL	--	--	<u>3.81E-06</u>	<u>4.19E-06</u>	1.64E-05	6.26E-05	2.54E-04	5.18E-04	1.42E-03

7.4. APPENDIX D - Photon absorbed fractions for juvenile *Lepus californicus*

TARGET	PHOTON ABSORBED FRACTIONS											
	Source = BONE											
	Energy (MeV)											
	0.01	0.015	0.02	0.03	0.05	0.1	0.2	0.5	1.0	1.5	2.0	4.0
BRAIN	1.12E-03	2.61E-03	3.50E-03	3.04E-03	1.58E-03	1.04E-03	1.14E-03	1.24E-03	1.17E-03	1.06E-03	9.74E-04	7.03E-04
HEART	5.31E-05	3.69E-04	8.53E-04	1.08E-03	6.83E-04	4.60E-04	5.05E-04	5.51E-04	5.22E-04	4.77E-04	4.43E-04	3.59E-04
LUNGS	5.77E-04	1.83E-03	2.89E-03	3.07E-03	1.93E-03	1.42E-03	1.55E-03	1.69E-03	1.60E-03	1.48E-03	1.38E-03	1.06E-03
LIVER	2.28E-04	1.08E-03	1.92E-03	2.17E-03	1.45E-03	1.15E-03	1.32E-03	1.46E-03	1.39E-03	1.32E-03	1.23E-03	9.73E-04
GALLBLADDER	--	--	<u>1.21E-05</u>	<u>1.63E-05</u>	<u>8.47E-06</u>	<u>8.01E-06</u>	<u>8.04E-06</u>	<u>9.46E-06</u>	<u>8.71E-06</u>	<u>8.03E-06</u>	<u>7.82E-06</u>	<u>7.04E-06</u>
GI TRACT	1.33E-04	1.10E-03	2.71E-03	4.02E-03	2.85E-03	2.23E-03	2.51E-03	2.74E-03	2.63E-03	2.46E-03	2.31E-03	1.85E-03
KIDNEYS	<u>2.46E-05</u>	1.78E-04	4.05E-04	5.75E-04	4.18E-04	3.50E-04	3.92E-04	4.30E-04	4.26E-04	3.98E-04	3.74E-04	2.97E-04
OVARIES	<u>1.09E-05</u>	7.80E-05	1.53E-04	1.73E-04	1.06E-04	6.48E-05	6.76E-05	7.29E-05	7.02E-05	6.36E-05	5.76E-05	4.58E-05
STOMACH CONTENTS	<u>1.23E-05</u>	1.56E-04	4.39E-04	6.93E-04	5.30E-04	3.96E-04	4.43E-04	4.81E-04	4.71E-04	4.40E-04	4.19E-04	3.45E-04
FECES	<u>1.07E-05</u>	3.23E-04	1.00E-03	1.66E-03	1.17E-03	8.75E-04	9.83E-04	1.06E-03	1.02E-03	9.37E-04	8.80E-04	7.26E-04
FAT	2.20E-04	6.35E-04	9.58E-04	1.04E-03	7.51E-04	7.10E-04	8.35E-04	9.11E-04	8.78E-04	8.00E-04	7.48E-04	5.81E-04
BLOOD	6.52E-04	2.60E-03	4.61E-03	5.15E-03	3.02E-03	1.92E-03	2.06E-03	2.23E-03	2.11E-03	1.94E-03	1.79E-03	1.40E-03
BONE	9.49E-01	8.69E-01	7.62E-01	5.29E-01	2.18E-01	5.43E-02	3.32E-02	3.19E-02	2.79E-02	2.38E-02	2.04E-02	1.31E-02
SKIN	2.57E-03	4.98E-03	5.95E-03	5.33E-03	3.06E-03	2.26E-03	2.60E-03	2.82E-03	2.54E-03	2.24E-03	2.01E-03	1.46E-03
BONE MARROW	3.82E-03	9.71E-03	1.43E-02	1.39E-02	6.47E-03	1.67E-03	1.01E-03	9.70E-04	8.91E-04	7.91E-04	7.00E-04	4.31E-04
MUSCLE	3.45E-02	6.41E-02	8.06E-02	7.70E-02	4.80E-02	3.67E-02	4.18E-02	4.58E-02	4.32E-02	3.93E-02	3.58E-02	2.63E-02
EXTERNAL	3.41E-04	6.37E-04	7.41E-04	6.44E-04	3.53E-04	2.33E-04	2.64E-04	2.60E-04	2.12E-04	1.91E-04	1.76E-04	1.37E-04

TARGET	PHOTON ABSORBED FRACTIONS												
	Source = MUSCLE												
	Energy (MeV)												
	0.01	0.015	0.02	0.03	0.05	0.1	0.2	0.5	1.0	1.5	2.0	4.0	
BRAIN	7.94E-05	1.94E-04	4.42E-04	6.74E-04	4.76E-04	3.41E-04	3.79E-04	4.22E-04	4.10E-04	3.80E-04	3.51E-04	2.78E-04	
HEART	1.37E-03	2.46E-03	2.76E-03	1.98E-03	9.07E-04	5.58E-04	6.01E-04	6.46E-04	6.13E-04	5.54E-04	5.13E-04	4.12E-04	
LUNGS	3.03E-03	4.93E-03	5.56E-03	4.40E-03	2.28E-03	1.53E-03	1.68E-03	1.80E-03	1.71E-03	1.57E-03	1.46E-03	1.13E-03	
LIVER	6.38E-03	9.47E-03	9.38E-03	6.29E-03	2.98E-03	2.10E-03	2.36E-03	2.58E-03	2.45E-03	2.25E-03	2.06E-03	1.56E-03	
GALLBLADDER	4.90E-05	6.90E-05	7.75E-05	5.30E-05	<u>2.39E-05</u>	<u>1.55E-05</u>	<u>1.80E-05</u>	<u>1.94E-05</u>	<u>1.90E-05</u>	<u>1.66E-05</u>	<u>1.70E-05</u>	<u>1.25E-05</u>	
GI TRACT	1.54E-02	2.52E-02	2.59E-02	1.65E-02	7.32E-03	5.01E-03	5.52E-03	5.95E-03	5.60E-03	5.14E-03	4.73E-03	3.59E-03	
KIDNEYS	3.02E-03	4.78E-03	4.51E-03	2.70E-03	1.20E-03	8.49E-04	9.56E-04	1.03E-03	9.69E-04	8.94E-04	8.17E-04	6.09E-04	
OVARIES	4.86E-04	6.90E-04	6.05E-04	3.47E-04	1.42E-04	8.29E-05	8.50E-05	9.04E-05	8.25E-05	7.45E-05	7.05E-05	5.17E-05	
STOMACH CONTENTS	1.17E-03	3.90E-03	4.80E-03	3.33E-03	1.52E-03	1.00E-03	1.10E-03	1.18E-03	1.11E-03	1.03E-03	9.39E-04	7.44E-04	
FECES	2.85E-03	7.98E-03	9.61E-03	6.57E-03	2.89E-03	1.90E-03	2.08E-03	2.23E-03	2.11E-03	1.94E-03	1.79E-03	1.39E-03	
FAT	5.01E-03	5.48E-03	4.55E-03	2.71E-03	1.35E-03	1.15E-03	1.32E-03	1.45E-03	1.35E-03	1.23E-03	1.13E-03	8.29E-04	
BLOOD	7.52E-03	1.19E-02	1.28E-02	9.49E-03	4.31E-03	2.48E-03	2.61E-03	2.80E-03	2.66E-03	2.43E-03	2.25E-03	1.73E-03	
BONE	9.49E-02	1.91E-01	2.51E-01	2.42E-01	1.17E-01	3.04E-02	1.76E-02	1.68E-02	1.57E-02	1.42E-02	1.30E-02	9.54E-03	
SKIN	2.87E-02	2.52E-02	1.82E-02	9.39E-03	3.93E-03	2.58E-03	2.92E-03	3.15E-03	2.78E-03	2.43E-03	2.18E-03	1.55E-03	
BONE MARROW	1.37E-04	5.99E-04	2.93E-03	6.73E-03	4.23E-03	1.16E-03	6.66E-04	6.18E-04	5.74E-04	5.37E-04	4.89E-04	3.82E-04	
MUSCLE	7.76E-01	5.47E-01	3.68E-01	1.81E-01	7.61E-02	5.20E-02	5.87E-02	6.36E-02	5.83E-02	5.17E-02	4.61E-02	3.22E-02	
EXTERNAL	2.92E-03	2.53E-03	1.81E-03	9.68E-04	3.97E-04	2.48E-04	2.76E-04	2.67E-04	2.22E-04	1.95E-04	1.79E-04	1.38E-04	

TARGET	PHOTON ABSORBED FRACTIONS											
	Source = LIVER											
	Energy (MeV)											
	0.01	0.015	0.02	0.03	0.05	0.1	0.2	0.5	1.0	1.5	2.0	4.0
BRAIN	0.00E+00	--	--	<u>3.62E-05</u>	1.00E-04	1.01E-04	1.21E-04	1.50E-04	1.57E-04	1.48E-04	1.38E-04	1.16E-04
HEART	<u>1.45E-05</u>	8.43E-04	2.55E-03	2.80E-03	1.37E-03	7.62E-04	7.98E-04	8.53E-04	8.06E-04	7.45E-04	6.95E-04	5.61E-04
LUNGS	5.76E-03	1.35E-02	1.86E-02	1.41E-02	6.08E-03	3.70E-03	3.95E-03	4.15E-03	3.88E-03	3.55E-03	3.28E-03	2.56E-03
LIVER	7.74E-01	5.04E-01	3.02E-01	1.18E-01	4.06E-02	2.79E-02	3.18E-02	3.37E-02	2.97E-02	2.52E-02	2.13E-02	1.25E-02
GALLBLADDER	2.46E-03	3.09E-03	2.19E-03	9.40E-04	3.31E-04	2.24E-04	2.51E-04	2.74E-04	2.54E-04	2.24E-04	1.99E-04	1.22E-04
GI TRACT	8.07E-03	2.59E-02	3.29E-02	2.29E-02	9.89E-03	6.39E-03	6.95E-03	7.43E-03	7.00E-03	6.42E-03	5.94E-03	4.64E-03
KIDNEYS	4.05E-03	6.54E-03	5.93E-03	3.58E-03	1.56E-03	1.06E-03	1.18E-03	1.27E-03	1.19E-03	1.08E-03	9.91E-04	7.30E-04
OVARIES	0.00E+00	0.00E+00	--	--	<u>9.21E-06</u>	--	<u>6.54E-06</u>	--	--	--	<u>7.97E-06</u>	<u>7.14E-06</u>
STOMACH CONTENTS	5.01E-03	2.12E-02	2.61E-02	1.60E-02	6.21E-03	3.87E-03	4.16E-03	4.38E-03	4.08E-03	3.74E-03	3.45E-03	2.64E-03
FECES	--	3.60E-04	1.78E-03	2.62E-03	1.47E-03	9.42E-04	1.02E-03	1.10E-03	1.05E-03	9.75E-04	9.02E-04	7.54E-04
FAT	6.16E-03	1.01E-02	8.74E-03	4.68E-03	2.08E-03	1.64E-03	1.87E-03	2.01E-03	1.89E-03	1.74E-03	1.59E-03	1.14E-03
BLOOD	3.96E-02	9.40E-02	9.95E-02	5.79E-02	2.09E-02	1.09E-02	1.12E-02	1.18E-02	1.11E-02	1.01E-02	9.32E-03	6.78E-03
BONE	1.36E-02	7.00E-02	1.32E-01	1.52E-01	7.70E-02	2.03E-02	1.11E-02	1.02E-02	9.65E-03	8.90E-03	8.27E-03	6.54E-03
SKIN	4.62E-04	3.27E-03	5.94E-03	5.93E-03	3.03E-03	1.97E-03	2.18E-03	2.34E-03	2.12E-03	1.90E-03	1.75E-03	1.40E-03
BONE MARROW	0.00E+00	--	3.25E-04	2.00E-03	1.89E-03	5.83E-04	3.10E-04	2.87E-04	2.66E-04	2.49E-04	2.30E-04	1.89E-04
MUSCLE	1.39E-01	2.10E-01	2.10E-01	1.40E-01	6.35E-02	4.16E-02	4.57E-02	4.96E-02	4.69E-02	4.30E-02	3.94E-02	3.00E-02
EXTERNAL	1.02E-04	7.07E-04	1.15E-03	9.92E-04	4.57E-04	2.56E-04	2.83E-04	2.64E-04	2.19E-04	1.99E-04	1.86E-04	1.60E-04

TARGET	PHOTON ABSORBED FRACTIONS												
	Source = OVARIES												
	Energy (MeV)												
	0.01	0.015	0.02	0.03	0.05	0.1	0.2	0.5	1.0	1.5	2.0	4.0	
BRAIN	0.00E+00	0.00E+00	--	--	<u>7.50E-06</u>	<u>9.13E-06</u>	<u>1.50E-05</u>	<u>2.24E-05</u>	<u>2.75E-05</u>	<u>2.82E-05</u>	<u>2.69E-05</u>	<u>2.41E-05</u>	
HEART	0.00E+00	0.00E+00	--	<u>1.09E-05</u>	<u>2.15E-05</u>	<u>1.86E-05</u>	2.29E-05	3.13E-05	<u>3.50E-05</u>	<u>3.65E-05</u>	<u>3.47E-05</u>	<u>3.04E-05</u>	
LUNGS	0.00E+00	0.00E+00	--	4.98E-05	7.23E-05	6.84E-05	8.38E-05	1.12E-04	1.25E-04	1.27E-04	1.24E-04	1.04E-04	
LIVER	0.00E+00	--	<u>3.15E-05</u>	2.51E-04	2.80E-04	2.33E-04	2.83E-04	3.45E-04	3.56E-04	3.41E-04	3.24E-04	2.86E-04	
GALLBLADDER	0.00E+00	0.00E+00	--	--	--	--	--	--	--	--	--	--	
GI TRACT	1.37E-02	4.67E-02	4.88E-02	2.84E-02	1.16E-02	7.60E-03	8.30E-03	8.82E-03	8.29E-03	7.62E-03	7.02E-03	5.16E-03	
KIDNEYS	--	1.22E-04	6.66E-04	9.89E-04	5.85E-04	4.20E-04	4.64E-04	5.02E-04	4.70E-04	4.38E-04	4.09E-04	3.37E-04	
OVARIES	6.17E-01	3.01E-01	1.48E-01	4.77E-02	1.33E-02	7.54E-03	8.42E-03	8.55E-03	6.33E-03	4.38E-03	3.13E-03	1.25E-03	
STOMACH CONTENTS	0.00E+00	--	5.89E-05	3.11E-04	2.60E-04	1.98E-04	2.20E-04	2.49E-04	2.46E-04	2.36E-04	2.27E-04	1.88E-04	
FECES	1.68E-03	1.24E-02	1.65E-02	1.14E-02	4.83E-03	3.04E-03	3.27E-03	3.45E-03	3.23E-03	2.97E-03	2.75E-03	2.12E-03	
FAT	4.45E-02	5.20E-02	3.65E-02	1.63E-02	6.70E-03	5.36E-03	6.19E-03	6.67E-03	6.22E-03	5.57E-03	4.95E-03	2.96E-03	
BLOOD	0.00E+00	0.00E+00	<u>1.47E-05</u>	2.16E-04	2.53E-04	1.87E-04	2.10E-04	2.71E-04	2.79E-04	2.80E-04	2.64E-04	2.32E-04	
BONE	1.83E-02	1.48E-01	2.95E-01	3.51E-01	1.74E-01	4.40E-02	2.43E-02	2.24E-02	2.07E-02	1.90E-02	1.75E-02	1.37E-02	
SKIN	<u>1.50E-05</u>	1.63E-03	4.63E-03	5.19E-03	2.92E-03	1.92E-03	2.11E-03	2.26E-03	2.09E-03	1.88E-03	1.73E-03	1.42E-03	
BONE MARROW	--	2.41E-04	3.42E-03	1.06E-02	6.87E-03	1.85E-03	1.00E-03	8.99E-04	8.43E-04	7.71E-04	7.11E-04	5.78E-04	
MUSCLE	3.05E-01	4.30E-01	3.80E-01	2.22E-01	9.75E-02	6.48E-02	7.12E-02	7.63E-02	7.15E-02	6.48E-02	5.88E-02	4.28E-02	
EXTERNAL	--	1.43E-04	4.57E-04	5.53E-04	3.06E-04	1.89E-04	2.14E-04	1.97E-04	1.63E-04	1.49E-04	1.40E-04	1.24E-04	

TARGET	PHOTON ABSORBED FRACTIONS												
	Source = LUNGS												
	Energy (MeV)												
	0.01	0.015	0.02	0.03	0.05	0.1	0.2	0.5	1.0	1.5	2.0	4.0	
BRAIN	0.00E+00	0.00E+00	--	8.11E-05	2.36E-04	2.23E-04	2.68E-04	3.02E-04	3.00E-04	2.85E-04	2.63E-04	2.19E-04	
HEART	1.20E-02	3.27E-02	3.43E-02	1.89E-02	6.84E-03	3.86E-03	4.05E-03	4.27E-03	3.98E-03	3.63E-03	3.31E-03	2.39E-03	
LUNGS	8.10E-01	5.48E-01	3.31E-01	1.29E-01	4.28E-02	2.69E-02	3.00E-02	3.18E-02	2.78E-02	2.34E-02	1.97E-02	1.11E-02	
LIVER	7.71E-03	1.78E-02	2.41E-02	1.81E-02	8.23E-03	5.55E-03	6.05E-03	6.38E-03	5.97E-03	5.47E-03	5.06E-03	3.95E-03	
GALLBLADDER	0.00E+00	<u>2.04E-05</u>	8.00E-05	9.53E-05	4.74E-05	3.21E-05	3.59E-05	3.70E-05	3.70E-05	<u>3.42E-05</u>	3.06E-05	2.51E-05	
GI TRACT	0.00E+00	1.86E-04	1.79E-03	3.75E-03	2.49E-03	1.78E-03	1.96E-03	2.14E-03	2.06E-03	1.92E-03	1.80E-03	1.48E-03	
KIDNEYS	0.00E+00	--	1.33E-04	4.24E-04	3.34E-04	2.45E-04	2.83E-04	3.12E-04	3.05E-04	2.85E-04	2.58E-04	2.21E-04	
OVARIES	0.00E+00	0.00E+00	--	--	--	--	--	--	--	--	--	--	
STOMACH CONTENTS	0.00E+00	1.80E-04	1.45E-03	2.45E-03	1.41E-03	9.39E-04	9.78E-04	1.04E-03	9.79E-04	9.11E-04	8.52E-04	6.96E-04	
FECES	0.00E+00	--	9.79E-05	5.06E-04	4.31E-04	3.19E-04	3.54E-04	4.17E-04	4.01E-04	3.79E-04	3.65E-04	3.04E-04	
FAT	--	9.92E-05	5.93E-04	8.77E-04	5.68E-04	4.82E-04	5.44E-04	5.99E-04	5.63E-04	5.18E-04	4.88E-04	4.09E-04	
BLOOD	3.70E-02	8.21E-02	9.30E-02	5.79E-02	2.19E-02	1.16E-02	1.19E-02	1.26E-02	1.17E-02	1.06E-02	9.72E-03	7.20E-03	
BONE	4.52E-02	1.59E-01	2.61E-01	2.79E-01	1.39E-01	3.62E-02	1.99E-02	1.83E-02	1.70E-02	1.56E-02	1.43E-02	1.10E-02	
SKIN	1.17E-04	1.40E-03	3.41E-03	4.42E-03	2.72E-03	1.87E-03	2.06E-03	2.23E-03	2.03E-03	1.83E-03	1.67E-03	1.35E-03	
BONE MARROW	--	2.39E-04	2.27E-03	6.28E-03	4.14E-03	1.15E-03	6.25E-04	5.68E-04	5.32E-04	4.91E-04	4.53E-04	3.59E-04	
MUSCLE	8.74E-02	1.42E-01	1.60E-01	1.27E-01	6.54E-02	4.48E-02	4.93E-02	5.30E-02	5.00E-02	4.58E-02	4.22E-02	3.26E-02	
EXTERNAL	<u>2.06E-05</u>	2.82E-04	6.13E-04	7.22E-04	4.00E-04	2.39E-04	2.65E-04	2.44E-04	2.03E-04	1.86E-04	1.76E-04	1.53E-04	

TARGET	PHOTON ABSORBED FRACTIONS												
	Source = KIDNEYS												
	Energy (MeV)												
	0.01	0.015	0.02	0.03	0.05	0.1	0.2	0.5	1.0	1.5	2.0	4.0	
BRAIN	0.00E+00	0.00E+00	--	<u>2.26E-05</u>	4.87E-05	5.17E-05	6.40E-05	8.07E-05	7.95E-05	7.89E-05	8.11E-05	6.69E-05	
HEART	0.00E+00	--	<u>3.26E-05</u>	1.85E-04	1.56E-04	1.10E-04	1.22E-04	1.36E-04	1.42E-04	1.33E-04	1.28E-04	1.06E-04	
LUNGS	0.00E+00	<u>1.23E-05</u>	3.09E-04	9.97E-04	7.26E-04	5.28E-04	5.62E-04	6.31E-04	6.13E-04	5.74E-04	5.40E-04	4.50E-04	
LIVER	1.24E-02	2.00E-02	1.82E-02	1.10E-02	4.75E-03	3.21E-03	3.55E-03	3.82E-03	3.58E-03	3.28E-03	3.02E-03	2.22E-03	
GALLBLADDER	0.00E+00	--	<u>2.58E-05</u>	4.01E-05	<u>2.43E-05</u>	<u>1.62E-05</u>	<u>1.82E-05</u>	<u>1.75E-05</u>	<u>1.79E-05</u>	<u>1.67E-05</u>	<u>1.65E-05</u>	<u>1.09E-05</u>	
GI TRACT	1.82E-02	6.74E-02	7.94E-02	4.86E-02	1.94E-02	1.24E-02	1.36E-02	1.44E-02	1.35E-02	1.24E-02	1.14E-02	8.72E-03	
KIDNEYS	7.48E-01	4.34E-01	2.31E-01	8.05E-02	2.64E-02	1.86E-02	2.15E-02	2.28E-02	1.95E-02	1.58E-02	1.27E-02	6.18E-03	
OVARIES	0.00E+00	<u>1.37E-05</u>	7.32E-05	1.10E-04	5.94E-05	3.33E-05	3.04E-05	3.34E-05	<u>3.21E-05</u>	<u>3.08E-05</u>	<u>2.80E-05</u>	2.27E-05	
STOMACH CONTENTS	2.67E-04	5.79E-03	1.06E-02	8.20E-03	3.47E-03	2.16E-03	2.30E-03	2.41E-03	2.27E-03	2.10E-03	1.94E-03	1.57E-03	
FECES	3.46E-03	2.03E-02	2.69E-02	1.74E-02	7.01E-03	4.31E-03	4.65E-03	4.91E-03	4.60E-03	4.27E-03	3.94E-03	3.07E-03	
FAT	3.92E-03	8.81E-03	9.11E-03	5.45E-03	2.49E-03	1.97E-03	2.24E-03	2.42E-03	2.26E-03	2.09E-03	1.91E-03	1.45E-03	
BLOOD	--	1.31E-03	4.91E-03	6.27E-03	3.24E-03	1.76E-03	1.80E-03	1.92E-03	1.84E-03	1.71E-03	1.57E-03	1.29E-03	
BONE	5.12E-03	3.63E-02	8.40E-02	1.20E-01	6.85E-02	1.86E-02	1.02E-02	9.38E-03	8.86E-03	8.20E-03	7.62E-03	6.16E-03	
SKIN	2.47E-03	9.20E-03	1.13E-02	8.07E-03	3.64E-03	2.28E-03	2.51E-03	2.73E-03	2.47E-03	2.22E-03	2.03E-03	1.59E-03	
BONE MARROW	0.00E+00	<u>1.29E-05</u>	6.16E-04	3.88E-03	3.36E-03	9.83E-04	5.33E-04	4.89E-04	4.52E-04	4.14E-04	3.87E-04	3.26E-04	
MUSCLE	2.01E-01	3.22E-01	3.05E-01	1.84E-01	7.85E-02	5.07E-02	5.58E-02	6.04E-02	5.70E-02	5.21E-02	4.78E-02	3.56E-02	
EXTERNAL	2.62E-04	1.12E-03	1.37E-03	9.66E-04	4.11E-04	2.38E-04	2.63E-04	2.39E-04	1.98E-04	1.82E-04	1.71E-04	1.45E-04	

TARGET	PHOTON ABSORBED FRACTIONS											
	Source = HEART											
	Energy (MeV)											
	0.01	0.015	0.02	0.03	0.05	0.1	0.2	0.5	1.0	1.5	2.0	4.0
BRAIN	0.00E+00	0.00E+00	--	3.76E-05	1.72E-04	1.91E-04	2.29E-04	2.56E-04	2.51E-04	2.35E-04	2.32E-04	1.90E-04
HEART	8.20E-01	5.56E-01	3.29E-01	1.23E-01	3.77E-02	2.20E-02	2.45E-02	2.59E-02	2.24E-02	1.84E-02	1.52E-02	7.72E-03
LUNGS	2.87E-02	7.90E-02	8.28E-02	4.61E-02	1.74E-02	1.06E-02	1.15E-02	1.22E-02	1.14E-02	1.04E-02	9.59E-03	6.87E-03
LIVER	<u>3.51E-05</u>	2.69E-03	7.94E-03	8.87E-03	4.61E-03	3.16E-03	3.43E-03	3.65E-03	3.41E-03	3.13E-03	2.93E-03	2.39E-03
GALLBLADDER	0.00E+00	--	<u>3.79E-05</u>	5.94E-05	3.45E-05	2.30E-05	2.47E-05	<u>2.67E-05</u>	<u>2.38E-05</u>	<u>2.33E-05</u>	<u>2.12E-05</u>	<u>1.65E-05</u>
GI TRACT	0.00E+00	<u>2.15E-05</u>	4.84E-04	1.71E-03	1.38E-03	1.02E-03	1.16E-03	1.32E-03	1.30E-03	1.23E-03	1.15E-03	9.54E-04
KIDNEYS	0.00E+00	--	<u>2.96E-05</u>	1.86E-04	1.87E-04	1.46E-04	1.72E-04	1.95E-04	1.91E-04	1.85E-04	1.71E-04	1.51E-04
OVARIES	0.00E+00	0.00E+00	--	--	--	--	--	--	--	--	--	--
STOMACH CONTENTS	0.00E+00	<u>2.38E-05</u>	4.67E-04	1.22E-03	8.10E-04	5.63E-04	6.05E-04	6.62E-04	6.40E-04	5.95E-04	5.47E-04	4.54E-04
FECES	0.00E+00	--	<u>3.52E-05</u>	2.57E-04	2.72E-04	2.16E-04	2.47E-04	2.96E-04	3.01E-04	2.85E-04	2.69E-04	2.29E-04
FAT	0.00E+00	--	1.24E-04	3.36E-04	2.74E-04	2.49E-04	2.87E-04	3.17E-04	3.11E-04	2.92E-04	2.74E-04	2.27E-04
BLOOD	4.41E-02	9.69E-02	9.87E-02	5.71E-02	2.10E-02	1.11E-02	1.15E-02	1.22E-02	1.14E-02	1.05E-02	9.60E-03	6.81E-03
BONE	9.87E-03	7.80E-02	1.85E-01	2.38E-01	1.25E-01	3.30E-02	1.81E-02	1.67E-02	1.55E-02	1.42E-02	1.32E-02	1.05E-02
SKIN	<u>3.21E-05</u>	1.83E-03	4.73E-03	5.36E-03	2.95E-03	1.99E-03	2.21E-03	2.39E-03	2.16E-03	1.95E-03	1.80E-03	1.46E-03
BONE MARROW	0.00E+00	1.20E-04	1.83E-03	5.94E-03	3.99E-03	1.09E-03	5.96E-04	5.36E-04	5.08E-04	4.74E-04	4.45E-04	3.56E-04
MUSCLE	9.70E-02	1.72E-01	1.94E-01	1.40E-01	6.71E-02	4.53E-02	4.99E-02	5.37E-02	5.06E-02	4.64E-02	4.27E-02	3.29E-02
EXTERNAL	--	2.45E-04	6.88E-04	8.02E-04	4.24E-04	2.54E-04	2.87E-04	2.55E-04	2.12E-04	1.93E-04	1.83E-04	1.60E-04

TARGET	PHOTON ABSORBED FRACTIONS												
	Source = GI TRACT												
	Energy (MeV)												
	0.01	0.015	0.02	0.03	0.05	0.1	0.2	0.5	1.0	1.5	2.0	4.0	
BRAIN	0.00E+00	0.00E+00	--	<u>2.18E-05</u>	5.13E-05	4.57E-05	5.80E-05	7.74E-05	7.99E-05	7.53E-05	7.13E-05	6.35E-05	
HEART	0.00E+00	--	7.56E-05	2.63E-04	2.06E-04	1.29E-04	1.44E-04	1.55E-04	1.56E-04	1.45E-04	1.40E-04	1.21E-04	
LUNGS	0.00E+00	7.50E-05	6.95E-04	1.44E-03	9.31E-04	6.18E-04	6.69E-04	7.33E-04	7.10E-04	6.65E-04	6.28E-04	5.12E-04	
LIVER	4.03E-03	1.30E-02	1.65E-02	1.15E-02	5.05E-03	3.33E-03	3.64E-03	3.89E-03	3.66E-03	3.39E-03	3.14E-03	2.44E-03	
GALLBLADDER	1.60E-04	1.87E-04	1.66E-04	1.11E-04	4.72E-05	2.78E-05	3.19E-05	<u>3.17E-05</u>	<u>3.11E-05</u>	<u>2.80E-05</u>	<u>2.63E-05</u>	1.99E-05	
GI TRACT	6.81E-01	4.45E-01	2.77E-01	1.15E-01	4.04E-02	2.68E-02	3.01E-02	<u>3.17E-02</u>	2.79E-02	2.38E-02	2.06E-02	1.28E-02	
KIDNEYS	3.01E-03	1.11E-02	1.31E-02	8.01E-03	3.27E-03	2.17E-03	2.37E-03	2.51E-03	2.35E-03	2.16E-03	1.99E-03	1.52E-03	
OVARIES	2.39E-04	8.27E-04	8.65E-04	4.96E-04	1.88E-04	9.93E-05	1.02E-04	1.07E-04	9.99E-05	9.07E-05	8.33E-05	6.13E-05	
STOMACH CONTENTS	2.69E-02	3.51E-02	2.99E-02	1.54E-02	5.68E-03	3.57E-03	3.92E-03	4.16E-03	3.88E-03	3.51E-03	3.15E-03	2.18E-03	
FECES	9.86E-02	1.10E-01	8.28E-02	3.84E-02	1.36E-02	8.60E-03	9.50E-03	1.01E-02	9.38E-03	8.33E-03	7.38E-03	4.85E-03	
FAT	8.17E-03	1.35E-02	1.21E-02	6.61E-03	2.93E-03	2.30E-03	2.62E-03	2.80E-03	2.62E-03	2.40E-03	2.18E-03	1.58E-03	
BLOOD	9.60E-04	5.51E-03	9.74E-03	8.90E-03	4.06E-03	2.16E-03	2.19E-03	2.33E-03	2.21E-03	2.06E-03	1.92E-03	1.55E-03	
BONE	4.04E-03	3.59E-02	9.32E-02	1.38E-01	7.78E-02	2.08E-02	1.12E-02	1.02E-02	9.55E-03	8.83E-03	8.24E-03	6.68E-03	
SKIN	2.34E-03	7.84E-03	1.06E-02	8.15E-03	3.75E-03	2.34E-03	2.55E-03	2.76E-03	2.50E-03	2.24E-03	2.06E-03	1.63E-03	
BONE MARROW	--	8.05E-05	1.37E-03	5.53E-03	4.07E-03	1.13E-03	6.16E-04	5.45E-04	5.11E-04	4.74E-04	4.37E-04	3.63E-04	
MUSCLE	1.68E-01	2.80E-01	2.89E-01	1.85E-01	8.02E-02	5.14E-02	5.62E-02	6.04E-02	5.67E-02	5.19E-02	4.76E-02	3.61E-02	
EXTERNAL	1.70E-04	7.50E-04	1.15E-03	9.20E-04	4.21E-04	2.38E-04	2.59E-04	2.41E-04	2.00E-04	1.82E-04	1.72E-04	1.47E-04	

TARGET	PHOTON ABSORBED FRACTIONS												
	Source = STOMACH CONTENTS												
	Energy (MeV)												
	0.01	0.015	0.02	0.03	0.05	0.1	0.2	0.5	1.0	1.5	2.0	4.0	
BRAIN	0.00E+00	0.00E+00	--	<u>1.76E-05</u>	6.45E-05	6.49E-05	8.48E-05	1.02E-04	1.10E-04	1.05E-04	9.79E-05	8.75E-05	
HEART	0.00E+00	<u>1.49E-05</u>	3.04E-04	7.94E-04	5.22E-04	3.12E-04	3.23E-04	3.53E-04	3.37E-04	3.16E-04	2.98E-04	2.37E-04	
LUNGS	--	2.81E-04	2.33E-03	4.03E-03	2.28E-03	1.43E-03	1.52E-03	1.61E-03	1.51E-03	1.39E-03	1.29E-03	1.06E-03	
LIVER	1.06E-02	4.45E-02	5.51E-02	3.37E-02	1.35E-02	8.77E-03	9.60E-03	1.01E-02	9.43E-03	8.70E-03	7.97E-03	6.15E-03	
GALLBLADDER	4.85E-04	1.03E-03	9.79E-04	5.09E-04	1.86E-04	1.28E-04	1.40E-04	1.50E-04	1.43E-04	1.31E-04	1.12E-04	8.26E-05	
GI TRACT	1.13E-01	1.47E-01	1.26E-01	6.47E-02	2.44E-02	1.58E-02	1.73E-02	1.84E-02	1.71E-02	1.54E-02	1.39E-02	9.68E-03	
KIDNEYS	1.82E-04	4.03E-03	7.40E-03	5.70E-03	2.49E-03	1.64E-03	1.77E-03	1.88E-03	1.77E-03	1.61E-03	1.49E-03	1.21E-03	
OVARIES	0.00E+00	--	--	<u>2.10E-05</u>	<u>1.86E-05</u>	<u>1.21E-05</u>	<u>1.29E-05</u>	<u>1.54E-05</u>	<u>1.46E-05</u>	<u>1.47E-05</u>	<u>1.20E-05</u>	<u>9.74E-06</u>	
STOMACH CONTENTS	8.06E-01	5.27E-01	3.04E-01	1.12E-01	3.62E-02	2.37E-02	2.68E-02	2.84E-02	2.47E-02	2.05E-02	1.71E-02	8.95E-03	
FECES	7.88E-03	1.46E-02	1.67E-02	1.13E-02	4.75E-03	2.94E-03	3.14E-03	3.35E-03	3.12E-03	2.85E-03	2.61E-03	2.02E-03	
FAT	2.55E-03	4.97E-03	5.67E-03	3.84E-03	1.85E-03	1.43E-03	1.63E-03	1.73E-03	1.62E-03	1.49E-03	1.36E-03	1.07E-03	
BLOOD	3.09E-03	1.88E-02	3.28E-02	2.62E-02	1.07E-02	5.57E-03	5.65E-03	5.88E-03	5.48E-03	5.03E-03	4.66E-03	3.70E-03	
BONE	1.53E-03	2.05E-02	6.30E-02	1.03E-01	6.06E-02	1.68E-02	8.93E-03	8.16E-03	7.68E-03	7.14E-03	6.65E-03	5.39E-03	
SKIN	1.58E-04	2.85E-03	6.40E-03	6.44E-03	3.24E-03	2.02E-03	2.22E-03	2.39E-03	2.17E-03	1.96E-03	1.79E-03	1.45E-03	
BONE MARROW	0.00E+00	--	2.04E-04	1.98E-03	2.00E-03	<u>6.35E-04</u>	<u>3.38E-04</u>	<u>3.03E-04</u>	<u>2.84E-04</u>	<u>2.61E-04</u>	<u>2.47E-04</u>	<u>2.01E-04</u>	
MUSCLE	5.38E-02	1.83E-01	2.27E-01	1.59E-01	7.04E-02	4.50E-02	4.89E-02	5.26E-02	4.97E-02	4.57E-02	4.23E-02	3.28E-02	
EXTERNAL	<u>3.00E-05</u>	5.40E-04	1.09E-03	9.93E-04	4.47E-04	2.50E-04	2.73E-04	2.53E-04	2.08E-04	1.88E-04	1.78E-04	1.54E-04	

TARGET	PHOTON ABSORBED FRACTIONS												
	Source = FECES												
	Energy (MeV)												
	0.01	0.015	0.02	0.03	0.05	0.1	0.2	0.5	1.0	1.5	2.0	4.0	
BRAIN	0.00E+00	0.00E+00	--	--	<u>2.26E-05</u>	<u>2.52E-05</u>	3.40E-05	4.33E-05	4.74E-05	4.85E-05	5.01E-05	4.59E-05	
HEART	0.00E+00	--	<u>1.17E-05</u>	1.02E-04	9.98E-05	7.01E-05	8.07E-05	9.14E-05	9.15E-05	9.36E-05	8.29E-05	7.54E-05	
LUNGS	0.00E+00	--	9.89E-05	4.49E-04	4.00E-04	2.94E-04	3.26E-04	3.83E-04	3.80E-04	3.49E-04	3.34E-04	2.76E-04	
LIVER	--	4.50E-04	2.18E-03	3.26E-03	1.89E-03	1.29E-03	1.42E-03	1.54E-03	1.48E-03	1.38E-03	1.29E-03	1.04E-03	
GALLBLADDER	0.00E+00	--	<u>2.06E-05</u>	<u>3.31E-05</u>	<u>1.62E-05</u>	<u>1.17E-05</u>	<u>1.23E-05</u>	<u>1.39E-05</u>	<u>1.16E-05</u>	<u>1.02E-05</u>	<u>1.19E-05</u>	<u>9.30E-06</u>	
GI TRACT	2.43E-01	2.71E-01	2.04E-01	9.47E-02	3.43E-02	2.23E-02	2.48E-02	2.65E-02	2.45E-02	2.18E-02	1.93E-02	1.26E-02	
KIDNEYS	1.39E-03	8.20E-03	1.09E-02	7.08E-03	2.94E-03	1.94E-03	2.09E-03	2.20E-03	2.07E-03	1.91E-03	1.79E-03	1.39E-03	
OVARIES	7.31E-05	5.21E-04	7.33E-04	4.98E-04	2.03E-04	1.05E-04	1.03E-04	1.10E-04	1.02E-04	9.49E-05	8.82E-05	6.74E-05	
STOMACH CONTENTS	4.59E-03	8.58E-03	9.83E-03	6.69E-03	2.81E-03	1.75E-03	1.88E-03	2.01E-03	1.88E-03	1.73E-03	1.57E-03	1.20E-03	
FECES	6.68E-01	4.15E-01	2.46E-01	9.52E-02	3.14E-02	2.03E-02	2.29E-02	2.41E-02	2.08E-02	1.73E-02	1.46E-02	8.43E-03	
FAT	1.19E-03	5.76E-03	7.40E-03	4.99E-03	2.36E-03	1.84E-03	2.06E-03	2.20E-03	2.04E-03	1.90E-03	1.75E-03	1.35E-03	
BLOOD	0.00E+00	7.87E-05	9.34E-04	2.31E-03	1.48E-03	8.47E-04	8.64E-04	9.58E-04	9.42E-04	8.72E-04	8.28E-04	6.86E-04	
BONE	9.84E-04	2.63E-02	8.48E-02	1.40E-01	8.04E-02	2.15E-02	1.15E-02	1.05E-02	9.75E-03	8.99E-03	8.31E-03	6.80E-03	
SKIN	1.83E-03	9.92E-03	1.34E-02	9.63E-03	4.23E-03	2.59E-03	2.83E-03	3.03E-03	2.71E-03	2.48E-03	2.29E-03	1.79E-03	
BONE MARROW	0.00E+00	1.44E-04	2.10E-03	7.30E-03	4.97E-03	1.36E-03	7.23E-04	6.48E-04	5.97E-04	5.53E-04	5.12E-04	4.15E-04	
MUSCLE	7.70E-02	2.19E-01	2.65E-01	1.82E-01	7.95E-02	5.06E-02	5.50E-02	5.90E-02	5.56E-02	5.11E-02	4.70E-02	3.63E-02	
EXTERNAL	9.30E-05	7.17E-04	1.17E-03	9.53E-04	4.29E-04	2.39E-04	2.62E-04	2.44E-04	2.05E-04	1.87E-04	1.76E-04	1.51E-04	

TARGET	PHOTON ABSORBED FRACTIONS											
	Source = SKIN											
	Energy (MeV)											
	0.01	0.015	0.02	0.03	0.05	0.1	0.2	0.5	1.0	1.5	2.0	4.0
BRAIN	--	1.44E-04	4.81E-04	7.43E-04	4.72E-04	3.37E-04	3.73E-04	4.18E-04	4.08E-04	3.90E-04	3.63E-04	2.83E-04
HEART	--	2.81E-04	7.31E-04	8.41E-04	4.71E-04	3.07E-04	3.38E-04	3.72E-04	3.56E-04	3.32E-04	2.98E-04	2.50E-04
LUNGS	4.53E-05	5.35E-04	1.29E-03	1.73E-03	1.09E-03	7.92E-04	8.98E-04	9.97E-04	9.65E-04	8.92E-04	8.30E-04	6.67E-04
LIVER	2.21E-04	1.60E-03	2.94E-03	2.98E-03	1.66E-03	1.26E-03	1.46E-03	1.63E-03	1.57E-03	1.47E-03	1.36E-03	1.09E-03
GALLBLADDER	--	<u>1.12E-05</u>	<u>2.56E-05</u>	<u>2.61E-05</u>	<u>1.50E-05</u>	<u>1.09E-05</u>	<u>1.26E-05</u>	<u>1.52E-05</u>	<u>1.30E-05</u>	<u>1.20E-05</u>	<u>1.11E-05</u>	<u>9.06E-06</u>
GI TRACT	2.32E-03	7.68E-03	1.04E-02	8.12E-03	3.97E-03	2.83E-03	3.20E-03	3.55E-03	3.40E-03	3.15E-03	2.94E-03	2.31E-03
KIDNEYS	4.09E-04	1.45E-03	1.79E-03	1.31E-03	6.41E-04	4.78E-04	5.56E-04	6.15E-04	5.86E-04	5.42E-04	5.15E-04	3.93E-04
OVARIES	--	<u>2.83E-05</u>	8.03E-05	8.93E-05	4.66E-05	2.91E-05	3.14E-05	3.40E-05	<u>3.13E-05</u>	<u>3.07E-05</u>	2.83E-05	2.54E-05
STOMACH CONTENTS	<u>3.85E-05</u>	6.72E-04	1.51E-03	1.53E-03	8.00E-04	5.61E-04	6.41E-04	7.05E-04	6.70E-04	6.24E-04	5.84E-04	4.82E-04
FECES	7.26E-04	3.95E-03	5.27E-03	3.81E-03	1.75E-03	1.20E-03	1.35E-03	1.47E-03	1.41E-03	1.30E-03	1.21E-03	9.57E-04
FAT	3.63E-04	8.84E-04	1.15E-03	9.98E-04	6.21E-04	5.47E-04	6.44E-04	7.25E-04	6.86E-04	6.48E-04	5.92E-04	4.74E-04
BLOOD	2.68E-04	2.16E-03	4.08E-03	4.53E-03	2.44E-03	1.48E-03	1.61E-03	1.78E-03	1.70E-03	1.58E-03	1.48E-03	1.20E-03
BONE	7.75E-02	1.61E-01	2.03E-01	1.87E-01	8.79E-02	2.28E-02	1.38E-02	1.36E-02	1.28E-02	1.16E-02	1.05E-02	7.56E-03
SKIN	3.23E-01	1.33E-01	6.44E-02	2.23E-02	7.30E-03	4.71E-03	5.35E-03	5.14E-03	3.66E-03	2.84E-03	2.33E-03	1.43E-03
BONE MARROW	<u>2.63E-05</u>	4.89E-04	2.29E-03	4.61E-03	2.80E-03	7.62E-04	4.57E-04	4.42E-04	4.17E-04	3.80E-04	3.56E-04	2.76E-04
MUSCLE	3.10E-01	2.73E-01	1.98E-01	1.04E-01	4.60E-02	3.25E-02	3.74E-02	4.15E-02	3.89E-02	3.48E-02	3.12E-02	2.23E-02
EXTERNAL	1.63E-02	6.97E-03	3.49E-03	1.34E-03	4.79E-04	2.73E-04	3.24E-04	3.29E-04	2.44E-04	1.93E-04	1.65E-04	1.09E-04

7.5. APPENDIX E - Electron absorbed fractions for juvenile *Lepus californicus*

ELECTRON ABSORBED FRACTIONS

Source = BONE

Energy (MeV)

TARGET	0.1	0.2	0.4	0.5	0.7	1.0	1.5	2.0	4.0
BRAIN	3.12E-04	1.02E-03	2.61E-03	3.36E-03	4.85E-03	6.82E-03	9.44E-03	1.11E-02	1.25E-02
HEART	--	<u>2.23E-05</u>	<u>5.22E-05</u>	7.32E-05	1.18E-04	2.14E-04	4.38E-04	7.26E-04	1.97E-03
LUNGS	6.78E-05	2.16E-04	6.16E-04	9.04E-04	1.59E-03	2.80E-03	4.78E-03	6.24E-03	8.93E-03
LIVER	<u>1.75E-05</u>	<u>5.08E-05</u>	1.34E-04	2.09E-04	4.01E-04	8.65E-04	1.83E-03	2.64E-03	4.39E-03
GALLBLADDER	--	--	--	--	--	--	--	--	<u>1.68E-05</u>
GI TRACT	--	<u>1.64E-05</u>	5.17E-05	7.81E-05	1.79E-04	4.26E-04	1.03E-03	1.71E-03	5.59E-03
KIDNEYS	--	--	<u>1.79E-05</u>	<u>2.69E-05</u>	4.88E-05	9.50E-05	1.90E-04	3.10E-04	8.74E-04
OVARIES	--	--	--	--	--	<u>1.76E-05</u>	8.05E-05	1.56E-04	5.32E-04
STOMACH CONTENTS	--	--	--	--	<u>2.75E-06</u>	<u>1.17E-05</u>	7.00E-05	1.71E-04	4.80E-04
FECES	--	--	3.15E-06	<u>3.10E-06</u>	<u>4.43E-06</u>	<u>6.03E-06</u>	3.50E-05	1.69E-04	1.97E-03
FAT	<u>4.59E-05</u>	1.42E-04	3.77E-04	5.22E-04	8.66E-04	1.42E-03	2.29E-03	3.12E-03	5.49E-03
BLOOD	7.39E-05	2.15E-04	5.99E-04	8.49E-04	1.48E-03	2.76E-03	5.13E-03	6.91E-03	1.02E-02
BONE	9.86E-01	9.56E-01	8.86E-01	8.53E-01	7.90E-01	7.05E-01	5.91E-01	5.10E-01	3.33E-01
SKIN	4.03E-04	1.35E-03	3.88E-03	5.55E-03	9.54E-03	1.47E-02	1.93E-02	2.12E-02	2.03E-02
BONE MARROW	8.20E-04	2.65E-03	6.85E-03	8.79E-03	1.25E-02	1.67E-02	1.90E-02	1.75E-02	1.04E-02
MUSCLE	1.14E-02	3.65E-02	9.29E-02	1.18E-01	1.64E-01	2.17E-01	2.75E-01	3.06E-01	3.26E-01
EXTERNAL	2.04E-04	3.70E-04	4.63E-04	5.76E-04	8.57E-04	1.33E-03	1.84E-03	2.07E-03	2.08E-03

ELECTRON ABSORBED FRACTIONS

Source = MUSCLE

Energy (MeV)

TARGET	0.1	0.2	0.4	0.5	0.7	1.0	1.5	2.0	4.0
BRAIN	--	--	<u>3.33E-05</u>	<u>4.86E-05</u>	7.85E-05	1.66E-04	4.49E-04	8.30E-04	2.12E-03
HEART	8.19E-05	2.62E-04	6.49E-04	8.23E-04	1.10E-03	1.40E-03	1.79E-03	2.09E-03	3.42E-03
LUNGS	1.88E-04	5.85E-04	1.46E-03	1.82E-03	2.49E-03	3.29E-03	4.42E-03	5.49E-03	8.58E-03
LIVER	3.57E-04	1.16E-03	2.95E-03	3.76E-03	5.21E-03	6.91E-03	8.97E-03	1.05E-02	1.30E-02
GALLBLADDER	--	--	<u>3.09E-05</u>	<u>3.54E-05</u>	<u>4.39E-05</u>	5.58E-05	6.32E-05	7.26E-05	9.67E-05
GI TRACT	8.55E-04	2.75E-03	6.92E-03	8.82E-03	1.23E-02	1.62E-02	2.09E-02	2.43E-02	3.17E-02
KIDNEYS	1.50E-04	4.68E-04	1.21E-03	1.56E-03	2.24E-03	3.13E-03	4.30E-03	5.12E-03	6.36E-03
OVARIES	<u>2.04E-05</u>	7.03E-05	1.79E-04	2.37E-04	3.35E-04	4.63E-04	6.00E-04	6.31E-04	6.01E-04
STOMACH CONTENTS	--	<u>3.81E-05</u>	1.14E-04	1.58E-04	3.15E-04	7.06E-04	1.62E-03	2.62E-03	5.56E-03
FECES	<u>4.38E-05</u>	1.42E-04	4.13E-04	6.03E-04	1.11E-03	2.13E-03	4.13E-03	5.89E-03	1.04E-02
FAT	3.80E-04	1.23E-03	3.08E-03	3.88E-03	5.36E-03	6.93E-03	8.38E-03	8.97E-03	9.30E-03
BLOOD	4.17E-04	1.32E-03	3.31E-03	4.20E-03	5.80E-03	7.58E-03	9.74E-03	1.13E-02	1.44E-02
BONE	4.00E-03	1.26E-02	3.21E-02	4.09E-02	5.68E-02	7.55E-02	9.62E-02	1.08E-01	1.15E-01
SKIN	3.13E-03	9.70E-03	2.17E-02	2.49E-02	2.76E-02	2.78E-02	2.67E-02	2.53E-02	2.15E-02
BONE MARROW	--	<u>2.63E-05</u>	6.51E-05	8.30E-05	1.19E-04	2.47E-04	9.67E-04	2.05E-03	4.03E-03
MUSCLE	9.89E-01	9.65E-01	9.13E-01	8.89E-01	8.45E-01	7.90E-01	7.17E-01	6.60E-01	5.17E-01
EXTERNAL	8.86E-04	1.46E-03	1.70E-03	1.91E-03	2.12E-03	2.17E-03	2.15E-03	2.10E-03	1.89E-03

ELECTRON ABSORBED FRACTIONS
Source = LIVER
Energy (MeV)

TARGET	0.1	0.2	0.4	0.5	0.7	1.0	1.5	2.0	4.0
BRAIN	--	--	--	--	--	--	--	--	--
HEART	--	--	<u>1.95E-06</u>	<u>2.21E-06</u>	<u>2.85E-06</u>	<u>3.30E-06</u>	<u>5.16E-06</u>	<u>7.30E-06</u>	6.88E-04
LUNGS	1.47E-04	5.51E-04	1.63E-03	2.21E-03	3.42E-03	5.05E-03	7.37E-03	9.26E-03	1.61E-02
LIVER	9.91E-01	9.73E-01	9.28E-01	9.07E-01	8.64E-01	8.06E-01	7.18E-01	6.43E-01	4.39E-01
GALLBLADDER	8.64E-05	2.65E-04	7.17E-04	9.85E-04	1.54E-03	2.39E-03	3.51E-03	4.14E-03	3.52E-03
GI TRACT	1.13E-04	3.52E-04	1.04E-03	1.49E-03	2.75E-03	5.33E-03	1.07E-02	1.61E-02	3.34E-02
KIDNEYS	1.41E-04	4.08E-04	1.17E-03	1.57E-03	2.41E-03	3.59E-03	5.33E-03	6.71E-03	8.46E-03
OVARIES	--	--	--	--	--	--	--	--	--
STOMACH CONTENTS	7.74E-05	2.40E-04	6.64E-04	8.97E-04	1.44E-03	2.52E-03	5.52E-03	9.81E-03	2.87E-02
FECES	--	--	<u>1.96E-06</u>	<u>2.10E-06</u>	<u>3.39E-06</u>	<u>3.76E-06</u>	6.22E-06	7.31E-06	5.33E-05
FAT	1.23E-04	4.53E-04	1.36E-03	2.05E-03	3.76E-03	6.69E-03	1.10E-02	1.41E-02	1.80E-02
BLOOD	6.56E-04	2.23E-03	6.65E-03	9.38E-03	1.59E-02	2.81E-02	4.95E-02	6.68E-02	9.97E-02
BONE	1.33E-04	3.73E-04	1.01E-03	1.43E-03	2.75E-03	5.77E-03	1.20E-02	1.77E-02	2.94E-02
SKIN	--	<u>2.65E-06</u>	<u>4.44E-06</u>	<u>5.56E-06</u>	8.05E-06	6.25E-05	5.53E-04	1.63E-03	5.78E-03
BONE MARROW	--	--	--	--	<u>1.69E-06</u>	<u>2.34E-06</u>	<u>3.12E-06</u>	<u>3.13E-06</u>	9.10E-05
MUSCLE	7.01E-03	2.21E-02	5.65E-02	7.20E-02	1.00E-01	1.32E-01	1.72E-01	2.01E-01	2.48E-01
EXTERNAL	--	--	--	--	--	5.05E-06	6.00E-05	2.10E-04	9.15E-04

TARGET	ELECTRON ABSORBED FRACTIONS									
	Source = OVARIES									
	Energy (MeV)									
	0.1	0.2	0.4	0.5	0.7	1.0	1.5	2.0	4.0	
BRAIN	0.00E+00	0.00E+00	--	--	--	--	--	--	--	--
HEART	0.00E+00	--	--	--	--	--	--	--	--	--
LUNGS	--	--	--	--	--	--	--	--	--	--
LIVER	--	--	--	--	--	--	--	<u>1.76E-06</u>	<u>4.54E-06</u>	
GALLBLADDER	--	--	--	--	--	--	--	--	--	
GI TRACT	<u>1.33E-05</u>	1.92E-05	4.62E-05	1.71E-04	1.13E-03	6.08E-03	2.24E-02	4.19E-02	7.39E-02	
KIDNEYS	--	--	--	--	--	--	<u>2.36E-06</u>	<u>3.50E-06</u>	<u>7.21E-06</u>	
OVARIES	9.79E-01	9.32E-01	8.21E-01	7.67E-01	6.62E-01	5.20E-01	3.46E-01	2.56E-01	1.28E-01	
STOMACH CONTENTS	--	--	--	--	--	--	--	1.30E-06	3.72E-06	
FECES	--	<u>6.01E-06</u>	9.37E-06	1.05E-05	1.30E-05	1.79E-05	8.54E-04	4.90E-03	2.08E-02	
FAT	2.17E-03	7.68E-03	2.18E-02	2.99E-02	4.68E-02	7.04E-02	1.01E-01	1.14E-01	8.99E-02	
BLOOD	--	--	--	--	--	--	--	<u>1.51E-06</u>	<u>3.49E-06</u>	
BONE	9.53E-05	1.48E-04	2.22E-04	2.91E-04	8.21E-04	5.57E-03	2.25E-02	4.47E-02	1.57E-01	
SKIN	--	--	<u>3.91E-06</u>	<u>4.62E-06</u>	5.87E-06	8.77E-06	1.26E-05	1.66E-05	6.48E-04	
BONE MARROW	--	--	<u>5.66E-06</u>	<u>6.79E-06</u>	7.49E-06	9.01E-06	1.25E-05	9.87E-05	4.03E-03	
MUSCLE	1.90E-02	6.01E-02	1.56E-01	2.01E-01	2.88E-01	3.95E-01	5.03E-01	5.33E-01	5.12E-01	
EXTERNAL	--	--	--	--	--	<u>9.40E-07</u>	<u>1.20E-06</u>	<u>1.43E-06</u>	2.03E-05	

ELECTRON ABSORBED FRACTIONS

Source = LUNGS

Energy (MeV)

TARGET	0.1	0.2	0.4	0.5	0.7	1.0	1.5	2.0	4.0
BRAIN	--	--	--	--	--	--	--	--	<u>4.49E-06</u>
HEART	1.47E-04	4.95E-04	1.51E-03	2.30E-03	4.55E-03	9.00E-03	1.76E-02	2.62E-02	4.46E-02
LUNGS	9.92E-01	9.75E-01	9.35E-01	9.15E-01	8.76E-01	8.21E-01	7.36E-01	6.60E-01	4.42E-01
LIVER	3.07E-04	9.17E-04	2.53E-03	3.43E-03	5.24E-03	7.75E-03	1.14E-02	1.43E-02	2.48E-02
GALLBLADDER	--	--	--	--	--	--	--	--	--
GI TRACT	--	--	<u>3.32E-06</u>	<u>3.59E-06</u>	<u>5.26E-06</u>	<u>7.16E-06</u>	1.03E-05	1.42E-05	3.11E-05
KIDNEYS	--	--	--	--	--	--	--	--	<u>4.90E-06</u>
OVARIES	--	0.00E+00	--	--	--	--	--	--	--
STOMACH CONTENTS	--	--	<u>2.10E-06</u>	<u>1.79E-06</u>	<u>2.67E-06</u>	<u>3.70E-06</u>	<u>5.56E-06</u>	7.06E-06	1.50E-05
FECES	--	--	--	--	--	--	<u>2.13E-06</u>	<u>2.55E-06</u>	<u>6.27E-06</u>
FAT	--	--	--	--	--	<u>2.10E-06</u>	<u>2.26E-06</u>	<u>3.67E-06</u>	8.59E-06
BLOOD	1.23E-03	3.89E-03	1.09E-02	1.48E-02	2.29E-02	3.43E-02	5.10E-02	6.49E-02	9.61E-02
BONE	6.92E-04	2.24E-03	6.32E-03	9.03E-03	1.60E-02	2.86E-02	4.88E-02	6.42E-02	9.23E-02
SKIN	--	--	<u>3.78E-06</u>	<u>4.19E-06</u>	5.43E-06	9.14E-06	9.91E-05	5.25E-04	3.26E-03
BONE MARROW	--	--	<u>3.81E-06</u>	<u>4.01E-06</u>	<u>5.12E-06</u>	2.23E-05	1.93E-04	7.41E-04	3.12E-03
MUSCLE	5.35E-03	1.71E-02	4.28E-02	5.41E-02	7.38E-02	9.71E-02	1.30E-01	1.62E-01	2.53E-01
EXTERNAL	--	--	--	--	--	<u>9.30E-07</u>	1.03E-05	6.08E-05	4.79E-04

ELECTRON ABSORBED FRACTIONS

Source = HEART

Energy (MeV)

TARGET	0.1	0.2	0.4	0.5	0.7	1.0	1.5	2.0	4.0
BRAIN	--	--	--	--	--	--	--	--	<u>3.67E-06</u>
HEART	9.91E-01	9.72E-01	9.27E-01	9.06E-01	8.64E-01	8.04E-01	7.13E-01	6.30E-01	3.85E-01
LUNGS	4.38E-04	1.42E-03	4.27E-03	6.45E-03	1.28E-02	2.55E-02	5.00E-02	7.41E-02	1.27E-01
LIVER	--	<u>4.21E-06</u>	<u>7.14E-06</u>	8.69E-06	1.09E-05	1.54E-05	2.22E-05	2.80E-05	2.98E-03
GALLBLADDER	--	--	--	--	--	--	--	--	--
GI TRACT	--	--	<u>1.60E-06</u>	<u>1.85E-06</u>	<u>2.88E-06</u>	<u>4.05E-06</u>	<u>6.08E-06</u>	8.59E-06	1.75E-05
KIDNEYS	--	--	--	--	--	--	--	--	<u>2.70E-06</u>
OVARIES	0.00E+00	0.00E+00	--	--	--	--	--	--	--
STOMACH CONTENTS	--	--	--	--	<u>1.69E-06</u>	<u>2.69E-06</u>	<u>3.32E-06</u>	<u>4.35E-06</u>	9.52E-06
FECES	--	--	--	--	--	--	--	<u>2.09E-06</u>	4.49E-06
FAT	--	--	--	--	--	--	<u>1.46E-06</u>	<u>1.81E-06</u>	<u>3.93E-06</u>
BLOOD	1.06E-03	3.52E-03	1.00E-02	1.44E-02	2.51E-02	4.31E-02	7.11E-02	9.19E-02	1.15E-01
BONE	2.10E-04	6.00E-04	1.57E-03	2.15E-03	3.53E-03	6.24E-03	1.26E-02	2.10E-02	5.79E-02
SKIN	--	--	<u>4.32E-06</u>	<u>4.83E-06</u>	7.03E-06	9.35E-06	1.40E-05	2.26E-05	3.29E-03
BONE MARROW	--	--	<u>3.38E-06</u>	<u>3.62E-06</u>	<u>4.72E-06</u>	<u>6.78E-06</u>	1.01E-04	4.58E-04	2.17E-03
MUSCLE	7.10E-03	2.24E-02	5.58E-02	6.96E-02	9.27E-02	1.18E-01	1.49E-01	1.76E-01	2.85E-01
EXTERNAL	--	--	--	--	--	<u>1.31E-06</u>	<u>1.83E-06</u>	2.30E-06	2.60E-04

ELECTRON ABSORBED FRACTIONS
Source = GI TRACT
Energy (MeV)

TARGET	0.1	0.2	0.4	0.5	0.7	1.0	1.5	2.0	4.0
BRAIN	0.00E+00	--	--	--	--	--	--	--	--
HEART	--	--	--	--	--	--	--	--	<u>2.27E-06</u>
LUNGS	--	--	--	--	<u>1.85E-06</u>	<u>2.54E-06</u>	<u>3.58E-06</u>	<u>5.28E-06</u>	1.02E-05
LIVER	<u>5.10E-05</u>	1.68E-04	5.28E-04	7.77E-04	1.43E-03	2.79E-03	5.58E-03	8.43E-03	1.75E-02
GALLBLADDER	--	<u>3.04E-05</u>	8.04E-05	1.02E-04	1.41E-04	1.79E-04	1.97E-04	2.10E-04	1.90E-04
GI TRACT	9.83E-01	9.46E-01	8.64E-01	8.26E-01	7.58E-01	6.80E-01	5.92E-01	5.31E-01	3.81E-01
KIDNEYS	<u>1.86E-05</u>	5.76E-05	1.84E-04	2.74E-04	6.32E-04	1.61E-03	4.10E-03	7.04E-03	1.65E-02
OVARIES	--	--	--	--	<u>1.52E-05</u>	7.29E-05	2.71E-04	5.05E-04	8.83E-04
STOMACH CONTENTS	1.58E-03	4.95E-03	1.24E-02	1.59E-02	2.21E-02	2.84E-02	3.41E-02	3.69E-02	3.89E-02
FECES	6.20E-03	1.94E-02	4.86E-02	6.19E-02	8.48E-02	1.07E-01	1.23E-01	1.27E-01	1.13E-01
FAT	2.24E-04	7.46E-04	2.17E-03	3.04E-03	5.11E-03	8.58E-03	1.40E-02	1.79E-02	2.33E-02
BLOOD	--	<u>2.42E-05</u>	6.29E-05	8.25E-05	1.28E-04	2.13E-04	6.33E-04	1.45E-03	5.20E-03
BONE	4.68E-05	1.01E-04	2.27E-04	3.38E-04	6.93E-04	1.57E-03	3.66E-03	6.12E-03	1.97E-02
SKIN	--	<u>3.60E-05</u>	1.03E-04	1.60E-04	4.27E-04	1.32E-03	3.20E-03	4.59E-03	8.50E-03
BONE MARROW	--	--	<u>3.17E-06</u>	<u>3.20E-06</u>	<u>4.10E-06</u>	4.98E-06	9.27E-06	5.43E-05	8.49E-04
MUSCLE	8.91E-03	2.80E-02	7.03E-02	8.98E-02	1.25E-01	1.65E-01	2.12E-01	2.46E-01	3.20E-01
EXTERNAL	--	--	<u>4.55E-06</u>	<u>6.38E-06</u>	1.40E-05	4.85E-05	1.40E-04	2.44E-04	6.37E-04

ELECTRON ABSORBED FRACTIONS

Source = STOMACH CONTENTS

Energy (MeV)

TARGET	0.1	0.2	0.4	0.5	0.7	1.0	1.5	2.0	4.0
BRAIN	--	--	--	--	--	--	--	--	--
HEART	--	--	--	--	--	--	--	<u>2.69E-06</u>	<u>5.37E-06</u>
LUNGS	--	--	<u>3.09E-06</u>	<u>3.46E-06</u>	<u>4.25E-06</u>	<u>5.81E-06</u>	8.46E-06	1.16E-05	2.40E-05
LIVER	1.46E-04	5.21E-04	1.52E-03	2.08E-03	3.37E-03	5.93E-03	1.30E-02	2.29E-02	6.67E-02
GALLBLADDER	<u>1.53E-05</u>	<u>5.14E-05</u>	1.56E-04	2.15E-04	3.38E-04	4.73E-04	6.23E-04	7.94E-04	1.55E-03
GI TRACT	6.97E-03	2.20E-02	5.51E-02	7.03E-02	9.75E-02	1.25E-01	1.50E-01	1.63E-01	1.72E-01
KIDNEYS	--	<u>2.73E-06</u>	<u>4.23E-06</u>	4.79E-06	6.60E-06	7.86E-06	2.03E-05	1.88E-04	4.82E-03
OVARIES	0.00E+00	--	--	--	--	--	--	--	--
STOMACH CONTENTS	9.92E-01	9.74E-01	9.34E-01	9.14E-01	8.75E-01	8.22E-01	7.39E-01	6.62E-01	4.20E-01
FECES	3.05E-04	9.20E-04	2.50E-03	3.40E-03	5.17E-03	7.66E-03	1.08E-02	1.28E-02	1.64E-02
FAT	8.39E-05	3.08E-04	8.98E-04	1.25E-03	2.00E-03	3.04E-03	4.54E-03	5.66E-03	8.11E-03
BLOOD	<u>1.97E-05</u>	5.60E-05	1.60E-04	2.22E-04	3.94E-04	1.14E-03	3.27E-03	6.07E-03	1.86E-02
BONE	<u>2.37E-05</u>	4.10E-05	5.55E-05	6.10E-05	8.45E-05	2.29E-04	1.13E-03	2.73E-03	7.69E-03
SKIN	--	<u>2.79E-06</u>	<u>5.23E-06</u>	5.72E-06	7.53E-06	1.14E-05	8.48E-05	3.04E-04	3.09E-03
BONE MARROW	--	--	--	--	<u>1.54E-06</u>	<u>2.39E-06</u>	<u>2.88E-06</u>	<u>3.69E-06</u>	6.89E-06
MUSCLE	--	1.69E-03	4.99E-03	7.27E-03	1.41E-02	3.17E-02	7.29E-02	1.17E-01	2.48E-01
EXTERNAL	--	--	--	--	--	<u>1.44E-06</u>	7.49E-06	3.09E-05	3.87E-04

TARGET	ELECTRON ABSORBED FRACTIONS								
	Source = FECES								
	Energy (MeV)								
	0.1	0.2	0.4	0.5	0.7	1.0	1.5	2.0	4.0
BRAIN	--	--	--	--	--	--	--	--	--
HEART	--	--	--	--	--	--	--	--	--
LUNGS	--	--	--	--	--	--	--	<u>2.43E-06</u>	<u>6.46E-06</u>
LIVER	--	--	<u>2.56E-06</u>	<u>3.16E-06</u>	<u>4.01E-06</u>	5.27E-06	7.74E-06	9.81E-06	7.16E-05
GALLBLADDER	--	--	--	--	--	--	--	--	--
GI TRACT	1.64E-02	5.13E-02	1.28E-01	1.63E-01	2.23E-01	2.81E-01	3.24E-01	3.34E-01	2.96E-01
KIDNEYS	--	<u>6.62E-06</u>	<u>1.65E-05</u>	<u>2.40E-05</u>	5.55E-05	2.70E-04	1.54E-03	3.73E-03	1.24E-02
OVARIES	--	--	--	--	--	--	<u>2.57E-05</u>	<u>1.53E-04</u>	<u>6.62E-04</u>
STOMACH CONTENTS	1.40E-04	4.96E-04	1.45E-03	1.97E-03	3.04E-03	4.49E-03	6.43E-03	7.64E-03	9.75E-03
FECES	9.82E-01	9.44E-01	8.58E-01	8.17E-01	7.42E-01	6.54E-01	5.51E-01	4.81E-01	3.26E-01
FAT	--	<u>1.74E-05</u>	5.33E-05	7.57E-05	1.37E-04	3.90E-04	1.66E-03	3.45E-03	1.07E-02
BLOOD	--	--	<u>1.57E-06</u>	--	<u>2.29E-06</u>	<u>3.61E-06</u>	<u>5.48E-06</u>	<u>7.51E-06</u>	<u>1.46E-05</u>
BONE	3.32E-05	5.24E-05	7.67E-05	8.39E-05	9.66E-05	1.20E-04	3.84E-04	1.62E-03	1.82E-02
SKIN	--	<u>5.53E-06</u>	8.25E-06	<u>9.98E-06</u>	2.08E-05	1.77E-04	1.78E-03	4.49E-03	1.17E-02
BONE MARROW	--	--	<u>3.76E-06</u>	<u>4.79E-06</u>	5.41E-06	6.49E-06	7.82E-06	2.15E-05	1.33E-03
MUSCLE	1.12E-03	3.66E-03	1.10E-02	1.60E-02	2.94E-02	5.67E-02	1.08E-01	1.56E-01	2.73E-01
EXTERNAL	--	--	--	--	<u>9.99E-07</u>	3.97E-06	5.31E-05	1.53E-04	5.87E-04

ELECTRON ABSORBED FRACTIONS

Source = SKIN

Energy (MeV)

TARGET	0.1	0.2	0.4	0.5	0.7	1.0	1.5	2.0	4.0
BRAIN	--	--	--	--	--	4.35E-05	3.26E-04	8.78E-04	2.45E-03
HEART	--	--	--	--	--	--	<u>1.87E-06</u>	<u>2.98E-06</u>	5.40E-04
LUNGS	--	--	--	<u>1.69E-06</u>	<u>2.22E-06</u>	<u>3.24E-06</u>	4.31E-05	2.30E-04	1.53E-03
LIVER	--	--	<u>2.34E-06</u>	<u>2.90E-06</u>	<u>4.73E-06</u>	4.01E-05	3.79E-04	1.16E-03	4.26E-03
GALLBLADDER	--	--	--	--	--	--	--	--	<u>1.19E-05</u>
GI TRACT	<u>1.37E-05</u>	<u>4.29E-05</u>	1.24E-04	2.03E-04	5.29E-04	1.65E-03	4.14E-03	6.04E-03	1.14E-02
KIDNEYS	--	--	--	<u>1.75E-05</u>	5.72E-05	1.77E-04	6.32E-04	1.19E-03	2.52E-03
OVARIES	--	--	--	--	--	--	--	--	<u>9.89E-06</u>
STOMACH CONTENTS	--	--	--	--	--	<u>2.59E-06</u>	<u>2.32E-05</u>	8.46E-05	9.48E-04
FECES	--	--	<u>3.19E-06</u>	<u>4.20E-06</u>	<u>8.45E-06</u>	8.19E-05	8.67E-04	2.23E-03	5.84E-03
FAT	--	--	<u>1.20E-05</u>	<u>2.90E-05</u>	1.16E-04	3.71E-04	9.09E-04	1.29E-03	1.82E-03
BLOOD	--	--	<u>3.23E-06</u>	<u>3.29E-06</u>	<u>5.88E-06</u>	2.01E-05	2.55E-04	1.13E-03	5.11E-03
BONE	1.81E-03	5.99E-03	1.70E-02	2.45E-02	4.24E-02	6.64E-02	8.98E-02	9.93E-02	9.56E-02
SKIN	9.33E-01	7.91E-01	5.00E-01	4.04E-01	2.87E-01	2.04E-01	1.40E-01	1.10E-01	6.31E-02
BONE MARROW	--	--	--	--	<u>1.71E-05</u>	1.75E-04	1.07E-03	1.72E-03	2.65E-03
MUSCLE	4.00E-02	1.23E-01	2.78E-01	3.20E-01	3.58E-01	3.65E-01	3.52E-01	3.36E-01	2.86E-01
EXTERNAL	2.14E-02	3.14E-02	2.49E-02	2.04E-02	1.47E-02	1.05E-02	7.35E-03	5.81E-03	3.47E-03

**7.6. APPENDIX F – Photon self-absorbed fractions for adult versus juvenile
*Lepus californicus***

**7.7. APPENDIX G – Electron self-absorbed fractions for adult versus juvenile
*Lepus californicus***

SOURCE/TARGET	ELECTRON SELF-ABSORBED FRACTIONS								
	0.1	0.2	0.4	0.5	0.7	1.0	1.5	2.0	4.0
BONE_ADULT	9.89E-01	9.64E-01	9.04E-01	8.75E-01	8.19E-01	7.45E-01	6.39E-01	5.59E-01	3.77E-01
BONE_JUVENILE	9.86E-01	9.56E-01	8.86E-01	8.53E-01	7.90E-01	7.05E-01	5.91E-01	5.10E-01	3.33E-01
MUSCLE_ADULT	9.92E-01	9.75E-01	9.34E-01	9.14E-01	8.79E-01	8.35E-01	7.75E-01	7.27E-01	5.97E-01
MUSCLE_JUVENILE	9.89E-01	9.65E-01	9.13E-01	8.89E-01	8.45E-01	7.90E-01	7.17E-01	6.60E-01	5.17E-01
LIVER_ADULT	9.94E-01	9.80E-01	9.47E-01	9.30E-01	8.98E-01	8.54E-01	7.87E-01	7.25E-01	5.29E-01
LIVER_JUVENILE	9.91E-01	9.73E-01	9.28E-01	9.07E-01	8.64E-01	8.06E-01	7.18E-01	6.43E-01	4.39E-01
TESTES_ADULT	9.92E-01	9.75E-01	9.33E-01	9.12E-01	8.74E-01	8.23E-01	7.49E-01	6.85E-01	4.83E-01
OVARIES_JUVENILE	9.79E-01	9.32E-01	8.21E-01	7.67E-01	6.62E-01	5.20E-01	3.46E-01	2.56E-01	1.28E-01
LUNGS_ADULT	9.95E-01	9.83E-01	9.55E-01	9.41E-01	9.15E-01	8.78E-01	8.20E-01	7.67E-01	5.94E-01
LUNGS_JUVENILE	9.92E-01	9.75E-01	9.35E-01	9.15E-01	8.76E-01	8.21E-01	7.36E-01	6.60E-01	4.42E-01
KIDNEYS_ADULT	9.92E-01	9.74E-01	9.31E-01	9.10E-01	8.70E-01	8.13E-01	7.24E-01	6.42E-01	3.88E-01
KIDNEYS_JUVENILE	9.91E-01	9.70E-01	9.23E-01	9.00E-01	8.54E-01	7.88E-01	6.86E-01	5.94E-01	3.35E-01
HEART_ADULT	9.95E-01	9.85E-01	9.59E-01	9.47E-01	9.23E-01	8.90E-01	8.37E-01	7.86E-01	6.04E-01
HEART_JUVENILE	9.91E-01	9.72E-01	9.27E-01	9.06E-01	8.64E-01	8.04E-01	7.13E-01	6.30E-01	3.85E-01
GITRACT_ADULT	9.86E-01	9.57E-01	8.88E-01	8.55E-01	7.98E-01	7.35E-01	6.60E-01	6.07E-01	4.69E-01
GITRACT_JUVENILE	9.83E-01	9.46E-01	8.64E-01	8.26E-01	7.58E-01	6.80E-01	5.92E-01	5.31E-01	3.81E-01
STOMACH_CONTENTS_ADULT	9.91E-01	9.71E-01	9.24E-01	9.01E-01	8.58E-01	8.01E-01	7.12E-01	6.29E-01	3.74E-01
STOMACH_CONTENTS_JUVENILE	9.92E-01	9.74E-01	9.34E-01	9.14E-01	8.75E-01	8.22E-01	7.39E-01	6.62E-01	4.20E-01
FECES_ADULT	9.81E-01	9.38E-01	8.39E-01	7.91E-01	7.05E-01	5.97E-01	4.64E-01	3.79E-01	2.37E-01
FECES_JUVENILE	9.82E-01	9.44E-01	8.58E-01	8.17E-01	7.42E-01	6.54E-01	5.51E-01	4.81E-01	3.26E-01
SKIN_ADULT	9.58E-01	8.68E-01	6.61E-01	5.66E-01	4.21E-01	3.04E-01	2.11E-01	1.66E-01	9.55E-02
SKIN_JUVENILE	9.33E-01	7.91E-01	5.00E-01	4.04E-01	2.87E-01	2.04E-01	1.40E-01	1.10E-01	6.31E-02
TESTES_ADULT_25g_HYP	9.92E-01	9.75E-01	9.35E-01	9.15E-01	8.78E-01	8.30E-01	7.59E-01	6.97E-01	4.99E-01
TESTES_ADULT_21g_MEASURED	9.92E-01	9.75E-01	9.33E-01	9.12E-01	8.74E-01	8.23E-01	7.49E-01	6.85E-01	4.83E-01
TESTES_ADULT_15g_HYP	9.91E-01	9.70E-01	9.22E-01	8.98E-01	8.53E-01	7.95E-01	7.11E-01	6.40E-01	4.34E-01

TESTES_ADULT_10g_HYP	9.89E-01	9.66E-01	9.09E-01	8.81E-01	8.29E-01	7.60E-01	6.64E-01	5.84E-01	3.77E-01
OVARIES_JUVENILE_1.0g_HYP	9.85E-01	9.54E-01	8.79E-01	8.42E-01	7.70E-01	6.73E-01	5.35E-01	4.26E-01	2.12E-01
OVARIES_JUVENILE_0.5g_HYP	9.79E-01	9.32E-01	8.21E-01	7.67E-01	6.62E-01	5.20E-01	3.46E-01	2.56E-01	1.28E-01
OVARIES_JUVENILE_0.2g_MEAS	9.79E-01	9.32E-01	8.21E-01	7.67E-01	6.62E-01	5.20E-01	3.46E-01	2.56E-01	1.28E-01
OVARIES_JUVENILE_0.1g_HYP	9.79E-01	9.32E-01	8.21E-01	7.67E-01	6.62E-01	5.20E-01	3.46E-01	2.56E-01	1.28E-01
OVARIES_JUVENILE_0.05g_HYP	9.72E-01	9.10E-01	7.68E-01	7.00E-01	5.70E-01	4.12E-01	2.57E-01	1.89E-01	9.54E-02

7.8. APPENDIX H – Electron and photon self-absorbed fractions for the sensitivity analysis on tissue composition in adult *Lepus californicus*

SOURCE/TARGET	ELECTRON SELF-ABSORBED			
	Energy (MeV)			
	0.1	0.5	1.0	1.5
BONE_MEASURED	9.89E-01	8.75E-01	7.45E-01	6.39E-01
BONE_ICRP Cortical	9.89E-01	8.74E-01	7.43E-01	6.37E-01
Bone Ratio	1.00E+00	1.00E+00	1.00E+00	1.00E+00
HEART_MEASURED	9.95E-01	9.47E-01	8.90E-01	8.37E-01
HEART_ICRP StriatedMuscle	9.95E-01	9.48E-01	8.92E-01	8.40E-01
Heart Ratio	1.00E+00	9.99E-01	9.98E-01	9.96E-01
KIDNEYS_MEASURED	9.92E-01	9.10E-01	8.13E-01	7.24E-01
KIDNEYS_ICRU FourComponent	9.92E-01	9.11E-01	8.16E-01	7.29E-01
Kidneys Ratio	1.00E+00	9.99E-01	9.96E-01	9.94E-01
LIVER_MEASURED	9.94E-01	9.30E-01	8.54E-01	7.87E-01
LIVER_ICRU FourComponent	9.94E-01	9.31E-01	8.56E-01	7.90E-01
Liver Ratio	1.00E+00	9.99E-01	9.97E-01	9.95E-01
LUNGS_MEASURED	9.95E-01	9.41E-01	8.78E-01	8.20E-01
LUNGS_ICRP Lung	9.95E-01	9.43E-01	8.82E-01	8.25E-01
Lungs Ratio	1.00E+00	9.98E-01	9.96E-01	9.94E-01
TESTES_MEASURED	9.92E-01	9.12E-01	8.23E-01	7.49E-01
TESTES_ICRP Testes	9.92E-01	9.14E-01	8.28E-01	7.55E-01
Testes Ratio	1.00E+00	9.98E-01	9.95E-01	9.92E-01
MUSCLE_MEASURED	9.92E-01	9.14E-01	8.35E-01	7.75E-01
MUSCLE_ICRP SkeletalMuscle	9.92E-01	9.16E-01	8.38E-01	7.79E-01
Muscle Ratio	1.00E+00	9.98E-01	9.96E-01	9.95E-01

PHOTON SELF-ABSORBED FRACTIONS
Energy (MeV)

SOURCE/TARGET	0.01	0.1	0.5	1.0	1.5	2.0	4.0
BONE_MEASURED	9.57E-01	7.27E-02	4.14E-02	3.68E-02	3.19E-02	2.78E-02	1.87E-02
BONE_ICRP_Cortical	9.58E-01	7.32E-02	4.13E-02	3.67E-02	3.17E-02	2.76E-02	1.86E-02
Bone Ratio	9.99E-01	9.93E-01	1.00E+00	1.00E+00	1.01E+00	1.00E+00	1.01E+00
HEART_MEASURED	8.81E-01	3.99E-02	4.67E-02	4.17E-02	3.60E-02	3.11E-02	1.88E-02
HEART_ICRP_StriatedMuscle	9.10E-01	4.24E-02	4.77E-02	4.26E-02	3.69E-02	3.19E-02	1.95E-02
Heart Ratio	9.68E-01	9.39E-01	9.78E-01	9.78E-01	9.76E-01	9.74E-01	9.62E-01
KIDNEYS_MEASURED	7.74E-01	2.25E-02	2.74E-02	2.37E-02	1.96E-02	1.62E-02	8.34E-03
KIDNEYS_ICRU_FourComponent	8.38E-01	2.39E-02	2.79E-02	2.42E-02	2.00E-02	1.66E-02	8.66E-03
Kidneys Ratio	9.24E-01	9.42E-01	9.82E-01	9.81E-01	9.78E-01	9.75E-01	9.63E-01
LIVER_MEASURED	8.18E-01	3.70E-02	4.41E-02	3.93E-02	3.38E-02	2.92E-02	1.79E-02
LIVER_ICRU_FourComponent	8.72E-01	3.96E-02	4.49E-02	4.01E-02	3.45E-02	3.00E-02	1.85E-02
Liver Ratio	9.38E-01	9.32E-01	9.81E-01	9.80E-01	9.79E-01	9.76E-01	9.65E-01
LUNGS_MEASURED	8.72E-01	4.52E-02	5.17E-02	4.63E-02	4.01E-02	3.52E-02	2.24E-02
LUNGS_ICRP_Lung	9.03E-01	4.86E-02	5.33E-02	4.78E-02	4.15E-02	3.65E-02	2.35E-02
Lungs Ratio	9.66E-01	9.30E-01	9.69E-01	9.68E-01	9.66E-01	9.64E-01	9.53E-01
TESTES_MEASURED	8.20E-01	3.20E-02	3.74E-02	3.31E-02	2.82E-02	2.41E-02	1.42E-02
TESTES_ICRP_Testes	8.63E-01	3.43E-02	3.84E-02	3.41E-02	2.91E-02	2.49E-02	1.48E-02
Testes Ratio	9.50E-01	9.34E-01	9.73E-01	9.72E-01	9.69E-01	9.67E-01	9.56E-01
MUSCLE_MEASURED	8.24E-01	7.21E-02	8.65E-02	8.01E-02	7.19E-02	6.49E-02	4.70E-02
MUSCLE_ICRP_SkeletalMuscle	8.63E-01	7.74E-02	8.86E-02	8.21E-02	7.37E-02	6.66E-02	4.86E-02
Muscle Ratio	9.55E-01	9.32E-01	9.76E-01	9.76E-01	9.75E-01	9.74E-01	9.68E-01

7.9. APPENDIX I – Electron and photon self-absorbed fractions for the sensitivity analysis on tissue density in adult *Lepus californicus*

ELECTRON SELF-ABSORBED

Energy (MeV)

0.1 0.5 1.0 1.5**SOURCE/TARGET**

BONE_1.0	9.83E-01	8.20E-01	6.51E-01	5.29E-01
BONE_1.2	9.86E-01	8.46E-01	6.96E-01	5.80E-01
BONE_1.4	9.88E-01	8.66E-01	7.31E-01	6.21E-01
BONE_1.5_MEASURED	9.89E-01	8.75E-01	7.45E-01	6.39E-01
BONE_1.6	9.90E-01	8.82E-01	7.58E-01	6.56E-01
BONE_1.8	9.91E-01	8.94E-01	7.80E-01	6.85E-01
BONE_2.0	9.92E-01	9.04E-01	7.98E-01	7.09E-01

ELECTRON SELF-ABSORBED

Energy (MeV)

0.1 0.5 1.0 1.5**SOURCE/TARGET**

HEART_0.9	9.94E-01	9.31E-01	8.60E-01	7.93E-01
HEART_1.0	9.94E-01	9.37E-01	8.72E-01	8.10E-01
HEART_1.1	9.95E-01	9.42E-01	8.81E-01	8.24E-01
HEART_1.2_MEASURED	9.95E-01	9.47E-01	8.90E-01	8.37E-01
HEART_1.3	9.96E-01	9.51E-01	8.97E-01	8.47E-01
HEART_1.4	9.96E-01	9.54E-01	9.03E-01	8.56E-01

ELECTRON SELF-ABSORBED

Energy (MeV)

0.1 0.5 1.0 1.5**SOURCE/TARGET**

KIDNEYS_0.9	9.90E-01	8.92E-01	7.79E-01	6.75E-01
KIDNEYS_1.0	9.91E-01	9.02E-01	7.97E-01	7.01E-01
KIDNEYS_1.1_MEASURED	9.92E-01	9.10E-01	8.13E-01	7.24E-01
KIDNEYS_1.2	9.92E-01	9.17E-01	8.27E-01	7.43E-01
KIDNEYS_1.3	9.93E-01	9.22E-01	8.38E-01	7.60E-01

SOURCE/TARGET	ELECTRON SELF-ABSORBED			
	Energy (MeV)			
	0.1	0.5	1.0	1.5
LIVER_0.9	9.92E-01	9.16E-01	8.27E-01	7.49E-01
LIVER_1.0	9.93E-01	9.24E-01	8.41E-01	7.69E-01
LIVER_1.1_MEASURED	9.94E-01	9.30E-01	8.54E-01	7.87E-01
LIVER_1.2	9.94E-01	9.35E-01	8.64E-01	8.01E-01
LIVER_1.3	9.95E-01	9.40E-01	8.73E-01	8.14E-01

SOURCE/TARGET	ELECTRON SELF-ABSORBED			
	Energy (MeV)			
	0.1	0.5	1.0	1.5
LUNGS_0.9	9.94E-01	9.32E-01	8.61E-01	7.96E-01
LUNGS_1.0	9.94E-01	9.39E-01	8.73E-01	8.13E-01
LUNGS_1.05_MEASURED	9.95E-01	9.41E-01	8.78E-01	8.20E-01
LUNGS_1.1	9.95E-01	9.44E-01	8.83E-01	8.27E-01

SOURCE/TARGET	ELECTRON SELF-ABSORBED FRACTIONS			
	Energy (MeV)			
	0.1	0.5	1.0	1.5
TESTES_0.9	9.90E-01	8.95E-01	7.92E-01	7.07E-01
TESTES_1.0	9.91E-01	9.04E-01	8.09E-01	7.30E-01
TESTES_1.1_MEASURED	9.92E-01	9.12E-01	8.23E-01	7.49E-01
TESTES_1.2	9.93E-01	9.19E-01	8.36E-01	7.66E-01
TESTES_1.3	9.93E-01	9.25E-01	8.46E-01	7.80E-01

ELECTRON SELF-ABSORBED**Energy (MeV)****0.1 0.5 1.0 1.5****SOURCE/TARGET**

MUSCLE_0.9	9.90E-01	8.97E-01	8.07E-01	7.40E-01
MUSCLE_1.0	9.91E-01	9.06E-01	8.22E-01	7.59E-01
MUSCLE_1.1_MEASURED	9.92E-01	9.14E-01	8.35E-01	7.75E-01
MUSCLE_1.2	9.93E-01	9.20E-01	8.45E-01	7.88E-01
MUSCLE_1.3	9.93E-01	9.26E-01	8.55E-01	8.00E-01

SOURCE/TARGET	PHOTON SELF-ABSORBED FRACTIONS						
	Energy (MeV)						
	0.01	0.1	0.5	1.0	1.5	2.0	4.0
BONE_1.0	9.36E-01	4.85E-02	2.77E-02	2.41E-02	2.04E-02	1.75E-02	1.13E-02
BONE_1.2	9.46E-01	5.82E-02	3.32E-02	2.92E-02	2.50E-02	2.16E-02	1.42E-02
BONE_1.4	9.54E-01	6.79E-02	3.87E-02	3.43E-02	2.96E-02	2.58E-02	1.72E-02
BONE_1.5_MEASURED	9.57E-01	7.27E-02	4.14E-02	3.68E-02	3.19E-02	2.78E-02	1.87E-02
BONE_1.6	9.59E-01	7.74E-02	4.41E-02	3.93E-02	3.42E-02	2.99E-02	2.03E-02
BONE_1.8	9.64E-01	8.71E-02	4.95E-02	4.44E-02	3.87E-02	3.41E-02	2.34E-02
BONE_2.0	9.68E-01	9.65E-02	5.48E-02	4.93E-02	4.33E-02	3.83E-02	2.65E-02

SOURCE/TARGET	PHOTON SELF-ABSORBED FRACTIONS						
	Energy (MeV)						
	0.01	0.1	0.5	1.0	1.5	2.0	4.0
HEART_0.9	8.46E-01	2.97E-02	3.50E-02	3.09E-02	2.61E-02	2.21E-02	1.22E-02
HEART_1.0	8.60E-01	3.31E-02	3.89E-02	3.45E-02	2.94E-02	2.51E-02	1.44E-02
HEART_1.1	8.71E-01	3.65E-02	4.28E-02	3.81E-02	3.27E-02	2.81E-02	1.66E-02
HEART_1.2_MEASURED	8.81E-01	3.99E-02	4.67E-02	4.17E-02	3.60E-02	3.11E-02	1.88E-02
HEART_1.3	8.89E-01	4.33E-02	5.06E-02	4.53E-02	3.92E-02	3.41E-02	2.10E-02
HEART_1.4	8.96E-01	4.67E-02	5.44E-02	4.89E-02	4.25E-02	3.71E-02	2.33E-02

SOURCE/TARGET	PHOTON SELF-ABSORBED FRACTIONS						
	Energy (MeV)						
	0.01	0.1	0.5	1.0	1.5	2.0	4.0
KIDNEYS_0.9	7.33E-01	1.84E-02	2.24E-02	1.90E-02	1.54E-02	1.24E-02	6.01E-03
KIDNEYS_1.0	7.55E-01	2.05E-02	2.49E-02	2.14E-02	1.75E-02	1.43E-02	7.13E-03
KIDNEYS_1.1_MEASURED	7.74E-01	2.25E-02	2.74E-02	2.37E-02	1.96E-02	1.62E-02	8.34E-03
KIDNEYS_1.2	7.90E-01	2.46E-02	3.00E-02	2.61E-02	2.17E-02	1.81E-02	9.57E-03
KIDNEYS_1.3	8.04E-01	2.66E-02	3.25E-02	2.84E-02	2.38E-02	2.00E-02	1.08E-02

SOURCE/TARGET	PHOTON SELF-ABSORBED FRACTIONS						
	Energy (MeV)						
	0.01	0.1	0.5	1.0	1.5	2.0	4.0
LIVER_0.9	7.86E-01	3.02E-02	3.62E-02	3.18E-02	2.71E-02	2.31E-02	1.35E-02
LIVER_1.0	8.04E-01	3.36E-02	4.01E-02	3.56E-02	3.05E-02	2.62E-02	1.57E-02
LIVER_1.1_MEASURED	8.18E-01	3.70E-02	4.41E-02	3.93E-02	3.38E-02	2.92E-02	1.79E-02
LIVER_1.2	8.31E-01	4.04E-02	4.80E-02	4.30E-02	3.71E-02	3.23E-02	2.01E-02
LIVER_1.3	8.42E-01	4.37E-02	5.20E-02	4.66E-02	4.05E-02	3.53E-02	2.24E-02

SOURCE/TARGET	PHOTON SELF-ABSORBED FRACTIONS						
	Energy (MeV)						
	0.01	0.1	0.5	1.0	1.5	2.0	4.0
LUNGS_0.9	8.54E-01	3.87E-02	4.44E-02	3.95E-02	3.40E-02	2.96E-02	1.82E-02
LUNGS_1.0	8.67E-01	4.30E-02	4.93E-02	4.40E-02	3.81E-02	3.33E-02	2.10E-02
LUNGS_1.05_MEASURED	8.72E-01	4.52E-02	5.17E-02	4.63E-02	4.01E-02	3.52E-02	2.24E-02
LUNGS_1.1	8.77E-01	4.74E-02	5.41E-02	4.85E-02	4.22E-02	3.71E-02	2.38E-02

SOURCE/TARGET	PHOTON SELF-ABSORBED FRACTIONS						
	Energy (MeV)						
	0.01	0.1	0.5	1.0	1.5	2.0	4.0
TESTES_0.9	7.87E-01	2.62E-02	3.06E-02	2.68E-02	2.25E-02	1.89E-02	1.06E-02
TESTES_1.0	8.05E-01	2.91E-02	3.40E-02	3.00E-02	2.54E-02	2.15E-02	1.24E-02
TESTES_1.1_MEASURED	8.20E-01	3.20E-02	3.74E-02	3.31E-02	2.82E-02	2.41E-02	1.42E-02
TESTES_1.2	8.32E-01	3.50E-02	4.08E-02	3.62E-02	3.11E-02	2.67E-02	1.61E-02
TESTES_1.3	8.43E-01	3.79E-02	4.41E-02	3.94E-02	3.39E-02	2.93E-02	1.79E-02

SOURCE/TARGET	PHOTON SELF-ABSORBED FRACTIONS						
	Energy (MeV)						
	0.01	0.1	0.5	1.0	1.5	2.0	4.0
MUSCLE_0.9	7.96E-01	5.90E-02	7.15E-02	6.59E-02	5.88E-02	5.28E-02	3.76E-02
MUSCLE_1.0	8.11E-01	6.56E-02	7.91E-02	7.30E-02	6.54E-02	5.89E-02	4.23E-02
MUSCLE_1.1_MEASURED	8.24E-01	7.21E-02	8.65E-02	8.01E-02	7.19E-02	6.49E-02	4.70E-02
MUSCLE_1.2	8.36E-01	7.87E-02	9.39E-02	8.71E-02	7.84E-02	7.09E-02	5.18E-02
MUSCLE_1.3	8.46E-01	8.53E-02	1.01E-01	9.41E-02	8.48E-02	7.69E-02	5.65E-02

7.10. APPENDIX J – Dose conversion factors for adult *Lepus californicus* derived from voxel model

Found online at: <http://www.rrjournal.org/doi/abs/10.1667/RR14162.1> and
https://www.dropbox.com/sh/2z8z88gx0fb1otg/AAAppfhRa8_Np2e4eQXKM5maa?dl=0

**7.11. APPENDIX K – Dose conversion factors for adult *Lepus californicus*
derived from ERICA Version 1.2**

Radionuclide	Scaled DCF uGy/hr per Bq/kg	uGy/d per Bq/kg
Am-241	3.20E-03	7.68E-02
Cs-134	1.45E-04	3.48E-03
Cs-137	1.59E-04	3.82E-03
Pu-238	3.17E-03	7.61E-02
Pu-239	2.97E-03	7.13E-02
Pu-240	2.98E-03	7.15E-02
Sr-90	5.58E-04	1.34E-02
 Cs-134, 137	3.04E-04	7.30E-03
Pu-239, 240	5.95E-03	1.43E-01
Pu-238, 239	6.14E-03	1.47E-01

Ellipsoid dimensions (mm)	
Length	345.4
Width	70.0
Height	242.6
Ellipsoid mass (kg)	
	2.1
Ellipsoid density (g/cm³)	
	1.00
Occupancy factors	
On-soil	0.5
In-soil	0.5

7.12. APPENDIX L – NTS, Hanford, Fukushima radionuclide concentration data

Found online at: <http://www.rrjournal.org/doi/abs/10.1667/RR14162.1> and
https://www.dropbox.com/sh/2z8z88gx0fb1otg/AAAppfhRa8_Np2e4eQXKM5maa?dl=0

7.13. APPENDIX M – NTS, Hanford, Fukushima, Maralinga organ dose rates

Found online at: <http://www.rrjournal.org/doi/abs/10.1667/RR14162.1> and

https://www.dropbox.com/sh/2z8z88gx0fb1otg/AAAppfhRa8_Np2e4eQXKM5maa?dl=0